



Mitogenomic phylogeny of mud snails of the mostly Atlantic/ Mediterranean genus *Tritia* (Gastropoda: Nassariidae)

Yi Yang, Samuel Abalde, Carlos Afonso, Manuel J Tenorio, Nicolas Puillandre, Jose Templado, Rafael Zardoya

► To cite this version:

Yi Yang, Samuel Abalde, Carlos Afonso, Manuel J Tenorio, Nicolas Puillandre, et al.. Mitogenomic phylogeny of mud snails of the mostly Atlantic/ Mediterranean genus *Tritia* (Gastropoda: Nassariidae). *Zoologica Scripta*, 2021, 50 (5), pp.571-591. 10.1111/zsc.12489 . hal-03172830

HAL Id: hal-03172830

<https://hal.science/hal-03172830>

Submitted on 19 Mar 2021

HAL is a multi-disciplinary open access archive for the deposit and dissemination of scientific research documents, whether they are published or not. The documents may come from teaching and research institutions in France or abroad, or from public or private research centers.

L'archive ouverte pluridisciplinaire **HAL**, est destinée au dépôt et à la diffusion de documents scientifiques de niveau recherche, publiés ou non, émanant des établissements d'enseignement et de recherche français ou étrangers, des laboratoires publics ou privés.



Distributed under a Creative Commons Attribution 4.0 International License

1 Submitted to:
2 *Zoologica Scripta*
3 Second revised version: March 8th, 2020

4
5
6
7 **Mitogenomic phylogeny of mud snails of the mostly Atlantic/Mediterranean**
8 **genus *Tritia* (Gastropoda: Nassariidae)**

9
10 Yi Yang¹, Samuel Abalde¹, Carlos L. M. Afonso², Manuel J. Tenorio³, Nicolas Puillandre⁴, José
11 Templado¹, and Rafael Zardoya¹
12

13 ¹Museo Nacional de Ciencias Naturales (MNCN-CSIC), José Gutiérrez Abascal 2, 28006, Madrid,
14 Spain;

15 ²Centre of Marine Sciences (CCMAR), Universidade do Algarve, Campus de Gambelas, 8005-139
16 Faro, Portugal

17 ³Departamento CMIM y Q. Inorgánica-INBIO, Facultad de Ciencias, Universidad de Cádiz; 11510
18 Puerto Real, Cádiz, Spain;

19 ⁴Institut de Systématique, Évolution, Biodiversité (ISYEB), Muséum National d'Histoire Naturelle,
20 CNRS, Sorbonne Université, EPHE, Université des Antilles, 57 rue Cuvier, CP 26, 75005 Paris,
21 France.

22

23

24 *Corresponding author (rafaz@mncn.csic.es)

25

26

27 **Abstract**

28 The mud snails endemic to the East Atlantic/Mediterranean region (genus *Tritia*; subfamily
29 Nassariinae) account for the second highest diversity within the family Nassariidae (Gastropoda:
30 Buccinoidea). In order to understand how the diversity of species, shell morphologies, and
31 ecological traits evolved within this genus, a robust phylogenetic framework is needed, yet still
32 unavailable due to high levels of homoplasy in shell morphology, the main trait used for their
33 taxonomic classification. Here, the near-complete mitogenomes of 20 species representing more
34 than half of the diversity of *Tritia* were sequenced. All mitogenomes of *Tritia* shared the same gene
35 order, which is identical to the consensus reported for caenogastropods. The reconstructed
36 phylogeny indicates that all analyzed *Tritia* species formed a natural group except *Tritia vaucheri*,
37 which was sister to an early diverging clade within subfamily Nassariinae that includes species of
38 genus *Reticunassa* sister to *Nassarius jacksonianus* and *Nassarius* sp. Within *Tritia*, the Northwest
39 Atlantic species *Tritia obsoleta* was placed as the sister group of three mostly East
40 Atlantic/Mediterranean clades (I-III), prompting the reinstatement of the genus *Ilyanassa*. The latter
41 three clades corresponded to different shell features (I, shell mostly with marked sculpture; II, shell
42 with strong nodules and small size; and III, smooth shell). For *Tritia incrassata*, the analyzed
43 specimens from Norway and from the Spanish Mediterranean coasts showed notable genetic
44 divergence, which may indicate the existence of cryptic species. The ancestral character state
45 reconstruction of protoconch inferred that the ancestor of *Tritia* had planktotrophic larvae, and that
46 a transition to lecithotrophy occurred independently at least three times within Nassariinae. The
47 reconstructed chronogram dated the origin of *Tritia* in the Oligocene and main diversification
48 events during the Miocene to Pleistocene, correlated with drastic shifts in local paleoecosystems
49 caused by cooling events, eustatic sea level changes, and the Messinian Salinity Crisis that favored
50 temperate taxa.

51

52 **KEYWORDS**

53 Nassariinae, *Tritia*, *Ilyanassa*, mitochondrial genome, phylogeny, chronogram

54

55 **1. INTRODUCTION**

56 Mud snails or dog whelks (family Nassariidae) are small- to medium-sized snails, readily
57 recognized by their fusiform, slender to broadly ovate shells of moderately sculptured surface (from
58 smooth to cancellate or reticulate) with more or less prominent axial and spiral ribs and cords
59 (Cernohorsky, 1984). The base of the shell aperture has a notch for extension of their long siphon.
60 The columella is short with a pronounced siphonal fold (Cossmann, 1901). The reduced operculum
61 is thin and corneous with a terminal nucleus and often marginally serrated. Most nassariids species
62 are facultative scavengers or non-selective predators (Morton, 2011). Their characteristic long
63 inhalant siphon (as long as their body) together with a well-developed osphradium allows acute
64 chemoreception and efficiently leads to carrion or prey. Their often very wide and flattened foot
65 enables these sea snails to glide quickly and easily over soft substrata.

66 The nassariids constitute an important component of the biodiversity of tropical and temperate
67 seas and attain their greatest diversity in the tropical Indo-Pacific (Cernohorsky, 1984). A few
68 species have reached the polar seas (Nekhaev, 2014). Mud snails inhabit predominantly in shallow
69 water soft bottoms, but some live in deep water, and many characterize certain types of sediments
70 where they are dominant (Harasewych, 1998; Hayashi, 2004). For instance, the species of the genus
71 *Bullia* are the most conspicuous surfing organisms of the swash zone of many sandy beaches in the
72 southern hemisphere, and some species of *Nassarius* and *Tritia* display dense populations in
73 estuaries and coastal lagoons. Several species have adapted to brackish water and a few have
74 successfully conquered freshwater habitats in Southeast Asia (Strong, Galindo, & Kantor, 2017).
75 Due to their abundance, nassariids have been well studied from different points of view. For
76 instance, many nassariid species are known to accumulate toxins and as such constitute a health
77 problem especially in Asia (Hwang et al., 2005); other species have been used as model organisms,
78 such as *Tritia obsoleta* (as *Ilyanassa obsoleta*) in developmental biology (Goulding & Lindberg,
79 2016) or *Bullia digitata* in ecological and behavioral studies (Brown, 1980). Furthermore, nassariids
80 have a rich fossil record (Gili & Martinell, 1993, Tracey, Todd, & Erwin, 1993; Haasl, 2000;
81 Harzhauser & Kowalke, 2004; Landau, da Silva, & Gili, 2009) since the lower Cretaceous (Taylor,
82 Morris, & Taylor, 1980) that should help understanding major evolutionary trends within the family
83 when interpreted within a phylogenetic framework.

84 The first thorough classification of nassariids was based on the shape of the shell columella
85 (Cossmann, 1901), and is still in use with slight modifications (Cernohorsky, 1984). The family was
86 traditionally divided into three subfamilies: Nassarinae, Dorsaniinae and Cyleninae, until Allmon
87 (1990) transferred several genera previously included in Dorsaniinae to establish the new subfamily
88 Bullinae. However, the taxonomy of these subfamilies, especially the status of genera and

89 subgenera, has remained far from resolved because of rampant convergence in shell morphology
90 and other phenotypic characters due to adaptations to similar environmental or selective pressures.
91 Moreover, most nassariids species were assigned by default to the genus *Nassarius* and many are
92 still provisionally included in this genus, which demands thorough revision.

93 Recently, a molecular phylogeny including more than 200 putative nassariid species was
94 reconstructed based on partial sequences of five (mitochondrial and nuclear) genes (Galindo et al.,
95 2016). This molecular phylogeny showed that the morphology-based taxonomy of the family
96 (Cernohorsky, 1984; Allmon, 1990; Haasl, 2000; Kantor, 2003) was dominated by homoplasy and
97 had little phylogenetic significance. Genera were redefined, the new subfamily Buccinanopsinae
98 was created, and the taxon Photinae was reestablished at subfamily level (Galindo et al., 2016).

99 The reconstructed phylogeny of Galindo et al. (2016) showed that the cosmopolitan subfamily
100 Nassariinae comprises about 80% of nassariid species diversity (MolluscaBase, 2020a). Up to five
101 strongly supported clades were recovered within this subfamily and were assigned to genera with
102 relatively distinct geographical distributions: the Indo-Pacific *Nassarius* and *Reticunassa* (the
103 “pauper-complex” *sensu* Kool & Dekker, 2006, 2007, Galindo, Kool, & Dekker, 2017); the mostly
104 Atlantic-Mediterranean *Tritia*; the (East and West) African *Naytia*; and the Caribbean-Panamanian
105 *Phrontis*. Furthermore, these genera showed different types of protoconch. The multispiral
106 protoconchs of species assigned to *Nassarius* and *Reticunassa* have one or two keels, whereas those
107 of species included within *Tritia*, *Naytia*, and *Phrontis* lack a keel (Galindo et al., 2016). Transitions
108 to a paucispiral protoconch have occurred independently within different genera (Galindo et al.,
109 2016).

110 Phylogenetic relationships among species within the different genera remained largely
111 unresolved in several cases (Galindo et al., 2016). After Galindo et al. (2016) around 60 species
112 were reclassified into genera other than *Nassarius* but more than 300 species remained tentatively in
113 this genus (MolluscaBase, 2020b) awaiting further phylogenetic studies. In this regard, two
114 subsequent mitogenomic studies that focused on the genus *Nassarius* improved the resolution of
115 phylogenetic relationships among species restricted to the China seas (Yang, Li, Kong, & Yu, 2019;
116 Yang et al., 2020), compared with previous attempts based on partial gene sequences (e.g., Zhang &
117 You, 2009; Chen & Zhang, 2012; Pu et al., 2017). As a result of these mitogenomic studies, the
118 composition of the genus *Nassarius* was refined, with *Nassarius jacksonianus* and *Nassarius* sp.
119 (incorrectly identified as *N. acuticostus*; see Supporting Information Figure S1) placed with strong
120 statistical support as sister to *Reticunassa* (Yang, Li, Kong, & Yu, 2019). Furthermore, another
121 mitogenomic phylogenetic study focused on genus *Reticunassa* revealed cryptic species (Yang, Li,
122 Kong, & Yu, 2018). These studies highlight the need of studying in depth the species composition

123 and phylogenetic relationships within the five recognized Nassariinae genera. They also confirm the
124 high levels of resolution achieved by complete mitochondrial genomes when inferring phylogenetic
125 relationships of gastropods below the family level (Uribe, Puillandre, & Zardoya, 2017).

126 The traditional taxonomy of the Atlantic/Mediterranean nassariids was mainly based on shell
127 characters, with species classified into different genera (*Hinia*, *Nassarius*, *Sphaeronassa*, *Naytiopsis*,
128 *Cyclope* and *Ilyanassa*). Even though species of *Cyclope* possess rather unique flattened shell
129 geometry, and *Ilyanassa* is restricted to the Northwest Atlantic, the molecular phylogeny of
130 Nassariidae found no evidence to support these genera, which were both synonymized with *Tritia*
131 (Galindo et al., 2016). At present, a total of 40 species are considered valid within *Tritia*
132 (MolluscaBase, 2020c), including four species endemic to the Gulf of Gabès that were recently
133 recognized as valid (Aissaoui, Galindo, Puillandre, & Bouchet, 2017). Several *Tritia* species extend
134 their range distribution to West African coasts living in sympatry with *Naytia* species.

135 In order to clarify the taxonomy of the genus *Tritia* in the Atlantic/ Mediterranean region, a
136 robust phylogeny of the group is needed. Thus far, only two complete mitochondrial genomes of
137 *Tritia* species are available i.e., *T. obsoleta* (DQ238598; Simison, Lindberg, & Boore, 2006, as
138 *Ilyanassa obsoleta*) and *T. reticulata* (EU827201; Cunha, Grande, & Zardoya, 2009). In the present
139 study, we sequenced the nearly complete (without the control region or partial gene sequences)
140 mitochondrial genomes of 21 specimens representing 20 species of *Tritia* (i.e., half of the diversity
141 of the genus) and of one specimen of the freshwater nassariid *Anentome* sp. as outgroup. Our aims
142 were: (1) to test the monophyly of the genus *Tritia* as currently defined (MolluscaBase, 2020c); (2)
143 to reconstruct robust phylogenetic relationships within the genus; (3) to date the origin and main
144 cladogenetic events during the diversification of this genus; and (4) to test the validity of shell
145 morphology in *Tritia* taxonomy.

146

147 2. MATERIALS AND METHODS

148 2.1. Samples and DNA extraction

149 The complete list of specimens analyzed in the present study, including their sampling sites,
150 collectors, and museum vouchers is shown in Table 1. Samples were stored in 100% ethanol at 4°C
151 or -20°C, and total genomic DNA was isolated from foot muscle using the DNeasy Blood & Tissue
152 Kit (Qiagen, Germany).

153

154 2.2. PCR amplification and sequencing

Nearly complete (without the control region or partial gene sequences) mt genomes were amplified in two main steps. First, fragments of *coxl*, *cox3*, *rrnS*, *rrnL*, and *cob* genes were amplified through standard PCRs, which were carried out in a total volume of 25 µl with 1 µl of template DNA (25–40 ng/µl), 2.5 µl of 10× buffer (Mg^{2+} plus), 0.5 µl of dNTPs (2.5 mM), 0.5 µl of each primers (10 µM), 0.2 µl of Taq DNA polymerase (5 U/µl), 0.25 µl of BSA (10 mg/ml) and 19.55 µl of DEPC water. The PCR conditions were as follows: an initial denaturing step at 94 °C for 5 min; 40 cycles of denaturing at 94 °C for 60 s, annealing at 39–48°C for 60 s, and extension at 72 °C for 90 s; and a final extension step at 72 °C for 10 min. Standard-PCR products were purified by ethanol precipitation, and Sanger sequenced at Macrogen (Seoul, Korea). Information on standard PCR primers is shown in Supporting Information Table S1.

In the second step, the obtained sequences were used to design specific primer pairs for long PCR amplification of the remaining mitogenome in four fragments (see Supporting Information Table S1). The long PCR reactions contained 2.5 µl of 10× buffer (Mg^{2+} plus), 3 µl of dNTPs (2.5 mM), 0.5 µl of each primers (10 µM), 0.8 µl of template DNA (25–40 ng/µl), 0.2 µl of TaKaRa LA Taq DNA polymerase (5 U/µl), 0.2 µl of BSA (10 mg/ml) and DEPC water up to 25 µl. The following PCR conditions were used: initial denaturing step at 94 °C for 60 s; 45 cycles of denaturing at 98 °C for 10 s, annealing at 53–56 °C for 30 s, and extension at 68 °C for 60 s per kb; final extension step at 68 °C for 10 min. Long PCR products were purified by ethanol precipitation, and fragments from the same mitogenome were pooled together in equimolar concentrations for high-throughput sequencing. For each mitogenome of *Tritia*, a separate indexed library was constructed using the NEXTERA XT DNA library prep Kit (Illumina, San Diego, CA, USA) and run in an Illumina MiSeq platform (2 × 150 paired-end) at AllGenetics (A Coruña, Spain) and NIMGenetics (Madrid, Spain). Among the 20 libraries, five contained also the mitogenomes of cones or buccinoids from different projects (see Supporting Information Table S1).

Due to the degraded condition of the source DNA of *T. ovoidea* and *T. tingitana*, the partial mt genomes of these species were mostly amplified through standard PCRs, as only few long PCRs worked (see Supporting Information Table S1). Those amplified fragments with sizes ≤ 1,000 bp were directly Sanger sequenced with the corresponding PCR primers, whereas the longer PCR products were Sanger sequenced using a primer walking strategy. Sequencing was performed in automated sequencers (ABI PRISM 3700) using the BigDye® Terminator v3.1 cycle-sequencing kit

185 (Applied Biosystems, Foster City, CA, USA), and following the manufacturer's instructions.

186 For some species with tentative identification, namely *N. jacksonianus* and *N. acusticostus*, or
187 of unexpected phylogenetic position, namely *T. ephamilla* and *T. vaucherii*, the barcoding *cox1*
188 fragment was PCR amplified and Sanger sequenced to double check species identity (see
189 Supporting Information Figure S1).

190

191 **2.3. Genome assembly and annotation**

192 The Sanger sequences were assembled using Sequencher 5.0.1. For the specimens from the MNHN
193 collections, some *cox1* sequences were downloaded from Genbank (see Supporting Information
194 Table S1). For Illumina sequence data, the reads corresponding to different individuals were sorted
195 by the corresponding library indices. Raw sequences were analyzed for quality control using
196 FastQC v.0.11.9 (Andrews, 2010), and trimmed and filtered out according to their quality scores
197 using PRINSEQ v.0.20.4 (Schmieder & Edwards, 2011). Assembly of the mitogenomes was
198 performed using Geneious Prime 2019.0.3 (Kearse et al., 2012). The mitogenomes were constructed
199 by repeatedly mapping the original reads (setting a minimum identity of 99%) to the Sanger
200 fragments from the same mitogenome.

201 The newly determined mt genomes were annotated with Geneious Prime 2019.0.3. Annotations
202 of protein-coding genes (PCGs) were defined by setting a limit of 75% nucleotide identity to
203 previously published nassariid mitogenomes (Table 1) in Geneious Prime 2019.0.3, and
204 corroborated using the MITOS Webserver (Bernt et al., 2013) with the invertebrate mitochondrial
205 genetic code. The transfer RNA (tRNA) genes were further identified using tRNA scan-SE 1.21
206 (Schattner, Brooks, & Lowe, 2005) and ARWEN (Laslett & Canbäck, 2008). The ribosomal RNA
207 (rRNA) genes were first identified using the MITOS Webserver (Bernt et al., 2013). The software
208 rendered shorter rRNA genes (due to sequence variability in the ends), and their boundaries were
209 assumed to be between the adjacent genes by comparison with other nassariid mt genomes.

210

211 **2.4. Sequence alignment**

212 The newly sequenced mitogenomes were aligned along with those of other nassariids available in
213 Genbank (Table 1). Representatives of different genera of Nassariinae were included in the ingroup
214 to test the monophyly of *Tritia*. The freshwater nassariid *Anentome* sp. (subfamily Anentominae)

215 was used as outgroup to root the tree (Galindo et al., 2016). A dataset concatenating the nucleotide
216 sequences of the 13 PCGs and two rRNA genes was constructed and analyzed.

217 The 13 PCGs were aligned separately guided by amino acid translations (according to the
218 invertebrate mitochondrial genetic code) using Translator X (Abascal, Zardoya, & Telford, 2010), .
219 Nucleotide sequences of the two rRNA genes were aligned separately using MAFFT v7 (Katoh &
220 Standley, 2013) with default parameters. Ambiguously aligned positions were removed using
221 Gblocks v.0.91b (Castresana, 2000) with the following settings: minimum sequence for flanking
222 positions: 85%; maximum contiguous non-conserved positions: 8; minimum block length: 10; gaps
223 in final blocks: no. Finally, the different single alignments were concatenated into a single data set
224 in Geneious Prime 2019.0.3. Sequences were converted into different formats for downstream
225 analyses using DAMBE5 (Xia, 2013).

226

227 **2.5. Phylogenetic analyses**

228 Pairwise uncorrected *p* sequence distances to delimit species were estimated based on the alignment
229 including the nucleotide sequences of the 13 PCGs and the two rRNA genes. Phylogenetic trees
230 were reconstructed using maximum likelihood (ML; Felsenstein, 1981) and Bayesian inference (BI;
231 Huelsenbeck & Ronquist, 2001). ML analyses were carried out using IQtree 1.6.10 (Nguyen,
232 Schmidt, Von Haeseler, & Minh, 2015) in the CIPRES gateway (Miller, Pfeiffer, & Schwartz, 2010),
233 allowing partitions to have different evolutionary rates (-spp option) and with 10,000 ultrafast
234 bootstrap pseudoreplications (-bb option). BI analyses were performed with MrBayes
235 v.3.1.2 (Ronquist & Huelsenbeck, 2003), running four simultaneous Monte Carlo Markov chains
236 (MCMC) for 10,000,000 generations, sampling every 1000 generations, and discarding the first 25%
237 generations as burn-in. Two independent runs were performed to increase the chance of adequate
238 mixing of the Markov chains and to increase the chance of detecting failure to converge, as
239 determined by using Tracer v1.6. The effective sample size (ESS) of all parameters was higher than
240 200. The resulting phylogenetic trees were visualized in FigTree v1.4.2.

241 The best partition schemes and best-fit substitution models for BI analysis of the data set were
242 determined (see Supporting Information Table S2 for selected best fit partitions and models) using
243 PartitionFinder 2 (Lanfear et al., 2017), under the Bayesian Information Criterion (BIC; Schwarz,
244 1978). For the 13 PCGs, the partitions tested were: all genes combined; all genes separated (except

245 *atp6-atp8* and *nad4-nad4L*); and genes grouped by subunits (*atp*, *cob*, *cox* and *nad*). Additionally,
246 these three partition schemes were tested considering separately the three codon positions. The two
247 rRNA genes were analyzed with two different schemes (genes grouped or separated). The best-fit
248 substitution models for ML analysis were calculated with ModelFinder (Kalyaanamoorthy, Minh,
249 Wong, Haeseler, & Jermiin, 2017) as implemented in IQ-TREE 1.6.10.

250

251 **2.6. Ancestral Character State Reconstruction**

252 The type of larval shell or protoconch with a single (paucispiral) or multiple whorls (multispiral)
253 was accessed based on literature (Galindo et al., 2016; Aissaoui, Galindo, Puillandre, & Bouchet,
254 2017) except for *T. vaucheri*, which was determined by direct examination of the shells (the number
255 of whorls was counted to the nearest quarter whorl; Modica et al., 2020). Both types of protoconch
256 were used as a proxy of the lecithotrophic (direct development using yolk reserves) or
257 planktotrophic (with a feeding veliger phase) modes of larval development (Strathmann, 1978). The
258 evolution of larval development was analyzed by performing an ancestral character state
259 reconstruction in Mesquite v3.6.1 (Maddison & Maddison, 2018) using the Tracing Character
260 History option under ML and mapping onto the identical topology inferred by the ML and BI
261 analyses.

262

263 **2.7. Estimation of divergence times**

264 The program BEAST v.1.10.4 (Drummond & Rambaut, 2007) was used to perform a Bayesian
265 estimation of divergence times among main nassariid lineages based on PCGs only. An uncorrelated
266 relaxed molecular clock was used to infer branch lengths and node ages. The tree topology was
267 fixed using the identical topology recovered by the ML and BI analyses. For the clock model, the
268 lognormal relaxed-clock model was selected, which allows rates to vary among branches without
269 any *a priori* assumption of autocorrelation between adjacent branches. For the tree prior, a Yule
270 process of speciation was employed. The partitions selected by PartitionFinder 2 (see above) were
271 applied. The final Markov chain was run twice for 100 million generations, sampling every 10,000
272 generations and the first 10 million were discarded as burn-in, according to the convergence of
273 chains checked with Tracer v.1.6. The effective sample size of all the parameters was above 200.

274 The posterior distribution of the estimated divergence times was obtained by specifying three

275 calibration points based on fossil data as priors for divergence times of the corresponding splits. The
276 prior distributions of the three calibration nodes were selected following Ho & Phillips (2009). For
277 the origin of the lineage leading to *T. neritea* and *T. pellucida*, a calibration point was set at the
278 minimum limit of 3.6 million years ago (Mya; exponential distribution, offset: 3.6; mean: 1.0) based
279 on the fossils of *Cyclope migliorinii* that are the oldest for the stem group (Gili & Martinell, 1999;
280 Landau, da Silva, & Grigis, 2009) and dated from the Pliocene (Placenzian; 3.6 - 2.6 Mya) of Spain
281 according to the Paleobiology Database (<https://paleobiodb.org>). A second calibration point was set
282 at the origin of *Tritia*. A lognormal distribution was applied, with the minimum of 23 Mya and a 95%
283 upper limit of 28.4 Mya (offset: 23; mean: 1.9; standard deviation: 1.9) based on *Nassarius (Hinia)*
284 *pygmaea* from Germany (Albright et al., 2019) and *Nassarius (Hinia) schlotheimi* from Hungary
285 (Báldi, 1973), both from the Oligocene (Chattian; 28.4 - 23.0 Mya), the oldest Nassariinae fossils in
286 Europe (Lozouet, 1999). A third calibration point was set at the root of the tree. A lognormal
287 distribution was applied, with the minimum of 55.8 Mya and a 95% upper limit of 58.7 Mya (offset:
288 55.8; mean: 1.0; standard deviation: 1.0) based on the oldest known Nassariinae fossil, which is
289 *Buccitriton sagenum* from the Paleocene (Thanetian; 58.7 - 55.8 Mya) of Louisiana, USA (Glawe,
290 Anderson, & Bell, 2014).

291

292 3. RESULTS

293 3.1. Sequencing and assembly

294 All newly sequenced mt genomes in the present study lacked the sequences of the *trnF* gene, the
295 control region, and the start of the *cox3* gene because the corresponding fragment could not be PCR
296 amplified. The number of reads, mean coverage, length, and accession number in Genbank of each
297 mitogenome are provided in Table 1. The mt genomes of *T. incrassata*-SP and *T. varicosa* received
298 the minimum (53x; 30,800 reads) and maximum (23,350x; 2,765,768 reads) coverage, respectively
299 (Table 1).

300

301 3.2. Genome organization

302 The newly determined *Tritia* mitogenomes encode for 13 PCGs, two rRNA and 22 tRNA genes (but
303 note that the *trnF* gene could not be determined in all mt genomes; see annotation of each mt
304 genome in Supporting Information Table S3). They all share the same genome organization

described for Caenogastropoda (Osca, Templado, & Zardoya, 2015), with most genes encoded by the major strand and a cluster of tRNA genes (*trnM*, *trnY*, *trnC*, *trnW*, *trnQ*, *trnG*, *trnE*) and the *trnT* gene encoded by the minor strand (Figure 1). All PCGs start with the conventional initiation codon ATG (but note that the start of the *cox3* gene could not be determined in all mt genomes; see Supporting Information Table S3). As for the termination codons, two genes (*cox2* and *atp8*) consistently ended with TAA and two (*nad4L* and *nad5*) stopped with TAG. The incomplete stop codon (TA-), which becomes functional after polyadenylation (Ojala et al., 1981), was observed in all *nad2* genes but that of *Tritia grana*, which ended with TAA. The remaining genes varied in their stop codons depending on the species (Supporting Information Table S3).

314

315 **3.3. Phylogenetic relationships**

316 Phylogenetic relationships of *Tritia* were reconstructed based on the nucleotide sequences of the
317 concatenated 13 PCGs and two rRNA genes using probabilistic methods (Figure 2). The final
318 matrix was 13,101 positions in length. According to the BIC, the best partition scheme for the PCGs
319 was the one combining genes by subunits but analyzing each codon position separately (Supporting
320 Information Table S2). For the rRNA genes, the best partition scheme was the one combining
321 together *rrnL* and *rrnS* genes. Both ML ($-lnL = 133,593.77$) and BI ($-lnL = 133,905.39$ for run 1;
322 $-lnL = 133,908.66$ for run 2) analyses arrived at identical topologies (Figure 2).

323 According to the reconstructed phylogeny, *N. jascksonianus* and *Nassarius* sp were recovered
324 closer to *Reticunassa* than to other *Nassarius* species (Figure 2). *Tritia vaucheri* was placed sister to
325 the clade including (*N. jascksonianus* and *Nassarius* sp.) + *Reticunassa*, and apart from the
326 remaining *Tritia* species, which formed a natural group. Within this latter group, the Northwest
327 Atlantic species *T. obsoleta* was placed as sister to three mostly Northeast Atlantic/ Mediterranean
328 clades (I-III). Clade I included ten species distributed into five lineages: (1) *T. ephamilla* (endemic
329 to New Zealand and southern Australia) and *T. ovoidea* + *T. elata*, (2) *T. denticulata*, (3) *T. tingitana*,
330 (4) *T. reticulata* and *T. nitida*, and (5) the “*T. cuvierii* complex” including *T. unifasciata* and *T.*
331 *cuvierii* + *T. tenuicosta*. This clade was sister to clades II and III (Figure 2). Clade II comprised *T.*
332 *varicosa* and *T. incrassata* (including one specimen from a Spanish Mediterranean population and
333 one from Norway). Clade III included *T. elongata* + (*T. pallaryana* and *T. corniculum*) sister to a
334 group formed by *T. grana* + (*T. neritea* and *T. pellucida*) and *T. pfeifferi* + *T. mutabilis* (Figure 2).

335

336 **3.4. Ancestral character state reconstruction**

337 The ancestral character state reconstruction analysis inferred that the Atlantic/Mediterranean
338 nassariids could have originated from an ancestor with a multispiral protoconch, which indicates a
339 planktotrophic mode of larval development (Figure 3). The “*T. cuvierii* complex”, clade III, and *T.*
340 *tingitana* were inferred to represent independent evolutionary transitions to a paucispiral protoconch,
341 suggesting a secondary loss of the planktotrophic mode of larval development to lecithotrophy.

342

343 **3.5. Divergence times**

344 Main cladogenetic events within *Tritia* were dated using an uncorrelated relaxed molecular clock
345 model, which was calibrated using three Atlantic fossils. The origin of the stem lineage leading to
346 genus *Tritia* (including *T. obsoleta* and without *T. vaucheri*) was dated 24.0 (26.2–23.1, 95% highest
347 posterior density interval, HPD) million years ago (Mya). The first event of diversification within
348 the crown group of *Tritia* was estimated at a mean of 20.4 (23.5–17.1) Mya, separating the
349 Northwest Atlantic *T. obsoleta* from *T. ephamilla* and East Atlantic/ Mediterranean *Tritia* species.
350 The branching of the three main East Atlantic/ Mediterranean clades was estimated to have occurred
351 around 18.9–17.6 (22.0–14.4) Mya. Finally, main diversification events leading to extant *Tritia*
352 species were estimated to have occurred between 16.9–3.9 (20.1–2.0) Mya, whereas divergences of
353 some closely-related species or populations were dated about 0.6–0.1 Mya (Figure 4).

354

355 **4. DISCUSSION**

356 **4.1. Taxonomy of the non-*Tritia* Nassariinae**

357 The often-ornamented shell of nassariids, which could in principle provide numerous characters for
358 taxonomic classification, and had been widely used in the past for this purpose, was found to be
359 prone to convergence at different taxonomic levels (particularly within Nassariinae) when a rather
360 comprehensive molecular phylogeny of the family was inferred (Galindo et al., 2016). This
361 phylogeny provided the long needed scaffold to continue resolving the systematics of the family
362 and opened the way to further phylogenetic studies focusing on relationships within particular
363 clades. Here, we focused on one of these clades, which included nassariinae mostly from the
364 Atlantic/Mediterranean region and was ascribed to genus *Tritia* (Galindo et al., 2016). We

365 sequenced the near-complete (without the control region or partial gene sequences) mitogenomes of
366 20 species belonging to *Tritia* and reconstructed a highly resolved phylogeny, which included more
367 than half of the species diversity of this genus (MolluscaBase, 2020c) as well as other nassariinae
368 genera and *Anentome* sp. (subfamily Anetominae) as outgroup.

369 Within the first offshoot of the tree, *N. jascksonianus* and *Nassarius* sp. were recovered closer
370 to *Reticunassa* than to other *Nassarius*, as previously suggested (Yang, Li, Kong, & Yu, 2019). This
371 is not surprising considering the geographic disparity of the samples and that not all species
372 ascribed to *Nassarius* were included in the molecular phylogeny of the family, impeding proper
373 assignment to clades (Galindo et al., 2016). Given the relative phylogenetic position of the two
374 species and the large uncorrected *p* distance separating them from other clades (16–18%), they
375 could be allocated in a new genus, whose formal description would need a larger taxon sampling
376 and thorough morphological revision beyond the scope of this study.

377 According to the reconstructed phylogeny, the ascription of *T. vaucheri* to genus *Tritia* was
378 strongly rejected. This taxon was originally described as *Nassa (Himia) vaucheri* (Pallary, 1906).
379 After examining the syntype of this species, Cernohorsky (1975), transferred it to genus *Chauvetia*
380 (in family Buccinidae). Later, Hoenselaar and Moolenbeek (1988) transferred the species to genus
381 *Nassarius* and designated a lectotype. Finally, the new combination *T. vaucheri* (currently accepted
382 in MolluscaBase, 2020c) was established in a checklist of marine mollusks recorded in Spanish
383 marine waters (Gofas et al., 2017). *Tritia vaucheri* was recovered as an early divergent lineage in
384 the phylogeny, sister to the Indo-Pacific clade (*N. jascksonianus* and *Nassarius* sp.) + *Reticunassa*,
385 although with low statistical support. Hence, this species does not belong to genus *Tritia*, but to
386 another Atlantic genus that is only distantly related and still needs to be determined (*Genus incertae
387 sedis*, *Gen. inc. sed.*). Therefore, the general shell morphology resemblance of this taxon to other
388 *Tritia* species would represent yet another case of convergence within Nassariidae (Galindo et al.,
389 2016). *Genus incertae sedis vaucheri* is found in the southwestern Mediterranean coasts of Spain
390 and in the nearby Atlantic coasts from south Portugal to Morocco being replaced by *Nassarius*
391 *argenteus* from Senegal down to the Gulf of Guinea (Gofas, 2011). This latter species was not
392 included in our study but may also belong to the same genus as *Gen. inc. sed. vaucheri*. The
393 above-mentioned distribution is typical of several species of *Tritia* but also of several sympatric
394 species of the African genus *Naytia*. Galindo et al. (2016) provisionally included in this latter genus

395 *N. glabrata* (type species), *N. granulosa*, *N. johni*, from West African coasts, and *N. priscardi* from
396 Madagascar, and they highlighted that the members of this genus were characterized by high
397 morphological disparity. The type species and *N. granulosa* exhibit a smooth shell, similar to that of
398 the species of the *Bullia* group, which led Simone & Pastorino (2014) to erroneously include *N.*
399 *granulosa* in the genus *Bullia*. Conversely, *N. johni* and *N. priscardi*, exhibit a reticulate shell
400 sculpture. *Gen. inc. sed. vaucheri* is quite similar to these two latter species, so it could be possible
401 that it belongs to *Naytia* (the position of this genus in the phylogeny of Galindo et al. 2016 is sister
402 to *Reticunassa*, although with low support). It will be necessary to include mitogenomes of species
403 from other genera (especially from West Africa) into the nassariid phylogeny in order to fully
404 resolve the phylogenetic position of *Gen. inc. sed. vaucheri* and its generic placement.

405 The first split among the species attributed to the genus *Tritia* separated the Northwest Atlantic
406 species *T. obsoleta* from the East Atlantic/Mediterranean species. This node is inconsistent with the
407 results reported for the nassariid phylogeny (Galindo et al., 2016), in which *T. obsoleta* emerged in
408 an internal position within *Tritia*, although with low bootstrap support. In the past, *T. obsoleta* was
409 assigned as the type species to genus *Ilyanassa* (Stimpson, 1865), which was a taxon that included
410 nassariids from North America (Cernohorsky, 1984). Although *Ilyanassa* had been widely used in
411 previous literature, the internal position of *T. obsoleta* within *Tritia* in Galindo et al. (2016), led
412 these authors to synonymize *Ilyanassa* with *Tritia*. In contrast, our results reveal a correlation
413 between the phylogenetic position of *T. obsoleta* and its geographical distribution, which together
414 with a significant level of genetic divergence (13.7%) support the reinstatement of the genus
415 *Ilyanassa*. To further resolve this part of the tree, it would be also necessary to include *I. trivittata*
416 and other Northwest Atlantic nassariids (Rosenberg, 2009) into the phylogeny, as well as *T.*
417 *buchardi* from southern Australia and New Zealand, which is close to *Ilyanassa* according to the
418 phylogeny of Galindo et al. (2016).

419

420 **4.2. Taxonomy of *Tritia***

421 Within the mostly East Atlantic/Mediterranean group, Clade I comprised 10 species, which are
422 characterized by the presence of a shell with a more or less marked sculpture. The first diverging
423 lineage of Clade I included *T. ephamilla* and *T. elata* + *T. ovoidea*. The former species is endemic to
424 New Zealand and southern Australia whereas the latter two are found in the Mediterranean Sea and

425 along the West African coasts down to Angola. The inclusion of *T. ephamilla* within *Tritia* was also
426 recovered by Galindo et al (2016), although its exact sister group was not resolved. In addition to
427 the geographic disparity, there is also a prominent morphological difference between *T. ephamilla*
428 (globose with nodulose shell sculpture) and *T. elata* and *T. ovoidea* (slender-ovoid with slight spiral
429 striations). The presence of *T. ephamilla* in this part of the tree could reflect a Thetyan origin of the
430 Northeast Atlantic/Mediterranean mud snails and a subsequent southwards expansion towards
431 tropical waters in the West Africa coasts (Galindo et al., 2016). A striking example of a similar
432 disjoint distribution is constituted by the seagrass genus *Posidonia*, which displays the same
433 contrasting biogeographic pattern. One species, *P. oceanica*, is distributed in the Mediterranean Sea
434 whereas the other species of the genus are restricted to subtropical and temperate Australian waters
435 (Aires et al., 2011). Other Northeast Atlantic/Mediterranean gastropods with a similar disjoint
436 distribution and suspected of having Thetyan origin are the top shell snails of the subfamily
437 Cantharidinae (Uribe et al., 2017b). In this case, the endemics to Oceania were recovered as sister to
438 all Atlantic/ Mediterranean taxa. *Tritia elata* is a circalittoral species typical of soft bottoms of the
439 continental shelf from the southern Iberian Peninsula to Angola. It shows a quite variable shell
440 sculpture along the West African coast where it has been sometimes recorded as *Nassarius*
441 *semistriatus*, a very similar fossil species extinct during the Pleistocene (Adam & Knudsen, 1984).
442 This last species, as well as the fossil species *Nassarius martinelli* (described by Gili, 1992 from the
443 West Mediterranean Pliocene and differing from *T. elata* by its paucispiral protoconch) likely
444 belong to the stem group of *Tritia*.

445 The other lineage within Clade I included *T. denticulata* sister to a rather diversified clade
446 including *T. tingitana* sister to the “*T. cuvierii* complex” plus *T. reticulata* and *T. nitida*. The relative
447 position of *T. denticulata* within clade I is in agreement with the Nassariidae molecular phylogeny
448 (Galindo et al., 2016) but here showing high statistical support. *Tritia denticulata* is another
449 circalittoral species distributed in the Alboran Sea and along the West African coasts down to
450 Angola, including the Canary, Madeira and Cabo Verde islands (Rolán & Hernández, 2005). This
451 species is morphologically similar to a group of West African species, namely *N. turbineus*, *N.*
452 *webbei*, *N. desmoulioides*, and *N. arcadioi* (Rolán & Hernández, 2005), whose ascription to *Tritia*
453 remains to be tested by their incorporation into the molecular phylogeny. In addition, the fossil
454 species *N. clathratus* (Rolán & Hernández, 2005) could belong to the stem lineage of *Tritia*. The

455 phylogenetic position of *T. tingitana* (endemic of the Strait of Gibraltar), as the second diverging
456 lineage within Clade I, is in clear disagreement with Galindo et al. (2016), who recovered *T.*
457 *tingitana* as sister to *T. corniculum* with maximal support in a clade equivalent to our Clade III (see
458 below). The two species are morphologically very different, and difficult to misidentify, suggesting
459 a possible mislabeling error.

460 The last lineage of Clade I included three species corresponding to the “*T. cuvierii* complex”
461 plus *T. reticulata* and *T. nitida* (Galindo et al., 2016; Aissaoui, Galindo, Puillandre, & Bouchet,
462 2017). Within the “*T. cuvierii* complex”, *T. cuvierii* and *T. unifasciata* are sympatric along the
463 Mediterranean coasts, and differ in the size of their shell, protoconch and egg capsules (Moreno &
464 Templado, 1994). *Tritia unifasciata* has faint axial ribs only in the first whorls of the shell. The third
465 species of the complex here studied was *T. tenuicosta*, endemic to the Gulf of Gabès, whose relative
466 position was in agreement to that recovered by Aissaoui, Galindo, Puillandre, & Bouchet (2017).
467 Another two endemic species of the Gulf of Gabès, *T. lanceolata* and *T. djerbaensis* also belong to
468 the “*T. cuvierii* complex”, and *T. cuvierii* may also include additional local cryptic species (Aissaoui,
469 Galindo, Puillandre, & Bouchet, 2017). According to Galindo et al. (2016), the West African *T.*
470 *miga* would be closely related to the “*T. cuvierii* complex”. Given its distribution and morphological
471 similarity, the endemic species from Cabo Verde islands, *T. caboverdensis* (Rolán, 1984) may also
472 belong to this complex (pending molecular confirmation).

473 The closely related and well-known species *T. reticulata* and *T. nitida* have been widely studied
474 from different viewpoints (see Rolán & Luque, 1994; Albaina et al., 2012; Couceiro et al., 2012,
475 and references therein). Both species, sometimes misidentified, share similar life histories and
476 dispersal capacities, but differ in their environmental affinities. The netted dogwhelk *T. reticulata*
477 inhabits a wide range of marine soft bottoms and is mainly an East Atlantic species with a more or
478 less continuous distribution from the British Isles to Morocco and the Canary Islands that enters
479 into western Mediterranean. The estuarine dog-welk *T. nitida* is restricted to sheltered brackish
480 habitats with a patchy distribution in the Mediterranean Sea and Black Sea coasts as well as in the
481 East Atlantic Ocean from Morocco to Norway (Albaina et al., 2012). Therefore, this latter species
482 probably diverged from *T. reticulata* by a habitat shift from marine to brackish waters.

483 Clade II in our phylogeny (also recovered in Galindo et al., 2016) included *T. varicosa* (often
484 previously recorded as *T. pygmaea*) and *T. incrassata*. Both species are sympatric in the

485 Mediterranean Sea and along the Northeast Atlantic coast from Sweden to the Iberian Peninsula.
486 They are similar in terms of shell size (about 10 mm) and ornament (little nodules on shell formed
487 by costae and spiral ridges), but the nodules of *T. varicosa* are much smaller, squarer and more
488 upstanding than those of *T. incrassata* (Fretter, Graham & Andrews, 1986). Divergence between
489 both species could have been caused by adaptation to dissimilar habitats: mainly rocky bottoms in *T.*
490 *incrassata* and soft bottoms with beds of *Zostera* and *Cymodocea* seagrasses in *T. varicosa* (JT, pers.
491 obs.). According to Galindo et al. (2016), *T. senegalensis* and *T. goreensis*, and several other species
492 endemic to Senegal, would be sister to the northern species within this clade.

493 With a planktotrophic larval stage, *T. incrassata* is widely distributed along the Mediterranean
494 and Northeast Atlantic region. The pairwise uncorrected *p* distance between the two studied
495 individuals of *T. incrassata* from two distant locations (Norway and the Spanish Mediterranean)
496 reached 3.8%, which was even higher than the value obtained for sibling species such as *T. neritea*
497 and *T. pellucida* (Supporting Information Table S4). This result indicates that the diversity of *T.*
498 *incrassata* was previously underestimated and that it may include putative cryptic species. This
499 hypothesis will need to be further confirmed by the inclusion of data from nuclear genes to discard
500 potential events of incomplete lineage sorting and hybridization (Alexander et al., 2017). A previous
501 phylogeographic study on *T. nitida* suggested the existence of two glacial refugia during the
502 Pleistocene, one in the Atlantic (around the Iberian Peninsula) and the other in the
503 Paleo-Mediterranean Sea (Albaina et al., 2012). It may well be the case that the observed genetic
504 divergence between the two populations of *T. incrassata*-NW and -SP is a result of isolation in the
505 two Pleistocene refugia. After the last glaciation, the Strait of Gibraltar and the Almeria-Oran
506 oceanographic front would have acted as well documented barriers to gene flow between the
507 Atlantic and Mediterranean populations, as reported for *T. nitida* (Albaina et al., 2012) and other
508 marine organisms (Patarnello, Volckaert, & Castilho, 2007). Our results show the need for further
509 studies with dense sampling at the population level along the distribution range of *T. incrassata* in
510 order to determine its diversity and elucidate the evolutionary processes driving its diversification.

511 Finally, Clade III in the reconstructed tree is composed of eight species with smooth (absence
512 of sculpture) shells as shared derived character. The absence of sculpture may have occurred
513 independently in several lineages of Nassariinae, some of which were already defined in the
514 Early-Middle Miocene (Manganelli, Spadini & Martini, 2010). Phylogenetic relationships within

515 Clade III are in agreement with those previously reported (Galindo et al., 2016; Aissaoui, Galindo,
516 Puillandre, & Bouchet, 2017), except for the relative phylogenetic position of *T. mutabilis*, which
517 here is moderately supported as sister to *T. pfeifferi* and was not resolved in previous studies. In
518 Galindo et al. (2016), *T. conspersa* was recovered as sister to *T. pfeifferi* within this clade. The
519 earliest divergent lineage within our Clade III includes species of the “*T. corniculum* complex”. The
520 pairwise uncorrected *p* distance obtained between *T. pallaryana* (a recently described species from
521 the Gulf of Gabès; Aissaoui, Galindo, Puillandre, & Bouchet, 2017) and *T. corniculum* showed the
522 least value of all comparisons (0.6%; Supporting Information Table S4), and could cast doubts on
523 the taxonomic validity of the former. However, we conservatively maintain *T. pallaryana* as valid
524 given significant ecological and morphological differences (Aissaoui, Galindo, Puillandre, &
525 Bouchet, 2017) as well as because the sequence divergence value falls within the so-called "grey
526 zone" of speciation (Roux et al., 2016). *Tritia elongata*, also endemic of the Gulf of Gabès, was also
527 recovered within the “*T. corniculum* complex”, in agreement with Aissaoui, Galindo, Puillandre, &
528 Bouchet (2017). *Tritia corniculum* inhabits sandy-muddy bottoms in shallow, sheltered waters of
529 brackish and marine environments, typically in coastal lagoons (Iannotta, Toscano, & Patti, 2009)
530 with a patchy distribution along the Mediterranean and Northeast Atlantic coasts. Its direct
531 development without a planktonic larval phase, together with the discontinuous distribution of its
532 habitat, may promote genetic isolation among populations and incipient speciation processes, which
533 are reflected in great intra-specific morphological variability (Iannotta, Toscano, & Patti, 2009;
534 Gofas, 2011).

535 The remaining species of Clade III were *T. mutabilis* (type species of the currently unaccepted
536 genus *Sphaeronassa*) and *T. pfeifferi* sister to a lineage comprising *T. grana* (type species of the
537 currently unaccepted genus *Naytiopsis*) and the flattened-shell sibling species *T. neritea* and *T.*
538 *pellucida* (previously assigned to the currently unaccepted genus *Cyclope*). While *T. mutabilis*
539 inhabits infralittoral fine sands and muddy sand banks along the Mediterranean coasts, *T. pfeifferi* is
540 an East Atlantic species (from northeastern Spain to Mauritania) adapted to shallow and intertidal
541 sheltered soft bottoms that is replaced by *T. conspersa* in Canary Islands (Gofas, 2011). On the
542 other hand, while *T. grana* inhabits clean, mobile, fine infralittoral sands in open waters, *T. neritea*
543 and *T. pellucida* are characteristic of sandy-muddy shallow bottoms in estuaries, sheltered bays and
544 marine lagoons, often subject to variable salinity (even brackish) waters (Gili & Martinell, 2000;

545 Gofas, 2011).

546

547 **4.3. Protoconch evolution**

548 The robust phylogeny of *Tritia* prompts some considerations about the evolution of the mode of
549 larval development within the genus. Since Thorson (1950), a large body of studies has focused on
550 the evolution of the mode of larval development in marine invertebrates. Transitions between modes
551 of development are considered highly asymmetrical from species with feeding larval stages
552 (planktotrophic) to species with non-feeding larval development (lecithotrophic), with the
553 evolutionary reversal of this transition considered very rare or impossible (Strathmann, 1978;
554 Modica et al., 2020). In both extant and fossil gastropods, the presence of a paucispiral or a
555 multispiral protoconch is used as proxy for the lecithotrophic and planktotrophic alternative modes
556 of development, respectively (Shuto, 1974; Jablonski & Lutz, 1980). The shift in mode of larval
557 development has important evolutionary consequences, as planktotrophic larvae are able to survive
558 longer in the water column and thus have higher dispersal capabilities than lecithotrophic larvae,
559 which barely move from the places where eggs were laid (Shank, 2009). Hence, species with
560 planktotrophic larvae usually are widely distributed and maintain high levels of gene flow between
561 populations, whereas species with lecithotrophic larvae show narrower distribution ranges and are
562 prone to allopatric speciation processes (Collin, 2001; Cunha et al., 2005; Abalde et al. 2017;
563 Modica, 2020).

564 The ancestor of the genus *Tritia* was inferred to have had planktotrophic veliger larvae, as is
565 widely assumed for caenogastropods (Ponder & Lindberg, 1997, 2019; Modica et al., 2020). The
566 lecithotrophic state is a derived condition, which evolved independently in at least three terminal
567 lineages: species within Clade III as well as species of the “*T. cuvierii* complex”, and *T. tingitana*
568 within Clade I. In addition, some but not all of the species of the “*T. denticulata* complex” have
569 planktotrophic development, and the potentially closely related *Nassarius turbineus* from the Gulf
570 of Guinea (not included in our phylogeny) exhibits paucispiral protoconch indicative of another
571 independent shift to lecithotrophy within Clade I. The loss of planktotrophy has occurred several
572 other times independently within Nassariinae including some *Reticunassa* species (Galindo et al.,
573 2016). Transitions from planktotrophic to lecithotrophic larval development have been recurrent in
574 diverse caenogastropod lineages (e.g. Lieberman, Allmon, & Eldredge, 1993; Reid, Rumbak, &

575 Thomas, 1996; Duda & Palumbi, 1999; Collin, 2004) and the fossil record from the Northeast
576 Atlantic and Mediterranean shows this trend towards the loss of planktotrophy in several taxa as
577 recently as the Pliocene and Pleistocene periods (Oliverio, 1996). During this evolutionary
578 transition, intermediate forms of development (facultative feeding larvae, short-lived planktotrophs,
579 species with dispersal polymorphisms, and species showing poecilogeny, i.e., the presence of the
580 two types of development) should appear (Collin, 2012). However, these intermediate stages are
581 generally ephemeral in evolutionary terms, and either go extinct or evolve into direct developers. In
582 rare cases, the phenotypically plastic intermediates might persist if they show a selective advantage
583 under heterogeneous environmental conditions compared to the two extremes (Collin, 2012). In
584 gastropods, the known cases of poecilogeny are prevalent among sea slugs in the suborder
585 Sacoglossa, short-lived planktotrophs are found among calyptaeids, and facultative lecithotrophy
586 has been reported in the nudibranch genus *Phestilla* (Collin, 2012).

587 The frequent and asymmetric transition to lecithotrophy may have key macroevolutionary
588 consequences because it implies shifts in rates of speciation and extinction. On the one hand,
589 species with lecithotrophic development have higher rates of speciation, and thus they are assumed
590 to progressively increase through time compared to widely dispersing species. For instance,
591 Harzhauser & Kowalke (2004) studied the nassariid gastropods from the Neogene Paratethys and
592 observed a trend in the fossil record towards the local appearance of species showing paucispiral
593 protoconch in rather short time periods. On the other hand, regional environmental perturbations
594 could cause the extinction of narrowly ranging species, whereas more broadly dispersed species
595 could survive elsewhere (e.g., Jablonski, 1986). Therefore, higher extinction rates would lower the
596 net diversity of lecithotrophs despite the fact that this condition originates frequently, and this
597 evolutionary pattern could explain the long-term maintenance of planktotrophy (Collin & Moran,
598 2018; Modica et al., 2020). In this regard, several authors have highlighted that planktotrophic
599 species are more resistant to extinction and persist longer on geological time scales relative to
600 lecithotrophic species (e.g. Hansen, 1980; Jablonski, 1986; Crampton et al., 2010). For instance,
601 planktotrophic species of the family Nassariidae from the Neogene fossil deposits of the
602 Atlantic/Mediterranean area had a mean duration of 9.8 million years, whereas the average duration
603 of several non-planktotrophic species was 2.8 million years (Gili & Martinell, 1994).

604 Given the high frequency of the transition to lecithotrophy (together with its enhancing effects

605 on extinction rates), it is likely that even if most living species of a taxon are included in a
606 molecular phylogeny, the total number of independent transitions to direct development will be
607 underestimated due to ignorance of what may have occurred in extinct lineages (Collin & Moran,
608 2018). Hence, fossil data appears necessary to testify and supplement the results of molecular data
609 to improve the knowledge of the evolution of this important trait in the life cycle in the East Atlantic
610 and Mediterranean nassariid gastropods (Lozouet & Galindo, 2015; Van Dingenen, Ceuleman,
611 Landau, & da Silva, 2015). For instance, the West Mediterranean Pliocene species *Nassarius*
612 *martinelli* is distinguished from the extant planktotrophic *T. elata* by its paucispiral protoconch,
613 indicative of lecithotrophic development (Gili, 1992). *Nassarius martinelli* was apparently quite
614 local in South France, inhabiting circallitoral bottoms, and became extinct at the end of the
615 Pliocene or during the first glacial period of the Pleistocene, probably as a consequence of
616 glacio-eustatic processes producing a sharp drop in sea level (Gili, 1992). *Tritia neritea* and *T.*
617 *pellucida* are the only extant species among Nassariinae gastropods with a depressed, discoidal shell,
618 dorsally convex and flatter in the ventral side. The early Pliocene fossil *Tritia migliorinii* (as
619 *Cyclope migliorinii*) shows the above-mentioned peculiar shell morphology (Gili & Martinell, 1999,
620 2000) and is considered a member of the stem group. It has a multispiral protoconch (i.e.,
621 planktotrophic larval development) implying a putative independent transition to direct
622 development within this lineage of Clade III. Another instance of shift in mode of larval
623 development could be that of some fossil forms closely related to *T. mutabilis* from the
624 Mediterranean and Atlantic Pliocene that may have had a rather short planktotrophic phase (Gili &
625 Martinell, 1990) suggesting yet another transition from planktotrophy to lecithotrophy within Clade
626 III.
627

628 **4.4. Tempo of diversification**

629 Our reconstructed time tree dates the origin of Nassariae genera throughout the Oligocene, which
630 is consistent with the fossil record (Lozouet & Galindo, 2015). A trend towards cooler conditions
631 during the Oligocene (Zachos et al., 2001) is likely to have favored temperate taxa (Uribe et al,
632 2017b). During this period, the onset of deep-water circulation between the Arctic and North
633 Atlantic Oceans (Davies et al., 2001) may have constituted a strong barrier to marine taxa dispersal
634 between North America and Eurasia. In this regard, the separation of *Ilyanassa* from *Tritia* at both

sides of the Atlantic and the subsequent diversification of the main eastern lineages occurred right after the Oligocene-Miocene transition. The late Oligocene is thought to have been a time of relatively warm global temperatures while in the early Miocene there was a rapid expansion of the Antarctica ice sheet and large-scale climate fluctuations attributed to an Earth orbital anomaly (Zachos et al., 2001). These global climate oscillations might have triggered diversification events leading to the extant genera within Nassariinae. In parallel, continental drift produced the collision of Laurasia and Gondwana about 19 Mya and the final closure of the Eastern Tethys Seaway (the so-called Terminal Tethyan event) around 14 Mya (Harzhauser et al., 2007; Okay, Zattin, & Cavazza, 2010; Hou & Li, 2018). The closure definitively ended the previous flow of tropical marine gastropods between the Indian Ocean and the proto-Mediterranean Basin (Hamon et al., 2013). In fact, fragmentation of the Tethys Ocean has been suggested as the main driver of the disjunct, endemic and relict distributions of many Tethyan lineages (i.e. Ozawa et al., 2009; Rodríguez-Flores et al., 2020). Accordingly, the puzzling phylogenetic position of the Australian and New Zealand endemic *T. ephamilla*, which diverged about 16 Mya from East Atlantic/Mediterranean taxa (as well as the sister relationship of the Australian *T. buchardi* and the Northwest Atlantic *I. obsoleta*; Galindo et al. 2016), would represent one of the latest split events prior to the closure.

The origin of extant species started at the end of the Miocene, when there was a sustained global cooling event that started about 12 Mya and culminated about 5.4 Mya (Herbert et al., 2016), causing an eustatic sea level drop of -10 to -30 m (Hodell et al., 2001). Simultaneously, and because of tectonic movements, the connection between the East Atlantic Ocean and the Mediterranean Sea at the Strait of Gibraltar was closed, resulting in the desiccation of the Mediterranean basin, the well-known Messinian Salinity Crisis (MSC, 5.96 to 5.33 Mya; Krijgsman et al., 1999). Altogether, these climatic, eustatic, and tectonic changes resulted in drastic shifts in the paleoecosystems of the East Atlantic/Mediterranean region that likely triggered speciation, as has been shown for other groups (Davis et al., 2016, Abalde et al., 2017; Uribe et al., 2017b). The ecological adaptation to the variable salinity waters of this period likely promoted the divergence between *T. nitida* and *T. reticulata*, between *T. mutabilis* and *T. pfeifferi*, and between *T. grana* and *T. neritea*/ *T. pellucida*, which were dated in the Miocene according to the chronogram. The independent transitions to the direct mode of larval development were also dated in this period. The transition from the Pliocene

665 to the Pleistocene was characterized by a sudden cooling (about 2.6 Mya) and subsequent
666 glacial-interglacial periods with extreme climate oscillations and drastic eustatic sea level changes
667 (Filippelli & Flores, 2009), which may explain the divergence between sibling taxa such as *T.*
668 *pallaryana* and *T. corniculum*, *T. neritea* and *T. pellucida*, and the two distant populations of *T.*
669 *incrassata*.

670 Our estimates of major divergence events within Nassariinae are about 11-24 Mya younger
671 than those previously reported in Galindo et al. (2016), which dated the origin of the lineage leading
672 to *Tritia* and *Ilyanassa* to 48 Mya (Eocene), separation of both genera at 32 Mya (Oligocene), and
673 the diversification of main lineages within *Tritia* during the Miocene. The main difference between
674 the two inferences relies on the calibration points, which in Galindo et al. (2016) were chosen to
675 date the much older Nassariidae origin within Buccinoidea (note that two calibration points were
676 the same in both studies) and the fewer representatives of *Tritia* in their chronogram. Given that our
677 calibration points were chosen to fit better in time the question at hand, and that there is congruence
678 of our estimated dates with climatic, eustatic, and tectonic changes, as well as the rich fossil record
679 of East Atlantic/Mediterranean Nassariinae during the Miocene and Pliocene (Cernohorsky, 1984),
680 we propose the present time tree as our preferred working hypothesis for the timing of the origin
681 and diversification of genus *Tritia*.

682

683 5. CONCLUSIONS

684 The reconstructed mitogenomic tree provided high resolution of *Tritia* phylogenetic relationships,
685 and allowed determining that *Gen. inc. sed. vaucheri* does not belong to the genus. Given its
686 distribution, this result calls for a morphological and ecological revision of the West African genus
687 *Naytia*. The strongly supported sister group relationship between the Northwest Atlantic *I. obsoleta*
688 and the three East Atlantic/Mediterranean clades (I-III), justify the reinstatement of the genus
689 *Ilyanassa*, and shows the need for a careful revision of the two genera. Within *Tritia*, the additional
690 described species endemic to West Africa need to be incorporated into the mitogenomic phylogeny.
691 In addition, the notable pairwise divergence between the two *T. incrassata* specimens from Norway
692 and the Spanish Mediterranean strongly suggests the possibility of the existence of cryptic species
693 that needs to be further confirmed with nuclear data and a larger sampling. The robust phylogeny
694 allowed inferring that the ancestor of Nassariinae had planktotrophic larvae and that several

695 independent transitions to lecithotrophic larvae occurred during the evolutionary history of the
696 group. Hence, it would be interesting to compare morphological and gene expression changes
697 during development of Nassariinae lecithotrophic larvae in search for footprints of convergence.
698 The inferred divergence dates suggest an important role of climatic, eustatic, and tectonic changes
699 during the Oligocene, Miocene, and Pleistocene influencing local Atlantic/Mediterranean
700 paleoecosystems and promoting the origin, main lineage diversification, and recent speciation
701 events within *Tritia*, respectively. Several recent divergences between some pairs of close species
702 could be due to a habitat shift from open marine to sheltered brackish waters. Our study indicates
703 that mt genomes could render similar robust results when applied to other Nassariinae genera and
704 would be highly useful in reconstructing a robust phylogeny of the entire Nassariidae family, hence
705 providing the long-needed framework to understand diversification and adaptation processes
706 underpinning the evolutionary success of this family.

707

708 **ACKNOWLEDGEMENTS**

709 We are grateful to the colleagues who helped us collect in the Gulf of Gabès or sent us specimens
710 from other Mediterranean, Atlantic, Australian and New-Zealand localities: Manuel Caballer, Serge
711 Gofas, Philippe Maestrati, Javier Martin, Jean Pierre Miquel, Leopoldo Moro, Marco Oliverio,
712 Gianni Spada, Jacques Pelorce, Emmanuel Vassard, and Bruce Marshall. Barbara Buge and Sadie
713 Mills are also thanked for their help in curating the MNHN and NIWA samples, respectively. We
714 thank two anonymous reviewers for detailed and insightful comments on a previous version of the
715 manuscript. This work was funded by the Spanish Ministry of Economy, Industry and
716 Competitiveness (CGL2016-75255-C2-1-P [AEI/FEDER, UE] to R.Z.; BES-2014-069575 to S.A.).
717 Yi Yang was supported by a scholarship from the China Scholarship Council (CSC-201806330034)
718 for studying and living abroad. The project has received funding from the European Research
719 Council (ERC) under the European Union's Horizon 2020 research and innovation programme
720 (grant agreement No. 865101) to NP.

721 REFERENCES

- 722 Abalde, S., Tenorio, M. J., Afonso, C. M., Uribe, J. E., Echeverry, A. M., & Zardoya, R. (2017).
723 Phylogenetic relationships of cone snails endemic to Cabo Verde based on mitochondrial
724 genomes. *BMC Evolutionary Biology*, 17, 231. <https://doi.org/10.1186/s12862-017-1069-x>
- 725 Abascal, F., Zardoya, R., & Telford, M. J. (2010). TranslatorX: multiple alignment of nucleotide
726 sequences guided by amino acid translations. *Nucleic Acids Research*, 38, W7–W13.
727 <https://doi.org/10.1093/nar/gkq291>
- 728 Adam, W., & Knudsen, J. (1984). Révision des Nassariidae (Mollusca: Gastropoda prosobranchia)
729 de l'Afrique occidentale. *Bulletin de l'Institut Royal des Sciences Naturelles de Belgique,*
730 *Biologie*, 55, 1–95, pls. 1–5.
- 731 Aires, T., Marbà, N., Cunha, R. L., Kendrick, G. A., Walker, D. I., Serrão, E. A., ... &
732 Arnaud-Haond, S. (2011). Evolutionary history of the seagrass genus *Posidonia*. *Marine*
733 *Ecology Progress Series*, 421, 117–130. <https://doi.org/10.3354/meps08879>
- 734 Aissaoui, C., Galindo, L. A., Puillandre, N., & Bouchet, P. (2017). The nassariids from the Gulf of
735 Gabès revisited (Neogastropoda, Nassariidae). *Marine Biology Research*, 13, 370–389.
736 <https://doi.org/10.1080/17451000.2016.1273528>
- 737 Albaina, N., Olsen, J. L., Couceiro, L., Ruiz, J. M., & Barreiro, R. (2012). Recent history of the
738 European *Nassarius nitidus* (Gastropoda): phylogeographic evidence of glacial refugia and
739 colonization pathways. *Marine biology*, 159, 1871–1884.
740 <https://doi.org/10.1007/s00227-012-1975-9>
- 741 Albright, L. B., Sanders, A. E., Weems, R. E., Cicimurri, D. J., & Knight, J. L. (2019). Cenozoic
742 vertebrate biostratigraphy of South Carolina, U.S.A. and additions to the fauna. *Bulletin of the*
743 *Florida Museum of Natural History*, 57, 77–236.
- 744 Alexander, A. M., Su, Y. C., Oliveros, C. H., Olson, K. V., Travers, S. L., & Brown, R. M. (2017).
745 Genomic data reveals potential for hybridization, introgression, and incomplete lineage sorting
746 to confound phylogenetic relationships in an adaptive radiation of narrow-mouth frogs.
747 *Evolution*, 71, 475–488. <https://doi.org/10.1111/evo.13133>

- 748 Allmon, W. D. (1990). Review of the *Bullia* group (Gastropoda: Nassariidae) with comments on its
749 evolution, biogeography, and phylogeny. *Bulletins of American Paleontology*, 99, 1–179.
- 750 Andrews, S. (2010). FastQC: a quality control tool for high throughput sequence data.
751 <http://www.bioinformatics.babraham.ac.uk/projects/fastqc/>
- 752 Báldi, T. (1973). *Mollusc fauna of the Hungarian Upper Oligocene (Egerian): Studies in*
753 *stratigraphy, palaeoecology, palaeogeography and systematics* (p. 511). Budapest: Akadémiai
754 Kiadó.
- 755 Bernt, M., Donath, A., Jühling, F., Externbrink, F., Florentz, C., Fritzsch, G., ... & Stadler, P. F.
756 (2013). MITOS: improved *de novo* metazoan mitochondrial genome annotation. *Molecular*
757 *Phylogenetics and Evolution*, 69, 313–319. <https://doi.org/10.1016/j.ympev.2012.08.023>
- 758 Bouchet, P., Rocroi, J. P., Hausdorf, B., Kaim, A., Kano, Y., Nützel, A., ... & Strong, E. E. (2017).
759 Revised classification, nomenclator and typification of gastropod and monoplacophoran
760 families. *Malacologia*, 61, 1–526. <https://doi.org/10.4002/040.061.0201>
- 761 Brown, A. C. (1982). The biology of sandy-beach whelks of the genus *Bullia* (Nassariidae).
762 *Oceanography and Marine Biology: An Annual Review*, 20, 309–361.
- 763 Castresana, J. (2000). Selection of conserved blocks from multiple alignments for their use in
764 phylogenetic analysis. *Molecular Biology and Evolution*, 17, 540–552.
765 <https://doi.org/10.1093/oxfordjournals.molbev.a026334>
- 766 Cernohorsky, W. O. (1975). The taxonomy of some West American and Atlantic Nassariidae based
767 on their type-specimens. *Records of the Auckland Institute and Museum*, 12, 121–173.
- 768 Cernohorsky, W. O. (1984). Systematics of the family Nassariidae (Mollusca: Gastropoda). *Bulletin*
769 *of the Auckland Institute and Museum*, 14, 1–356.
- 770 Chen, Z. Y., & Zhang, S. P. (2012). Molecular phylogeny of *Nassarius* (Gastropoda, Nassariidae)
771 based on 16s rRNA gene sequences. *Acta Zootaxonomica Sinica*, 37, 467–472.
- 772 Collin R. (2001). The effects of mode of development on phylogeography and population structure
773 of North Atlantic *Crepidula* (Gastropoda: Calyptraeidae). *Molecular Ecology*, 10, 2249–2262.
774 <https://doi.org/10.1046/j.1365-294x.2001.01372.x>

- 775 Collin, R. (2004). Phylogenetic effects, the loss of complex characters, and the evolution of
776 development in calyptraeid gastropods. *Evolution*, 58, 1488–1502.
777 <https://doi.org/10.1111/j.0014-3820.2004.tb01729.x>
- 778 Collin, R. (2012). Non-traditional life history choices: what can “intermediates” tell us about
779 evolutionary transitions between modes of invertebrate development? *Integrative and*
780 *Comparative Biology*, 52, 128–137. <https://doi.org/10.1093/icb/ics065>
- 781 Collin, R., & Moran, A. (2018). Evolutionary transitions in mode of development. In: T. J. Carrier,
782 A. M. Reitzel & A. Heyland (Eds.), *Evolutionary Ecology of Marine Invertebrate Larvae* (pp.
783 51–66). Oxford University Press. <https://doi.org/10.1093/oso/9780198786962.003.0004>
- 784 Cossmann, M. (1901). Essais de paléoconchologie comparée, 4. Paris (Cossmann): 293 pp., 10 pls.
- 785 Couceiro, L., López, L., Sotka, E. E., Ruiz, J. M., & Barreiro, R. (2012). Molecular data delineate
786 cryptic *Nassarius* species and characterize spatial genetic structure of *N. nitidus*. *Journal of the*
787 *Marine Biological Association of the UK*, 92, 1175–1182.
- 788 Crampton, J. S., Cooper, R. A., Beu, A. G., Foote, M., & Marshall, B. A. (2010). Biotic influences
789 on species duration: interactions between traits in marine molluscs. *Paleobiology*, 36, 204–223.
790 <https://doi.org/10.1666/09010.1>
- 791 Cunha, R.L., Castilho, R., Rüber, R. & Zardoya, R. (2005) Patterns of cladogenesis in the
792 venomous marine gastropod genus *Conus* from the Cape Verde Islands. *Systematic Biology*, 54,
793 634–650. <https://doi.org/10.1080/106351591007471>
- 794 Cunha, R. L., Grande, C., & Zardoya, R. (2009). Neogastropod phylogenetic relationships based on
795 entire mitochondrial genomes. *BMC Evolutionary Biology*, 9, 210.
796 <https://doi.org/10.1186/1471-2148-9-210>
- 797 Davis, K. E., Hill, J., Astrop, T. I., & Wills, M. A. (2016). Global cooling as a driver of
798 diversification in a major marine clade. *Nature Communications*, 7, 13003.
799 <https://doi.org/10.1038/ncomms13003>
- 800 Davies, R., Cartwright, J., Pike, J. & Line, C. (2001) Early Oligocene initiation of North Atlantic
801 deep water formation. *Nature*, 410, 917–920. <https://doi.org/10.1038/35073551>
- 802 Drummond, A., & Rambaut, A. (2007). BEAST: Bayesian evolutionary analysis by sampling trees.
803 *BMC Evolutionary Biology*, 7, 214. <https://doi.org/10.1186/1471-2148-7-214>

- 804 Duda, T. F., & Palumbi, S. R. (1999). Developmental shifts and species selection in gastropods.
805 *Proceedings of the National Academy of Sciences USA*, 96, 10272–10277.
806 <https://doi.org/10.1073/pnas.96.18.10272>
- 807 Felsenstein, J. (1981). Evolutionary trees from DNA sequences: a maximum likelihood approach.
808 *Journal of Molecular Evolution*, 17, 368–376. <https://doi.org/10.1007/BF01734359>
- 809 Filippelli, G. M., & Flores, J. A. (2009). From the warm Pliocene to the cold Pleistocene: A tale of
810 two oceans. *Geology*, 37, 959–960. <https://doi.org/10.1130/focus102009.1>
- 811 Fretter, V., Graham, A., & Andrews, E. (1986). The Prosobranch molluscs of Britain and Denmark.
812 Part 8 : Neogastropoda. *Journal of Molluscan Studies*, Suppl. 15, 435–556.
- 813 Galindo, L. A., Kool, H. H., & Dekker, H. (2017). Review of the *Nassarius pauper* (Gould, 1850)
814 complex (Gastropoda, Nassariidae). Part 3, reinstatement of the genus *Reticunassa*, with the
815 description of six new species. *European Journal of Taxonomy*, 275, 1–43.
816 <https://doi.org/10.5852/ejt.2017.275>
- 817 Galindo, L. A., Puillandre, N., Utge, J., Lozouet, P., & Bouchet, P. (2016). The phylogeny and
818 systematics of the Nassariidae revisited (Gastropoda, Buccinoidea). *Molecular Phylogenetics*
819 and Evolution, 99, 337–353. <https://doi.org/10.1016/j.ympev.2016.03.019>
- 820 Gili, C. (1992). *Nassarius martinelli* (Neogastropoda: Nassariidae) del Plioceno del Mediterráneo
821 occidental. *Revista Española de Paleontología*, 7, 167–173.
- 822 Gili, C., & Martinell, J. (1990). Aportación al conocimiento de subgénero *Sphaeronassa* (Locard,
823 Neogastropoda) del Plioceno del mediterráneo y del Atlántico adyacente. *Revista Española de*
824 *Paleontología*, 5, 19–33.
- 825 Gili, C., & Martinell, J. (1993). The distribution of Pliocene Nassariidae (Mollusca, Gastropoda)
826 from the Western Mediterranean: palaeoecological and historical considerations. *Mededelingen*
827 van de Werkgroep voor Tertiaire en Kwartaire Geologie, 30(1–2), 29–39.
- 828 Gili, C., & Martinell, J. (1994). Relationships between species longevity and larval ecology in
829 nassariid gastropods. *Lethaia*, 27, 291–299.
830 <https://doi.org/10.1111/j.1502-3931.1994.tb01577.x>
- 831 Gili, C., & Martinell, J. (1999). Revisión del género *Cyclope* Risso, 1826 (Gastropoda: Nassariidae)

- 832 en el Plioceno mediterráneo. *Revista Española de Paleontología*, 14, 149–158.
- 833 Gili, C., & Martinell, J. (2000). Phylogeny, speciation and species turnover. The case of the
834 Mediterranean gastropods of genus *Cyclope* Risso, 1826. *Lethaia*, 33, 236–250.
835 <https://doi.org/10.1080/00241160025100080>
- 836 Glawe, L. N., Anderson, J. F., & Bell, D. E. (2014). Late Paleocene examples of residual coloration
837 and embryonic features in juvenile marine mollusks from Northwest Louisiana. *Palaeontologia
838 Electronica*, 17, 30A.
- 839 Gofas, S. (2011). Familia Nassariidae. In: Moluscos marinos de Andalucía, vol. 1. (Gofas, S.,
840 Moreno, D., & Salas, C. Coords.). Servicio de Publicaciones e Intercambio Científico,
841 Universidad de Málaga, pp. 297–305.
- 842 Gofas, S., Luque, Á, Templado, J., & Salas, C. (2017). A national checklist of marine Mollusca in
843 Spanish waters. *Scientia Marina*, 81, 241-254
- 844 Goulding, M. Q., & Lambert, J. D. (2016). Mollusc models I. The snail *Ilyanassa*. *Current Opinion
845 in Genetics & Development*, 39, 168–174. <https://doi.org/10.1016/j.gde.2016.07.007>
- 846 Haasl, D. M. (2000). Phylogenetic relationships among nassariid gastropods. *Journal of
847 Paleontology*, 74, 839–852. <https://doi.org/10.1017/S0022336000033047>
- 848 Hamon, N., Sepulchre, P., Lefebvre, V., & Ramstein, G. (2013). The role of eastern Tethys seaway
849 closure in the Middle Miocene Climatic Transition (ca. 14 Ma). *Climate of the Past*, 9, 2687–
850 2702. <https://doi.org/10.5194/cp-9-2687-2013>
- 851 Hansen, T. A. (1980). Influence of larval dispersal and geographic distribution on species longevity
852 in neogastropods. *Paleobiology*, 6, 193–207. <https://doi.org/10.1017/S0094837300006758>
- 853 Harasewych, M. G. (1998). Family Nassariidae. In P. L. Beesley, G. J. B Ross & A. Wells (Eds.),
854 *Mollusca: the southern synthesis. Fauna of Australia* (pp. 829–831). Melbourne, CSIRO
855 Publishing.
- 856 Harzhauser, M., & Kowalke, T. (2004). Survey of the nassariid gastropods in the Neogene
857 Paratethys. *Archiv für Molluskenkunde*, 133(1–2), 1–63.
- 858 Harzhauser, M., Kroh, A., Mandic, O., Piller, W. E., Göhlich, U., Reuter, M., & Berning, B. (2007).
859 Biogeographic responses to geodynamics: a key study all around the Oligo–Miocene Tethyan

- 860 Seaway. *Zoologischer Anzeiger-A Journal of Comparative Zoology*, 246, 241–256.
861 <https://doi.org/10.1016/j.jcz.2007.05.001>
- 862 Hayashi, S. (2004). The molecular phylogeny of the Buccinidae (Caenogastropoda: Neogastropoda)
863 as inferred from the complete mitochondrial 16S rRNA gene sequences of selected
864 representatives. *Molluscan Research*, 25, 85–98.
- 865 Herbert, T. D., Lawrence, K. T., Tzanova, A., Peterson, L. C., Caballero-Gill, R., & Kelly, C. S.
866 (2016). Late Miocene global cooling and the rise of modern ecosystems. *Nature Geoscience*, 9,
867 843–847. <https://doi.org/10.1038/ngeo2813>
- 868 Ho, S. Y., & Phillips, M. J. (2009). Accounting for calibration uncertainty in phylogenetic
869 estimation of evolutionary divergence times. *Systematic Biology*, 58, 367-380.
- 870 Hodell, D. A., Curtis, J. H., Sierro, F. J., & Raymo, M. E. (2001). Correlation of late Miocene to
871 early Pliocene sequences between the Mediterranean and North Atlantic. *Paleoceanography*, 16,
872 164–178. <https://doi.org/10.1029/1999PA000487>
- 873 Hoenselaar, H.J., & Moolenbeek, R.G. (1988). The identity of *Nassarius vaucheri* (Pallary, 1906)
874 (Gastropoda Prosobranchia). *Basteria*, 52, 45–47.
- 875 Hou, Z., & Li, S. (2018). Tethyan changes shaped aquatic diversification. *Biological Reviews*, 93,
876 874–896. <https://doi.org/10.1111/brv.12376>
- 877 Huelsenbeck, J., & Ronquist, F. (2001). MrBayes: Bayesian inference of phylogenetic trees.
878 *Bioinformatics*, 17, 754–755.
- 879 Hwang, P. A., Tsai, Y.H., Deng, J.F., Cheng, C.A., Ho, P.H., & Hwang, D.F. (2005) Identification of
880 tetrodotoxin in a marine gastropod (*Nassarius glans*) responsible for human morbidity and
881 mortality in Taiwan. *Journal of Food Protection*, 68, 1696–1701.
882 <https://doi.org/10.4315/0362-028x-68.8.1696>
- 883 Iannotta, M. A., Toscano, F., & Patti, F. (2009). *Nassarius corniculus* (Olivi, 1792)
884 (Caenogastropoda: Nassariidae): a model of environmental complexity of Italian brackish and
885 marine habitats. *Marine Ecology*, 30, 106–115.
886 <https://doi.org/10.1111/j.1439-0485.2008.00263.x>
- 887 Jablonski, D. & Lutz, R. A. (1980) Molluscan larval shell morphology: ecological and
888 paleontological applications. In Rhoads, D.C. and Lutz, R.A. (eds) *Skeletal growth of aquatic*

- 889 organisms. New York: Plenum Press, pp. 323–377.
- 890 Jablonski, D. (1986). Larval ecology and macroevolution of marine invertebrates. *Bulletin of*
891 *Marine Sciences*, 39, 565–587.
- 892 Kalyaanamoorthy, S., Minh, B. Q., Wong, T. K. F., von Haeseler, A., & Jermiin, L. S. (2017).
893 ModelFinder: Fast model selection for accurate phylogenetic estimates. *Nature Methods*, 14,
894 587–589. <https://doi.org/10.1038/nmeth.4285>
- 895 Katoh, K., & Standley, D. M. (2013). MAFFT multiple sequence alignment software version 7:
896 improvements in performance and usability. *Molecular Biology and Evolution*, 30, 772–780.
897 <https://doi.org/10.1093/molbev/mst010>
- 898 Kearse, M., Moir, R., Wilson, A., Stones-Havas, S., Cheung, M., Sturrock, S., ... & Thierer, T.
899 (2012). Geneious Basic: an integrated and extendable desktop software platform for the
900 organization and analysis of sequence data. *Bioinformatics*, 28, 1647–1649.
901 <https://doi.org/10.1093/bioinformatics/bts199>
- 902 Kool, H. H., & Dekker, H. (2006). Review of the *Nassarius pauper* (Gould, 1850) complex
903 (Gastropoda, Nassariidae). Part. 1, with the description of four new species from the
904 Indo-West-Pacific. *Visaya*, 1, 56–77.
- 905 Kool, H. H., & Dekker, H. (2007). Review of the *Nassarius pauper* (Gould, 1850) complex
906 (Gastropoda, Nassariidae). Part 2, the Western Indian Ocean species, with the description of
907 two new species and introducing a nomen novum. *Visaya*, 2, 62–77.
- 908 Krijgsman, W., Hilgen, F. J., Raffi, I., Sierro, F. J., & Wilson, D. S. (1999). Chronology, causes and
909 progression of the Messinian salinity crisis. *Nature*, 400, 652–655.
910 <https://doi.org/10.1038/23231>
- 911 Landau, B., Marquet, R. & Grigis, M. (2003) The Early Pliocene Gastropoda (Mollusca) of
912 Estepona, Southern Spain. Part 1: Vetigastropoda. *Paleontos* 3, 1–87
- 913 Landau, B., da Silva, C. M., & Gili, C. (2009). The early Pliocene Gastropoda (Mollusca) of
914 Estepona, southern Spain, 8. Nassariidae. *Palaeontos*, 17, 1-101.
- 915 Lanfear, R., Frandsen, P. B., Wright, A. M., Senfeld, T., & Calcott, B. (2017). PartitionFinder 2:
916 new methods for selecting partitioned models of evolution for molecular and morphological

- 917 phylogenetic analyses. *Molecular Biology and Evolution*, 34, 772–773.
- 918 <https://doi.org/10.1093/molbev/msw260>
- 919 Laslett, D., & Canbäck, B. (2008). ARWEN: a program to detect tRNA genes in metazoan
- 920 mitochondrial nucleotide sequences. *Bioinformatics*, 24, 172–175.
- 921 <https://doi.org/10.1093/bioinformatics/btm573>
- 922 Lieberman, B. S., Allmon, W. D., & Eldredge, N. (1993). Levels of selection and
- 923 macroevolutionary patterns in the turritellid gastropods. *Paleobiology*, 19, 205–215.
- 924 Lozouet, P. (1999). Nouvelles espèces de gastéropodes (Mollusca: Gastropoda) de l’Oligocène et du
- 925 Miocène inférieur d’Aquitaine (Sud-Ouest de la France). Partie 2. *Cossmanniana*, 6, 1–68.
- 926 Lozouet, P., & Galindo, L. A. (2015). Resolution of the confused classification of some Miocene
- 927 Nassariidae, and reappraisal of their paleobiodiversity on the French Atlantic seaboard
- 928 (Gastropoda: Neogastropoda). *Archiv Für Molluskenkunde: International Journal of*
- 929 *Malacology*, 144, 31–50. <https://doi.org/10.1127/arch.moll/1869-0963/144/031-050>
- 930 Maddison, W. P., & Maddison, D. R. (2018). Mesquite: a modular system for evolutionary analysis.
- 931 Version 3.6. <http://www.mesquiteproject.org>
- 932 Manganelli, G., Spadini, V., & Martini, I. (2010) Rediscovery of an enigmatic Euro-Mediterranean
- 933 Pliocene nassariid species: *Nassarius crassiusculus* Bellardi, 1882 (Gastropoda: Nassariidae).
- 934 *Bollettino della Società Paleontologica Italiana*, 49, 195-202.
- 935 Miller, M., Pfeiffer, W., & Schwartz, T. (2010). Creating the CIPRES Science Gateway for
- 936 inference of large phylogenetic trees. Proceedings of the Gateway Computing Environments
- 937 Workshop (GCE), New Orleans, LA, pp. 1–8.
- 938 Modica, M.V., Gorson, J., Fedosov, A.E., Malcolm, G., Terryn, Y., Puillandre, N. & Holford, M.
- 939 (2020) Macroevolutionary analyses suggest that environmental factors, not venom apparatus,
- 940 play key role in Terebridae marine snail diversification. *Systematic Biology*, 69, 413–430.
- 941 <https://doi.org/10.1093/sysbio/syz059>
- 942 MolluscaBase (2020a) Nassariidae Iredale, 1916 (1835). Accessed through: *World Register of*
- 943 *Marine Species*. Retrieved from:

- 944 <http://www.marinespecies.org/aphia.php?p=taxdetails&id=151> Accessed 2020-04-10.
- 945 MolluscaBase (2020b). MolluscaBase. *Nassarius* Duméril, 1805. Accessed through: *World Register*
946 *of Marine Species*. Retrieved from:
947 <http://www.marinespecies.org/aphia.php?p=taxdetails&id=138235> on 2020-07-18
- 948 MolluscaBase (2020c). *Tritia* Risso, 1826. Accessed through: *World Register of Marine Species*.
949 Retrieved from: <http://www.marinespecies.org/aphia.php?p=taxdetails&id=246140> Accessed
950 2020-04-10.
- 951 Moreno, D. & Templado, J. (1994). The species complex “*Nassarius cuvierii* – *N. unifasciatus*”
952 (Gastropoda, Nassariidae) in the SE of Spain. *Iberus*, 12, 33–47.
- 953 Morton, B. (2011) Behaviour of *Nassarius bicallosus* (Caenogastropoda) on a northwestern Western
954 Australian surf beach with a review of feeding in the Nassariidae. *Molluscan Research*, 31,
955 89-94
- 956 Nekhaev, I. O. (2014). Marine shell-bearing Gastropoda of Murman (Barents Sea): an annotated
957 check-list. *Ruthenica*, 24, 75–121.
- 958 Nguyen, L. T., Schmidt, H. A., Von Haeseler, A., & Minh, B. Q. (2015). IQ-TREE: a fast and
959 effective stochastic algorithm for estimating maximum-likelihood phylogenies. *Molecular*
960 *Biology and Evolution*, 32, 268–274. <https://doi.org/10.1093/molbev/msu300>
- 961 Ojala, D., Montoya J., & Attardi, G. (1981) tRNA punctuation model of RNA processing in human
962 mitochondria. *Nature*, 290, 470–474.
- 963 Okay, A. I., Zattin, M., & Cavazza, W. (2010). Apatite fission-track data for the Miocene
964 Arabia-Eurasia collision. *Geology*, 38, 35–38. <https://doi.org/10.1130/G30234.1>
- 965 Oliverio, M. (1996). Contrasting developmental strategies and speciation in NE Atlantic
966 prosobranchs: a preliminary analysis. *Origin and Evolutionary Radiation of the Mollusca*, 22,
967 261–266.
- 968 Osca, D., Templado, J., & Zardoya, R. (2015). Caenogastropod mitogenomics. *Molecular*
969 *Phylogenetics and Evolution*, 93, 118–128. <https://doi.org/10.1016/j.ympev.2015.07.011>
- 970 Ozawa, T., Köhler, F., Reid, D. G., & Glaubrecht, M. (2009). Tethyan relicts on continental

- 971 coastlines of the northwestern Pacific Ocean and Australasia: molecular phylogeny and fossil
972 record of batillariid gastropods (Caenogastropoda, Cerithioidea). *Zoologica Scripta*, 38, 503–
973 525. <https://doi.org/10.1111/j.1463-6409.2009.00390.x>
- 974 Pallary, P. (1906). Diagnoses de nouvelles coquilles du Maroc. Oran, privately printed 3 pp.
- 975 Patarnello, T., Volckaert, F. A., & Castilho, R. (2007). Pillars of Hercules: is the Atlantic–
976 Mediterranean transition a phylogeographical break? *Molecular ecology*, 16, 4426–4444.
977 <https://doi.org/10.1111/j.1365-294X.2007.03477.x>
- 978 Ponder, W. F., & Lindberg, D. R. (1997). Towards a phylogeny of gastropod molluscs: an analysis
979 using morphological characters. *Zoological Journal of the Linnean Society*, 119, 83–265.
980 <https://doi.org/10.1111/j.1096-3642.1997.tb00137.x>
- 981 Ponder, W. F., & Lindberg, D. R. (2019). *Biology and evolution of the Mollusca*. Boca Raton, FL.
982 CRC press.
- 983 Pu, C., Li, H., Zhu, A., Chen, Y., Zhao, Y., & Zhan, A. (2017). Phylogeography in *Nassarius* mud
984 snails: Complex patterns in congeneric species. *PLoS ONE*, 12,
985 e0180728. <https://doi.org/10.1371/journal.pone.0180728>
- 986 Reid, D. G., Rumbak, E., & Thomas, R. H. (1996). DNA, morphology and fossils: phylogeny and
987 evolutionary rates of the gastropod genus *Littorina*. *Philosophical Transactions of the Royal
988 Society of London B*, 351, 877–895. <https://doi.org/10.1098/rstb.1996.0082>
- 989 Rodríguez-Flores, P.C., Buckley, D., MacPherson, E., Corbari, L., & Machordom, A. (2020)
990 Deep-sea squat lobster biogeography (Munidopsidae: Leiogalathea) unveils Tethyan vicariance
991 and evolutionary patterns shared by shallow-water relatives. *Zoologica Scripta*, 49, 340–356.
992 <https://doi.org/10.1111/zsc.12414>
- 993 Rolán E. (1984). Descripción de una nueva especie del género *Hinia* Leach in Gray, 1847 (Mollusca,
994 Gastropoda) procedente del Archipiélago de Cabo Verde. *Bulletin Malacológico* 29, 167–174.
- 995 Rolán E., Luque, A.A. (1994). *Nassarius reticulatus* (Linnaeus, 1758) y *Nassarius nitidus* (Jeffreys,
996 1867) (Gastropoda, Nassariidae), dos especies válidas de los mares de Europa. *Iberus*, 12, 59–
997 76.

- 998 Rolán, E., & Hernandez, J. M. (2005). The West African species of the group *Nassarius*
999 *denticulatus* (Mollusca, Neogastropoda), with the description of a new species. *Journal of*
1000 *Conchology*, 38, 499–511.
- 1001 Ronquist, F., & Huelsenbeck, J. P. (2003). MrBayes 3: Bayesian phylogenetic inference under
1002 mixed models. *Bioinformatics*, 19, 1572–1574. <https://doi.org/10.1093/bioinformatics/btg180>
- 1003 Rosenberg, G. (2009). Malacolog 4.1.1: a database of Western Atlantic marine Mollusca. [www
1004 database (version 4.1.1)]. <http://www.malacolog.org/>.
- 1005 Roux, C., Fraisse, C., Romiguier, J., Anciaux, Y., Galtier, N., & Bierne, N. (2016). Shedding light
1006 on the grey zone of speciation along a continuum of genomic divergence. *PLoS biology*, 14,
1007 e2000234. <https://doi.org/10.1371/journal.pbio.2000234>
- 1008 Schattner, P., Brooks, A. N., & Lowe, T. M. (2005). The tRNAscan-SE, snoScan and snoGPS web
1009 servers for the detection of tRNAs and snoRNAs. *Nucleic Acids Research*, 33, W686-W689.
1010 <https://doi.org/10.1093/nar/gki366>
- 1011 Schmieder, R., & Edwards, R. (2011). Quality control and preprocessing of metagenomic datasets.
1012 *Bioinformatics*, 27, 863–864. <https://doi.org/10.1093/bioinformatics/btr026>
- 1013 Schwarz, G. (1978). Estimating the dimension of a model. *The Annals of Statistics*, 6, 461–464.
- 1014 Shank, A.L. 2009. Pelagic larval duration and dispersal distance revisited. *Biological Bulletin*, 216,
1015 373–385.
- 1016 Shuto, T. (1974). Larval ecology of prosobranch gastropods and its bearing on biogeography and
1017 paleontology. *Lethaia*, 7, 239–256.
- 1018 Simison, W. B., Lindberg, D. R., & Boore, J. L. (2006). Rolling circle amplification of metazoan
1019 mitochondrial genomes. *Molecular Phylogenetics and Evolution*, 39, 562–567.
1020 <https://doi.org/10.1016/j.ympev.2005.11.006>
- 1021 Simone, L. R. L., & Pastorino, G. (2014). Comparative Morphology of *Dorsanum miran* and *Bullia*
1022 *granulosa* from Morocco (Mollusca: Caenogastropoda: Nassariidae). *African Invertebrates*, 55,
1023 125–142. <https://doi.org/10.5733/afin.055.0107>
- 1024 Strathmann, R. R. (1978). The evolution and loss of feeding larval stages of marine invertebrates.

- 1025 *Evolution*, 32, 894–906. <https://doi.org/10.2307/2407502>
- 1026 Strong, E. E., Galindo, L. A., & Kantor, Y. I. (2017). Quid est *Clea helena*? Evidence for a
1027 previously unrecognized radiation of assassin snails (Gastropoda: Buccinoidea: Nassariidae).
1028 *PeerJ*, 5, e3638. <https://doi.org/10.7717/peerj.3638>
- 1029 Taylor, J. D., Morris, N. J., & Taylor, C. N. (1980). Food specialization and the evolution of
1030 predatory prosobranch gastropods. *Palaentology*, 23, 375–409.
- 1031 Thorson, G. (1950). Reproductive and larval ecology of marine bottom invertebrates. *Biological
1032 Reviews*, 25, 1–45.
- 1033 Tracey, S., Todd, J. A., & Erwin, D. H. (1993). Mollusca: Gastropoda. In M. J. Benton (Ed.). *The
1034 Fossil Record 2* (pp. 131–167). London, Chapman & hall.
- 1035 Uribe, J. E., Puillandre, N., & Zardoya, R. (2017). Beyond *Conus*: phylogenetic relationships of
1036 Conidae based on complete mitochondrial genomes. *Molecular Phylogenetics and Evolution*,
1037 107, 142–151. <https://doi.org/10.1016/j.ympev.2016.10.008>
- 1038 Uribe, J.E., Williams, S. T., Templado, J., Buge, B. & Zardoya, R. (2017b) Phylogenetic
1039 relationships of Mediterranean and North-East Atlantic Cantharidinae and notes on
1040 Stomatellinae (Vetigastropoda: Trochidae). *Molecular Phylogenetics and Evolution*, 107, 64–
1041 79. <https://doi.org/10.1016/j.ympev.2016.10.009>.
- 1042 Van Dingenen F, Ceulemans L, Landau M & da Silva C M. (2015).The family Nassariidae from the
1043 late Neogene of northwestern France. *Cainozoic Research*, 15(1-2), 75-122.
- 1044 Xia, X. (2013). DAMBE5: A comprehensive software package for data analysis in molecular
1045 biology and evolution. *Molecular Biology and Evolution*, 30, 1720–1728.
1046 <https://doi.org/10.1093/molbev/mst064>
- 1047 Yang, Y., Li, Q., Kong, L., & Yu, H. (2018). Comparative mitogenomic analysis reveals cryptic
1048 species in *Reticunassa festiva* (Neogastropoda: Nassariidae). *Gene*, 662, 88–96.
1049 <https://doi.org/10.1016/j.gene.2018.04.001>
- 1050 Yang, Y., Li, Q., Kong, L., & Yu, H. (2019). Mitogenomic phylogeny of *Nassarius* (Gastropoda:
1051 Neogastropoda). *Zoologica Scripta*, 48, 302–312. <https://doi.org/10.1111/zsc.12343>

- 1052 Yang, Y., Liu, H., Qi, L., Kong, L., & Li, Q. (2020). Complete Mitochondrial Genomes of Two
1053 Toxin-Accumulated Nassariids (Neogastropoda: Nassariidae: *Nassarius*) and Their Implication
1054 for Phylogeny. *International Journal of Molecular Sciences*, 21, 3545.
1055 <https://doi.org/10.3390/ijms21103545>
- 1056 Zachos, J. C., Shackleton, N.J., Revenaugh, J.S., Pälike, H. & Flower, B. P. (2001), Climate
1057 response to orbital forcing across the Oligocene–Miocene boundary. *Science*, 292, 274– 278.
1058 <https://doi.org/10.1126/science.1058288>
- 1059 Zhang, A. J., & You, Z. J. (2009). Molecular phylogenetic relationships of some species of
1060 *Nassarius* (Gastropoda, Prosobranchia, Neogastropoda, Nassariidae) based on 16S rRNA
1061 fragment sequence. *Acta Zootaxonomica Sinica*, 33, 549–552.

1062 **Figure captions**

1063

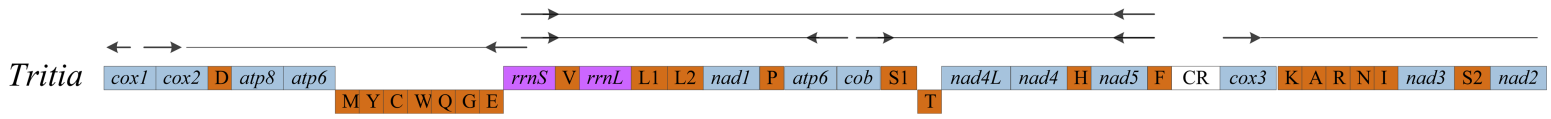
1064 Figure 1. Gene order of *Tritia* mitogenomes. All newly sequenced mt genomes shared identical
1065 genome organization. The genes encoded in the major and minor strands are shown in the
1066 top and bottom rows, respectively. Genes encoding for proteins (blue), rRNAs (pink), and
1067 tRNAs (red) are depicted with different colors. The relative positions of the primers for
1068 long PCR are shown.

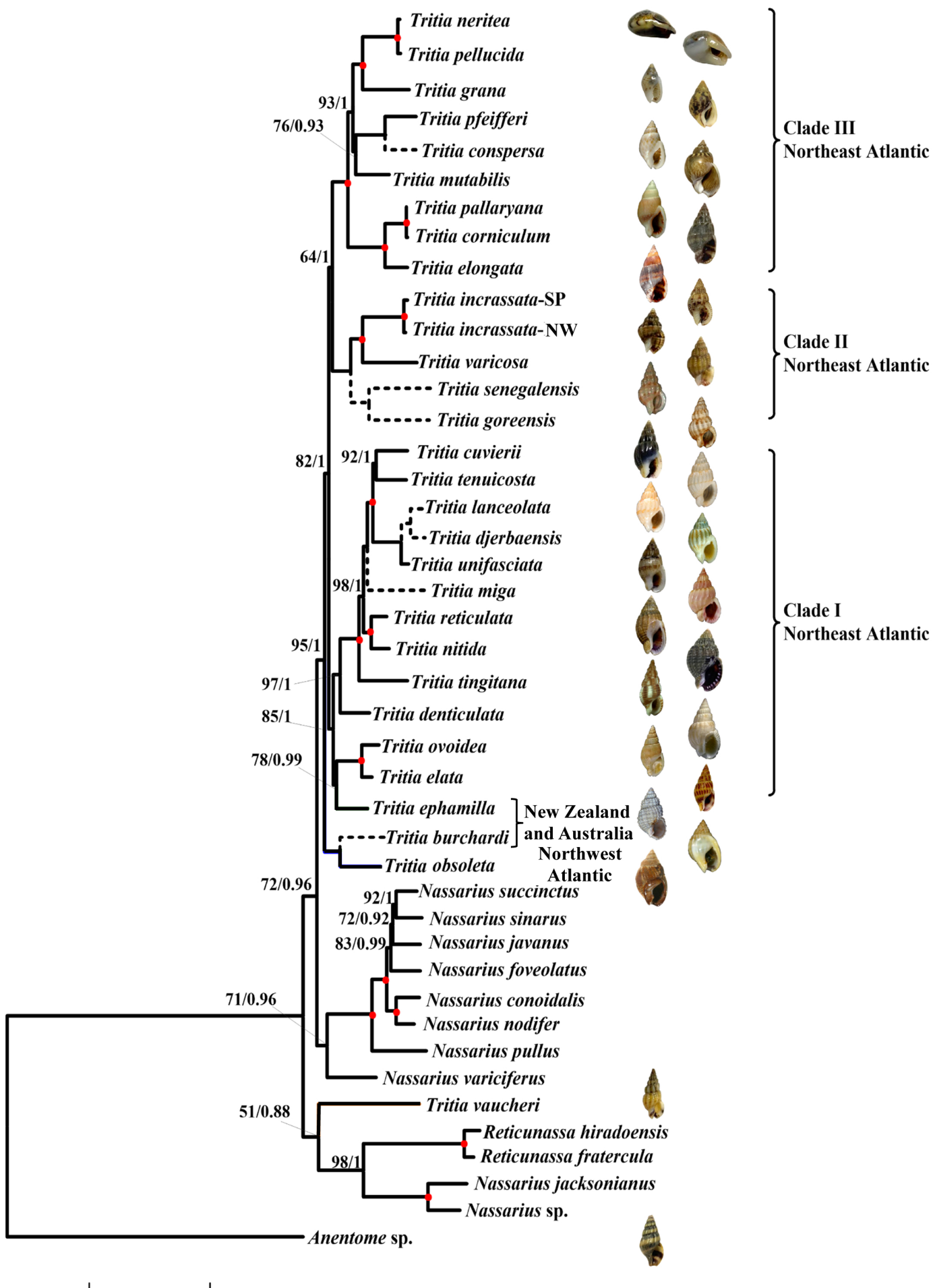
1069 Figure 2. Phylogenetic relationships within Nassariinae based on the nucleotide sequences of 13
1070 protein-coding genes plus two rRNA genes. The Bayesian inference (BI) phylogram is
1071 shown. The non-nassariinae *Anentome* sp. was used as outgroup. The three Northeast
1072 clades are indicated. Numbers at nodes are statistical support values for ML (bootstrap
1073 proportions in percentage)/BI (posterior probabilities). Solid red circles represent nodes
1074 with maximum support values. The bar indicates substitutions per site. Additional *Tritia*
1075 species whose relative phylogenetic positions were resolved in Galindo et al. (2016) but
1076 were not included in this study are shown with a dashed line. Ventral images of the
1077 voucher specimens are shown.

1078 Figure 3. Ancestral character state reconstruction of *Tritia* protoconch (paucispiral *versus*
1079 multispiral) using the ML model Mk1 in Mesquite. Pie charts represent the statistical
1080 support at every node.

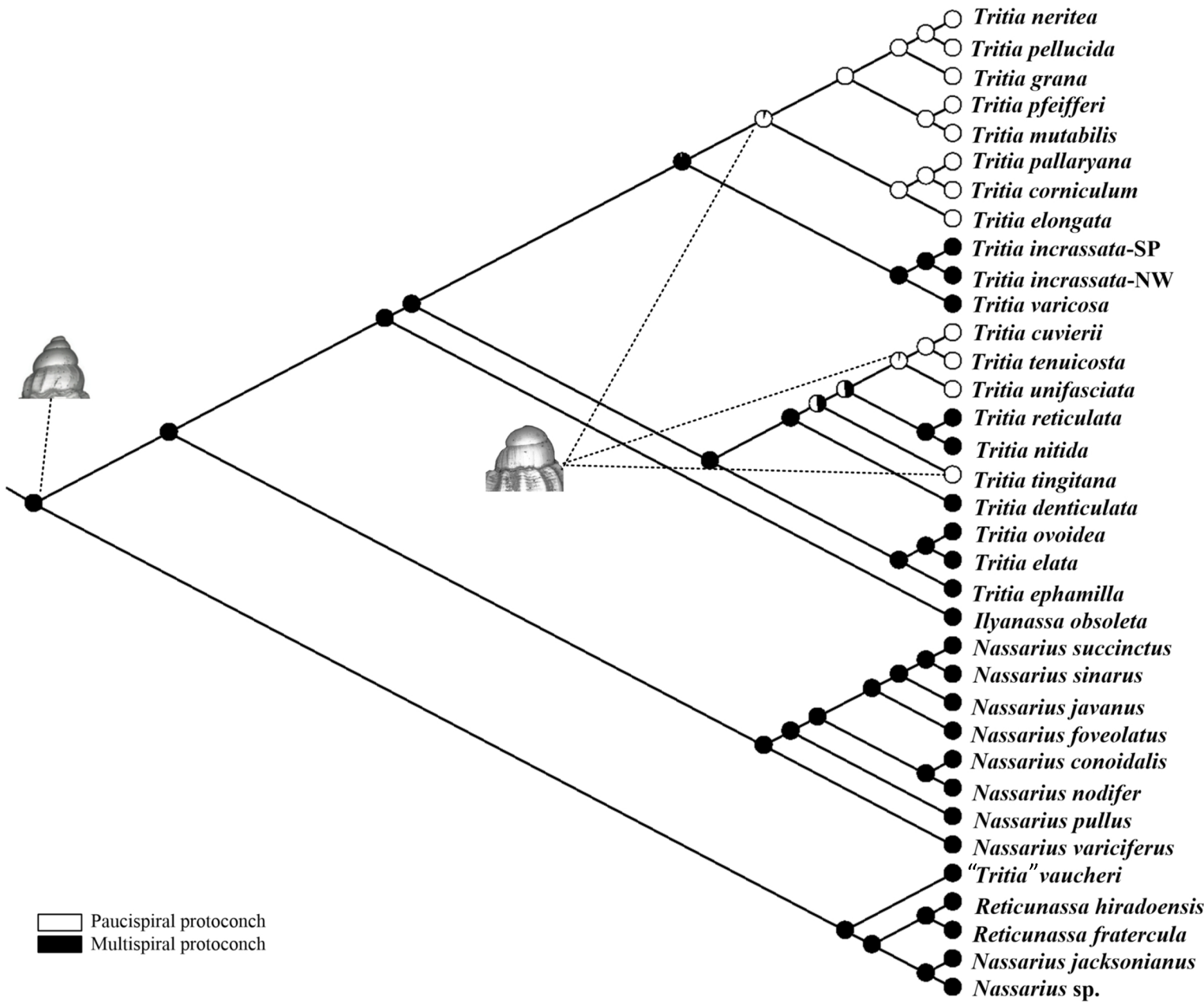
1081 Figure 4. Chronogram with age estimates of major divergence events within Nassariinae based on
1082 the nucleotide sequences of the concatenated mitochondrial protein coding genes, and
1083 using Bayesian relaxed dating methods (BEAST). Horizontal bars represent 95% credible
1084 intervals of relevant nodes, and calibration constraints are indicated with an asterisk on
1085 the corresponding nodes. Dates (and highest posterior density intervals, HPD) are in
1086 millions of years. Geological epochs are indicated.

1087





1



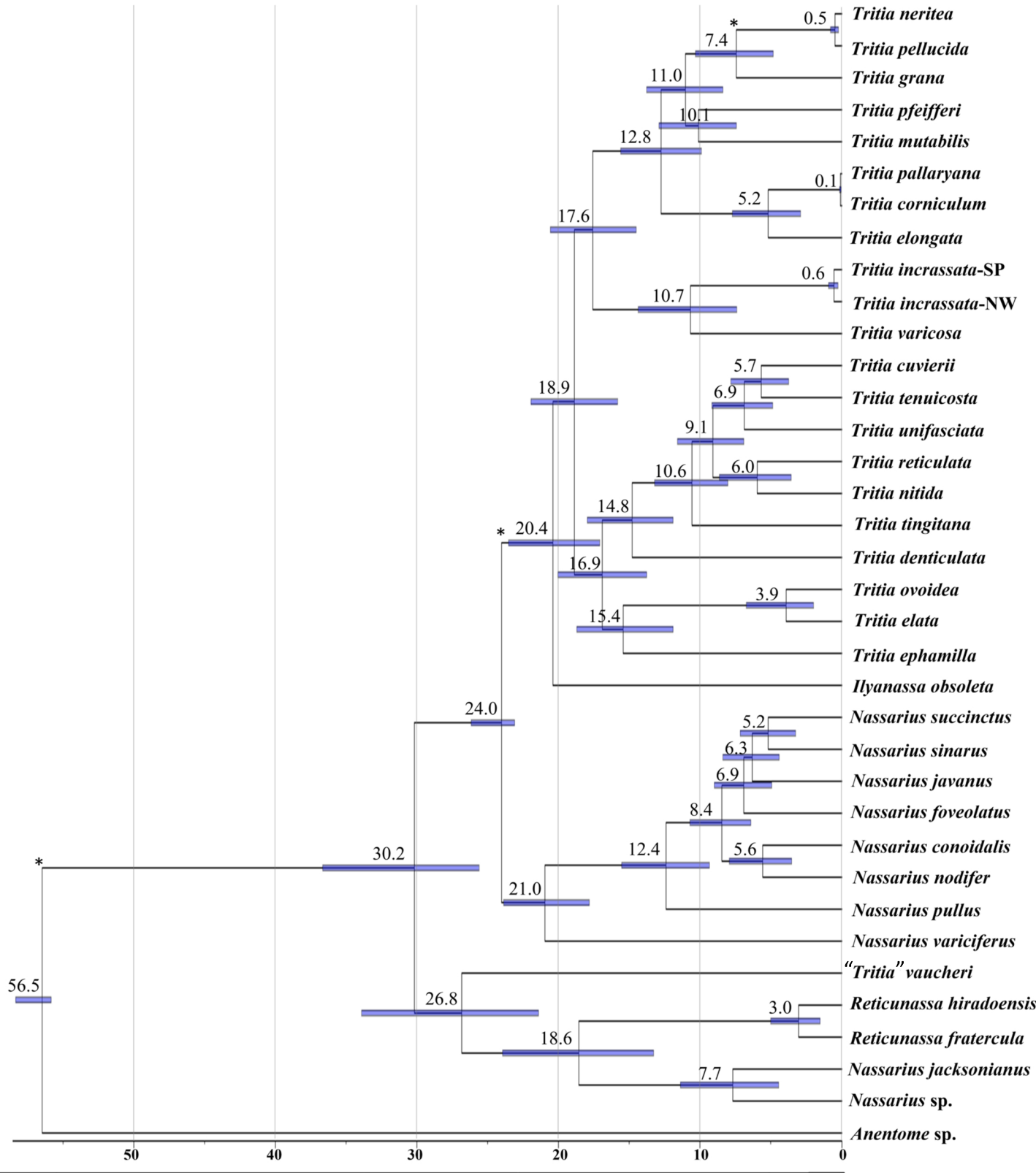


Table 1. Mitochondrial (mt) genomes analyzed in this study.

New mt genomes							
Species	Location	Collector	No. reads	Coverage (x)	Length (bp)	Genbank Acc. No.	Voucher
<i>Tritia corniculum</i>	Ilha da Armona, Portugal	CLMA	34 502	75	15 114	MT755650	MNCN:ADN: 118970
<i>Tritia cuvierii</i>	Cabo de Palos, Spain	JT	36 582	306	15 185	MT755651	MNCN:ADN: 118971
<i>Tritia grana</i>	Cabo de Palos, Spain	JT	40 296	131	15 198	MT762151	MNCN:ADN: 118972
<i>Tritia incrassata</i> -SP	Cabo de Palos, Spain	JT	30 800	53	15 159	MT762153	MNCN:ADN: 118973
<i>Tritia incrassata</i> -NW	Bergen, Norway	David Osca	38 716	151	15 170	MT762152	MNCN:ADN: 118974
<i>Tritia mutabilis</i>	Market, Madrid, Spain	YY	40 182	250	15 148	MT762154	MNCN:ADN: 118975
<i>Tritia neritea</i>	Vigo, Spain	SA	35 082	216	15 179	MT762155	MNCN:ADN: 118976
<i>Tritia pellucida</i>	Mar Menor, Spain	JT	40 234	317	15 175	MT768039	MNCN:ADN: 118977
<i>Tritia pfeifferi</i>	Praia dos Cavacos, Portugal	CLMA	43 804	76	15 142	MT768040	MNCN:ADN: 118978
<i>Tritia unifasciata</i>	Mar Menor, Spain	JT	43 288	322	15 168	MT768043	MNCN:ADN: 118979
<i>Tritia vaucheri</i>	Isla Canela, Spain	CLMA	58 170	83	15 153	MT768044	MNCN:ADN: 118980
<i>Tritia denticulata</i>	Candelaria, Spain	—	2 142 656	19 059	15 167	MT755652	MNHN-IM-2009-21546
<i>Tritia ephamilla</i>	Kermadec Ridge, New Zealand	—	1 849 562	14 802	15 157	MT755654	MNHN-IM-2009-24014
<i>Tritia pallaryana</i>	Golfe de Gabès, Tunisie	Chrifa Aissaoui	2 515 502	21 974	15 144	MT762157	MNHN-IM-2009-30939
<i>Tritia tenuicosta</i>	Golfe de Gabès, Tunisie	Chrifa Aissaoui	2 494 246	19 378	15 169	MT768042	MNHN-IM-2013-31865
<i>Tritia elongata</i>	Errimel, Tunisie	Chrifa Aissaoui	2 133 232	18 698	15 145	MT755653	MNHN-IM-2013-32570
<i>Tritia nitida</i>	Vigo, Spain	Samuel Abalde	2 415 740	21 498	15 157	MT762156	MNCN:ADN: 118981
<i>Tritia varicosa</i>	Ponta da Piedade, Portugal	CLMA	2 765 768	23 350	15 142	MT768041	MNCN:ADN: 118982
<i>Tritie elata</i>	Ponta da Piedade, Portugal	CLMA	2 493 798	21 897	15 167	MT768045	MNCN:ADN: 118983
<i>Tritia tingitana</i>	Isla de Tarifa, Spain	Serge Gofas	—	—	13 337	MW194096	MNCN:ADN: 118984
<i>Tritia ovoidea</i>	Cañón de Carchuna, Spain	Serge Gofas	—	—	14 889	MW194095	MNCN:ADN: 118985
<i>Anentome</i> sp.	Aquarium market, Madrid, Spain	YY	2 528 802	19 514	15 069	MT755649	MNCN:ADN: 118986

Genbank mt genomes

Species	Length (bp)	Accession No.	Reference
<i>Tritia obsoleta</i>	15 263	DQ238598	Simison, Lindberg, & Boore, 2006
<i>Tritia reticulata</i>	15 271	EU827201	Cunha, Grande, & Zardoya, 2009
<i>Nassarius variciferus</i>	15 269	KM603509	Yang, Li, Kong, & Yu, 2018
<i>Nassarius succinctus</i>	15 329	KT768016	Yang, Li, Kong, & Yu, 2019
<i>Nassarius nodifer</i>	15 337	KT818617	Yang, Li, Kong, & Yu, 2019
<i>Nassarius conoidalis</i>	15 332	KT826694	Yang, Li, Kong, & Yu, 2019
<i>Nassarius pullus</i>	15 278	KT900947	Yang, Li, Kong, & Yu, 2019
<i>Nassarius sinarus</i>	15 325	MH346208	Yang, Li, Kong, & Yu, 2019
<i>Nassarius foveolatus</i>	15 343	MH346209	Yang, Li, Kong, & Yu, 2019
<i>Nassarius javanus</i>	15 325	MH346210	Yang, Li, Kong, & Yu, 2019
<i>Reticunassa fratercula</i>	15 174	KT826695	Yang, Li, Kong, & Yu, 2018
<i>Reticunassa hiradoensis</i>	15 194	MG744569	Yang, Li, Kong, & Yu, 2018
<i>Nassarius jacksonianus</i>	15 234	MH346212	Yang, Li, Kong, & Yu, 2019
<i>Nassarius</i> sp.	15 240	MH346211	Yang, Li, Kong, & Yu, 2019

Table S1. Standard and Long PCR primers for *Tritia* mitogenomes.

<i>Tritia corniculum</i>	Sequenced by Allgenetics, with a buccinoid species in the same library	
Long PCR		
Primer	Sequence 5'-3'	Fragment (bp)
cox1laF	AAYATRCGATGACGAGGRATRCARTTTGA	<i>cox1-rrnS</i> (4K)
12SlaR	ATAGGCTGCACCTTGATCTGACGTYTT	
12SlaF	CAGTTTGTATAACCGTCGTCGTCAAGGT	<i>rrnS-cob</i> (4.5K)
cobra2R	GGRTTAGCWGGRATAAARTTYTCWGGRTC	
cobra2F	CCYTGAGGTCARATATCYTTYGAGGRGC	<i>cob-trnF</i> (4.3K)
trnF-R	CACCCTAGCATCTCAGTGCTATGCTCT	
cox3la2F	ATGGCRCGNAATCCTTTCATTAGTWGARTT	<i>cox3-cox1</i> (2.5K)
cox1laR	CGAGGAAAAGCYATRTCAGGAGC	
Primer Link <i>cox1</i>		
Primer	Sequence 5'-3'	Fragment (bp)
COI-tritiaF	ACWGCYCAYGCTTYGTAATAAT	<i>cox1</i> (400)
COI-tritiaR	TGYATNCCTCGTCATCGYATRTT	
<i>Tritia cuvierii</i>	Sequenced by Allgenetics, in a whole library	
Long PCR		
Primer	Sequence 5'-3'	Fragment (bp)
cox1laF	AAYATRCGATGACGAGGRATRCARTTTGA	<i>cox1-rrnS</i> (4K)
12SlaR	ATAGGCTGCACCTTGATCTGACGTYTT	
12SlaF	CAGTTTGTATAACCGTCGTCGTCAAGGT	<i>rrnS-cob</i> (4.5K)
cobra2R	GGRTTAGCWGGRATAAARTTYTCWGGRTC	
cobra2F	CCYTGAGGTCARATATCYTTYGAGGRGC	<i>cob-trnF</i> (4.3K)
trnF-R	CACCCTAGCATCTCAGTGCTATGCTCT	
cox3la2F	ATGGCRCGNAATCCTTTCATTAGTWGARTT	<i>cox3-cox1</i> (2.5K)
cox1laR	CGAGGAAAAGCYATRTCAGGAGC	
Primer Link <i>cox1</i>		
Primer	Sequence 5'-3'	Fragment (bp)
LCO1490 F	GGTCAACAAATCATAAAGATATTGG	<i>cox1</i> (709)
HCO2198 R	TTAACCTCAGGGTGACCAAAAAATCA	
<i>Tritia grana</i>	Sequenced by Allgenetics, with a cone species in the same library	
Long PCR		
Primer	Sequence 5'-3'	Fragment (bp)
cox1laF	AAYATRCGATGACGAGGRATRCARTTTGA	<i>cox1-rrnS</i> (4K)
12SlaR	ATAGGCTGCACCTTGATCTGACGTYTT	
12SlaF	CAGTTTGTATAACCGTCGTCGTCAAGGT	<i>rrnS-cob</i> (4.5K)
cobra2R	GGRTTAGCWGGRATAAARTTYTCWGGRTC	
cobra2F	CCYTGAGGTCARATATCYTTYGAGGRGC	<i>cob-trnF</i> (4.3K)
trnF-R	CACCCTAGCATCTCAGTGCTATGCTCT	

cox3la2F	ATGGCRCGNAATCCTTTCATTAGTWGARTT	<i>cox3-cox1</i> (2.5K)
cox1laR	CGAGGAAAAGCYATRTCAGGAGC	

Primer Link *cox1*

Primer	Sequence 5'-3'	Fragment (bp)
LCO1490 F	GGTCAACAAATCATAAAGATATTGG	<i>cox1</i> (709)
HCO2198 R	TTAACTTCAGGGTGACCAAAAAATCA	

Tritia incrassata-sp Sequenced by Allgenetics, with a cone species in the same library

Long PCR

Primer	Sequence 5'-3'	Fragment (bp)
cox1laF	AAYATRCGATGACGAGGRATRCARTTTGA	<i>cox1-rnS</i> (4K)
12SlaR	ATAGGCTGCACCTTGATCTGACGTYTT	
12SlaF	CAGTTTGTATAACCGTCTCGTCAGGT	<i>rnS-cob</i> (4.5K)
cobra2R	GGRTTAGCWGGRATAAARTTYTCWGGRTC	
cobra2F	CCYTGAGGTCARATATCYTTYGAGGRGC	<i>cob-trnF</i> (4.3K)
trnF-R	CACCCTAGCATCTTCAGTGCTATGCTCT	
cox3la2F	ATGGCRCGNAATCCTTTCATTAGTWGARTT	<i>cox3-cox1</i> (2.5K)
cox1laR	CGAGGAAAAGCYATRTCAGGAGC	

Primer Link *cox1*

Primer	Sequence 5'-3'	Fragment (bp)
COINassaF	TCTACAAATCATAAAGACATTGG	<i>cox1</i> (700)
COINassaR	ACYTCAGGATGACCAAARAATCA	

Tritia incrassata-nw Sequenced by Allgenetics, in a whole library

Long PCR

Primer	Sequence 5'-3'	Fragment (bp)
cox1laF	AAYATRCGATGACGAGGRATRCARTTTGA	<i>cox1-rnS</i> (4K)
12SlaR	ATAGGCTGCACCTTGATCTGACGTYTT	
12SlaF	CAGTTTGTATAACCGTCTCGTCAGGT	<i>rnS-cob</i> (4.5K)
cobra2R	GGRTTAGCWGGRATAAARTTYTCWGGRTC	
cobra2F	CCYTGAGGTCARATATCYTTYGAGGRGC	<i>cob-trnF</i> (4.3K)
trnF-R	CACCCTAGCATCTTCAGTGCTATGCTCT	
cox3la2F	ATGGCRCGNAATCCTTTCATTAGTWGARTT	<i>cox3-cox1</i> (2.5K)
cox1laR	CGAGGAAAAGCYATRTCAGGAGC	

Primer Link *cox1*

Primer	Sequence 5'-3'	Fragment (bp)
COINassaF	TCTACAAATCATAAAGACATTGG	<i>cox1</i> (700)
COINassaR	ACYTCAGGATGACCAAARAATCA	

Tritia mutabilis Sequenced by Allgenetics, in a whole library

Long PCR

Primer	Sequence 5'-3'	Fragment (bp)
cox1laF	AAYATRCGATGACGAGGRATRCARTTTGA	<i>cox1-rnS</i> (4K)
12SlaR	ATAGGCTGCACCTTGATCTGACGTYTT	

12SlaF	CAGTTTGTATAACCGTCGTCGTCAAGGT	<i>rrnS-cob</i> (4.5K)
cobra2R	GGRTTAGCWGGRATAAARTTYTCWGGRTC	
cobra2F	CCYTGAGGTCARATATCYTTYTGAGGRGC	<i>cob-trnF</i> (4.3K)
trnF-R	CACCCTAGCATCTCAGTGTATGCTCT	
cox3la2F	ATGGCRCGNAATCCTTTCATTAGTWGARTT	<i>cox3-cox1</i> (2.5K)
cox1laR	CGAGGAAAAGCYATRTCAGGAGC	

Primer Link *cox1*

Primer	Sequence 5'-3'	Fragment (bp)
COINassaF	TCTACAAATCATAAAGACATTGG	<i>cox1</i> (700)
COINassaR	ACYTCAGGATGACCAAARAATCA	

Tritia neritea Sequenced by Allgenetics, in a whole library

Long PCR

Primer	Sequence 5'-3'	Fragment (bp)
cox1laF	AAYATRCGATGACGAGGRATRCARTTTGA	<i>cox1-rrnS</i> (4K)
12SlaR	ATAGGCTGCACCTTGATCTGACGTYTT	
12SlaF	CAGTTTGTATAACCGTCGTCGTCAAGGT	<i>rrnS-cob</i> (4.5K)
cobra2R	GGRTTAGCWGGRATAAARTTYTCWGGRTC	
cobra2F	CCYTGAGGTCARATATCYTTYTGAGGRGC	<i>cob-trnF</i> (4.3K)
trnF-R	CACCCTAGCATCTCAGTGTATGCTCT	
cox3la2F	ATGGCRCGNAATCCTTTCATTAGTWGARTT	<i>cox3-cox1</i> (2.5K)
cox1laR	CGAGGAAAAGCYATRTCAGGAGC	

Primer Link *cox1*

Primer	Sequence 5'-3'	Fragment (bp)
LCO1490 F	GGTCAACAAATCATAAAGATATTGG	<i>cox1</i> (709)
HCO2198 R	TTAACCTCAGGGTGACCAAAAAATCA	

Tritia pellucida Sequenced by Allgenetics, in a whole library

Long PCR

Primer	Sequence 5'-3'	Fragment (bp)
cox1laF	AAYATRCGATGACGAGGRATRCARTTTGA	<i>cox1-rrnS</i> (4K)
12SlaR	ATAGGCTGCACCTTGATCTGACGTYTT	
12SlaF	CAGTTTGTATAACCGTCGTCGTCAAGGT	<i>rrnS-cob</i> (4.5K)
cobra2R	GGRTTAGCWGGRATAAARTTYTCWGGRTC	
cobra2F	CCYTGAGGTCARATATCYTTYTGAGGRGC	<i>cob-trnF</i> (4.3K)
trnF-R	CACCCTAGCATCTCAGTGTATGCTCT	
cox3la2F	ATGGCRCGNAATCCTTTCATTAGTWGARTT	<i>cox3-cox1</i> (2.5K)
cox1laR	CGAGGAAAAGCYATRTCAGGAGC	

Primer Link *cox1*

Primer	Sequence 5'-3'	Fragment (bp)
LCO1490 F	GGTCAACAAATCATAAAGATATTGG	<i>cox1</i> (709)
HCO2198 R	TTAACCTCAGGGTGACCAAAAAATCA	

Tritia pfeifferi Sequenced by Allgenetics, with a buccinoid species in the same library

Long PCR		
Primer	Sequence 5'-3'	Fragment (bp)
cox1laF	AAYATRCGATGACGAGGRATRCARTTTGA	<i>cox1-rrnS</i> (4K)
12SlaR	ATAGGCTGCACCTTGATCTGACGTYTT	
12SlaF	CAGTTTGTATAACCGTCGTCGTCAAGGT	<i>rrnS-cob</i> (4.5K)
cobra2R	GGRTTAGCWGGRATAAARTTYTCWGGRTC	
cobra2F	CCYTGAGGTCARATATCYTTYTGAGGRGC	<i>cob-trnF</i> (4.3K)
trnF-R	CACCCTAGCATCTTCAGTGCTATGCTCT	
cox3la2F	ATGGCRCGNAATCCTTTCATTAGTWGARTT	<i>cox3-cox1</i> (2.5K)
cox1laR	CGAGGAAAAGCYATRTCAGGAGC	
Primer Link <i>cox1</i>		
Primer	Sequence 5'-3'	Fragment (bp)
COINassaF	TCTACAAATCATAAAGACATTGG	<i>cox1</i> (700)
COINassaR	ACYTCAGGATGACCAAARAATCA	
<i>Tritia unifascita</i>	Sequenced by Allgenetics, in a whole library	
Long PCR		
Primer	Sequence 5'-3'	Fragment (bp)
cox1laF	AAYATRCGATGACGAGGRATRCARTTTGA	<i>cox1-rrnS</i> (4K)
12SlaR	ATAGGCTGCACCTTGATCTGACGTYTT	
12SlaF	CAGTTTGTATAACCGTCGTCGTCAAGGT	<i>rrnS-cob</i> (4.5K)
cobra2R	GGRTTAGCWGGRATAAARTTYTCWGGRTC	
cobra2F	CCYTGAGGTCARATATCYTTYTGAGGRGC	<i>cob-trnF</i> (4.3K)
trnF-R	CACCCTAGCATCTTCAGTGCTATGCTCT	
cox3la2F	ATGGCRCGNAATCCTTTCATTAGTWGARTT	<i>cox3-cox1</i> (2.5K)
cox1laR	CGAGGAAAAGCYATRTCAGGAGC	
Primer Link <i>cox1</i>		
Primer	Sequence 5'-3'	Fragment (bp)
LCO1490 F	GGTCAACAAATCATAAAGATATTGG	<i>cox1</i> (709)
HCO2198 R	TTAACCTCAGGGTGACCAAAAAATCA	
<i>Tritia vaucheri</i>	Sequenced by Allgenetics, with a buccinoid species in the same library	
Long PCR		
Primer	Sequence 5'-3'	Fragment (bp)
cox1laF	AAYATRCGATGACGAGGRATRCARTTTGA	<i>cox1-rrnS</i> (4K)
12SlaR	ATAGGCTGCACCTTGATCTGACGTYTT	
12SlaF	CAGTTTGTATAACCGTCGTCGTCAAGGT	<i>rrnS-cob</i> (4.5K)
cobra2R	GGRTTAGCWGGRATAAARTTYTCWGGRTC	
cobra2F	CCYTGAGGTCARATATCYTTYTGAGGRGC	<i>cob-trnF</i> (4.3K)
trnF-R	CACCCTAGCATCTTCAGTGCTATGCTCT	
cox3la2F	ATGGCRCGNAATCCTTTCATTAGTWGARTT	<i>cox3-cox1</i> (2.5K)
cox1laR	CGAGGAAAAGCYATRTCAGGAGC	
Primer Link <i>cox1</i>		
Primer	Sequence 5'-3'	Fragment (bp)

COINassaF	TCTACAAATCATAAAGACATTGG	<i>cox1</i> (700)
COINassaR	ACYTCAGGATGACCAAARAATCA	

Tritia denticulata Sequenced by NIMGenetics, in a whole library

Long PCR

Primer	Sequence 5'-3'	Fragment (bp)
cox1laF	AAYATRCGATGACGAGGRATRCARTTTGA	<i>cox1-rrnS</i> (4K)
12SlaR	ATAGGCTGCACCTTGATCTGACGTYTT	
12SlaF	CAGTTTGTATAACCGTCGTCGTCAGGT	<i>rrnS-cob</i> (4.5K)
cobla2R	GGRTTAGCWGGRATAAARTTYTCWGGRTC	
coblaF	GAYCCWGARAAYTTATYCCTGCTAAYCC	<i>cob-trnF</i> (4.0K)
trnF-R	CACCCTAGCATCTCAGTGCTATGCTCT	
cox3la2F	ATGGCRCGNAATCCTTTCATTAGTWGARTT	<i>cox3-cox1</i> (2.5K)
cox1laR	CGAGGAAAAGCYATRTCAGGAGC	

cox1 Genbank Acc. No: KY451292

Primer Link *cytb*

Primer	Sequence 5'-3'	Fragment (bp)
cytbF	GGWTAYGTWYTWCCTGRGGWCARAT	<i>cytb</i> (0.5K)
cytbR	GCRTAWGCRAAWARRAARTAYCAYTCWGG	

Tritia ephamilla Sequenced by NIMGenetics, in a whole library

Long PCR

Primer	Sequence 5'-3'	Fragment (bp)
cox1laF	AAYATRCGATGACGAGGRATRCARTTTGA	<i>cox1-rrnS</i> (4K)
12SlaR	ATAGGCTGCACCTTGATCTGACGTYTT	
12SlaF	CAGTTTGTATAACCGTCGTCGTCAGGT	<i>rrnS-cob</i> (4.4K)
coblaR	GCYCCTCARAARGATATYTGACCTCARGG	
coblaF	GAYCCWGARAAYTTATYCCTGCTAAYCC	<i>cob-trnF</i> (4.0K)
trnF-R	CACCCTAGCATCTCAGTGCTATGCTCT	
cox3la2F	ATGGCRCGNAATCCTTTCATTAGTWGARTT	<i>cox3-cox1</i> (2.5K)
cox1laR	CGAGGAAAAGCYATRTCAGGAGC	

cox1 Genbank Acc. No: KY451298

Primer Link *cytb*

Primer	Sequence 5'-3'	Fragment (bp)
cytbF	GGWTAYGTWYTWCCTGRGGWCARAT	<i>cytb</i> (0.5K)
cytbR	GCRTAWGCRAAWARRAARTAYCAYTCWGG	

Tritia pallaryana Sequenced by NIMGenetics, in a whole library

Long PCR

Primer	Sequence 5'-3'	Fragment (bp)
cox1laF	AAYATRCGATGACGAGGRATRCARTTTGA	<i>cox1-rrnS</i> (4K)
12SlaR	ATAGGCTGCACCTTGATCTGACGTYTT	
12SlaF	CAGTTTGTATAACCGTCGTCGTCAGGT	<i>rrnS-cob</i> (4.5K)

cobra2R	GGRTTAGCWGGRATAAARTTYTCWGGRTC	
cobra2F	CCYTGAGGT CARATATCYTTYGAGGRGC	<i>cob-trnF</i> (4.3K)
trnF-R	CACCC TAGCATCTCAGTGCTATGCTCT	
cox3la2F	ATGGCRCGNAATCCTTTCAATTAGTWGARTT	<i>cox3-cox1</i> (2.5K)
cox1laR	CGAGGAAAAGCYATRTCAGGAGC	

Primer Link *cox1*

Primer	Sequence 5'-3'	Fragment (bp)
COI-tritiaF	ACWG CYCAYGCT TTYGTAATAAT	<i>cox1</i> (400)
COI-tritiaR	TGYATNCCTCGTCATCGYATRTT	

Tritia tenuicosta Sequenced by NIMGenetics, in a whole library

Long PCR

Primer	Sequence 5'-3'	Fragment (bp)
cox1laF	AAYATRCGATGACGAGGRATRCARTTTGA	<i>cox1-rrnS</i> (4K)
12SlaR	ATAGGCTGCACCTTGATCTGACGTYTT	
12SlaF	CAGTTGTATA CGTCGTCGT CAGGT	<i>rrnS-cob</i> (4.4K)
cobraR	GCYCCTCARAARGATATYTGACCTCARGG	
cobraF	GAYCCWGARAAYTTATY CCTGCTAAYCC	<i>cob-trnF</i> (4.0K)
trnF-R	CACCC TAGCATCTCAGTGCTATGCTCT	
cox3la2F	ATGGCRCGNAATCCTTTCAATTAGTWGARTT	<i>cox3-cox1</i> (2.5K)
cox1laR	CGAGGAAAAGCYATRTCAGGAGC	

cox1 Genbank Acc. No: KY489424

Primer Link *cytb*

Primer	Sequence 5'-3'	Fragment (bp)
cytbF	GGWTAYGTWYT WCCWTGRGGWCARAT	<i>cytb</i> (0.5K)
cytbR	GCRTAWGCRAAWARRAARTAYCAYTCWGG	

Tritia elongata Sequenced by NIMGenetics, in a whole library

Long PCR

Primer	Sequence 5'-3'	Fragment (bp)
cox1laF	AAYATRCGATGACGAGGRATRCARTTTGA	<i>cox1-rrnS</i> (4K)
12SlaR	ATAGGCTGCACCTTGATCTGACGTYTT	
12SlaF	CAGTTGTATA CGTCGTCGT CAGGT	<i>rrnS-cob</i> (4.5K)
cobra2R	GGRTTAGCWGGRATAAARTTYTCWGGRTC	
cobra2F	CCYTGAGGT CARATATCYTTYGAGGRGC	<i>cob-trnF</i> (4.3K)
trnF-R	CACCC TAGCATCTCAGTGCTATGCTCT	
cox3la2F	ATGGCRCGNAATCCTTTCAATTAGTWGARTT	<i>cox3-cox1</i> (2.5K)
cox1laR	CGAGGAAAAGCYATRTCAGGAGC	

cox1 Genbank Acc. No: KY489440

Tritia nitida Sequenced by NIMGenetics, in a whole library

Long PCR

Primer	Sequence 5'-3'	Fragment (bp)
cox1laF	AAYATRCGATGACGAGGRATRCARTTTGA	<i>cox1-rrnS</i> (4K)

12SlaR	ATAGGCTGCACCTTGATCTGACGTYTT	
12SlaF	CAGTTGTATAACCGTCGTCGTCAGGT	<i>rrnS-cob</i> (4.5K)
cobra2R	GGRTTAGCWGRATAAARTTYTCWGGRTC	
cobra2F	CCYTGAGGTCARATATCYTTYGAGGRGC	<i>cob-trnF</i> (4.3K)
trnF-R	CACCCTAGCATCTCAGTGCTATGCTCT	
cox3la2F	ATGGCRCGNAATCCTTTCATTAGTWGARTT	<i>cox3-cox1</i> (2.5K)
cox1laR	CGAGGAAAAGCYATRTCAGGAGC	

Primer Link *cox1*

Primer	Sequence 5'-3'	Fragment (bp)
LCO1490 F	GGTCAACAAATCATAAAGATATTGG	<i>cox1</i> (709)
HCO2198 R	TTAACCTCAGGGTGACCAAAAAATCA	

Tritia varicosa Sequenced by NIMGenetics, in a whole library

Long PCR

Primer	Sequence 5'-3'	Fragment (bp)
cox1laF	AAYATRCGATGACGAGGRATRCARTTTGA	<i>cox1-rrnS</i> (4K)
12SlaR	ATAGGCTGCACCTTGATCTGACGTYTT	
12SlaF	CAGTTGTATAACCGTCGTCGTCAGGT	<i>rrnS-cob</i> (4.5K)
cobra2R	GGRTTAGCWGRATAAARTTYTCWGGRTC	
16slaF	GTGCAAAGGTAGCATAATCATTGCCT	<i>rrnL-trnF</i> (6.1K)
trnF-R	CACCCTAGCATCTCAGTGCTATGCTCT	
cox3la2F	ATGGCRCGNAATCCTTTCATTAGTWGARTT	<i>cox3-cox1</i> (2.5K)
cox1laR	CGAGGAAAAGCYATRTCAGGAGC	

Primer Link *cox1*

Primer	Sequence 5'-3'	Fragment (bp)
COINassaF	TCTACAAATCATAAAGACATTGG	<i>cox1</i> (700)
COINassaR	ACYTCAGGATGACCAAARAATCA	

Tritia elata Sequenced by NIMGenetics, in a whole library

Long PCR

Primer	Sequence 5'-3'	Fragment (bp)
cox1laF	AAYATRCGATGACGAGGRATRCARTTTGA	<i>cox1-rrnS</i> (4K)
12SlaR	ATAGGCTGCACCTTGATCTGACGTYTT	
12SlaF	CAGTTGTATAACCGTCGTCGTCAGGT	<i>rrnS-cob</i> (4.5K)
cobra2R	GGRTTAGCWGRATAAARTTYTCWGGRTC	
16slaF	GTGCAAAGGTAGCATAATCATTGCCT	<i>rrnL-trnF</i> (6.1K)
trnF-R	CACCCTAGCATCTCAGTGCTATGCTCT	
cox3la2F	ATGGCRCGNAATCCTTTCATTAGTWGARTT	<i>cox3-cox1</i> (2.5K)
cox1laR	CGAGGAAAAGCYATRTCAGGAGC	

Primer Link *cox1*

Primer	Sequence 5'-3'	Fragment (bp)
COINassaF	TCTACAAATCATAAAGACATTGG	<i>cox1</i> (700)
COINassaR	ACYTCAGGATGACCAAARAATCA	

<i>Tritia ovoidea</i>	Sequenced by Sanger	
Long PCR		
Primer	Sequence 5'-3'	Fragment (bp)
cox1laF	AAYATRCGATGACGAGGRATRCARTTGA	<i>cox1-rrnS</i> (5.7K)
16SlaR	ATGCTGTTATCCCTACGGTAACATAATT	
16SZouF	GCGGTACTCTGACCGTGCAA	<i>rrnL-cob</i> (2.5K)
cobraR	GCYCCTCARAARGATATYTGACCTCARGG	
cox3la2F	ATGGCRCNAATCCTTCATTAGTWGARTT	<i>cox3-cox1</i> (2.5K)
cox1laR	CGAGGAAAAGCYATRTCAGGAGC	
15F	TCAGCYTGTGGATTGRARAT	<i>trnH-trnF</i> (1.6K)
trnF-R	CACCCTAGCATCTCAGTGCTATGCTCT	
Walking Primers		
Primer	Sequence 5'-3'	Fragment (bp)
1F	TGATTCTTARGAGAGGTTCA	<i>TrnQ-rrnS</i> (1K)
1R	TGCTATGTTACGACTTATCTC	
2F	AAGCTRTTGGGTTCATACCCC	<i>TrnM-TrnE</i> (0.5K)
2R	TAGATTTCATCTAAARGRATA	
3F	ATGCTTAGACATTTTCTTC	<i>atp6-trnC</i> (0.9K)
3R	TCGATTTGCARRTCGATGTT	
4F	TTTAYGGTCARTGTTCYGAAAT	<i>cox2-atp6</i> (0.8K)
4R	ACAATATGYCCRGCYCTTATRTT	
5F	ATGAGCCTATGAGGACAAYTAGGATT	<i>cox2-trnD</i> (0.7K)
5R	GYRACRTAACRGCTGACAAYCT	
6F	GAYATTATRCTYCAYGAYAHTAYTA	<i>cox1-cox2</i> (0.7K)
6R	TCATAGCTTCARTATCATGRTG	
7F	AAYATRCGATGACGAGGRATRCA	<i>cox1</i> (0.9K)
7R	GCYTCYCABACAATTACYATRAA	
9F	AGGGCTGCTAACITGTTTG	<i>trnS-cox1</i> (1.1K)
9R	ACRTTRTAAAGTTGRTCRTCACCC	
10F	CTAGCTGTTAATTAGRAGAAT	<i>trnN-nd2</i> (0.75K)
10R	ATRAARTAYTTWACRGCGYAYTG	
11F	TTYTTYTGAGCTTAYTTCAAG	<i>cox3-trnI</i> (0.87K)
11R	ACATCAATGATTYCCGTTCAT	
15F	TCAGCYTGTGGATTGRARAT	<i>nd5</i> (0.9K)
15R	TTRTGRATAAATATHCCDGCRCA	
16F	ATTGGNGCHAAYTAYGAAAAYGA	<i>nd5-trnF</i> (0.9K)
trnF-R	CACCCTAGCATCTCAGTGCTATGCTCT	
Standard PCR		
Primer	Sequence 5'-3'	Fragment (bp)
12F	ATGGCRCGTAATCCTTTCATTT	<i>cox3-trnA</i> (0.8K)
12R	CTRAATGCAAATCARRTCTTT	
13F	TTTGAAGCTCTTAATTCCWAC	<i>nd4-trnH</i> (0.8K)
13R	ATYTYCAAATCCACARGCTGA	
cobraF	GAYCCWGARAAYTTATYCCTGCTAAYCC	<i>cob-nd4</i> (0.9K)

14R	TTKACYCTATTTGMCTYGCTAA	
18F	DCATTCTGCCTGTTAKCAA	<i>rrnL-trnL2</i> (0.8K)
18R	GGGCTTAAACCTAATGCACTT	
19F	AATGCAATTGACTTAGGMTCA	<i>trnL1-trnP</i> (1K)
19R	ACCCAAGCTYTAGCTTCCAAT	
20F	TTGGCAGTCGCTTTTACTCT	<i>nd1-nd6</i> (1K)
20R	CTAAARAYAATTARYGCTCTCAT	
21F	ATTAGCATTGGAAGCTARAGC	<i>trnP-cob</i> (0.6K)
21R	AARATRGGRGTGHACTTTCGAAT	
22F	ATGCGAAGTCCYATTCGAAAAGT	<i>cob</i> (1K)
22R	ACMGGACAAGCYCCAATTCAWGT	
LCO1490 F	GGTCAACAAATCATAAAGATATTGG	<i>cox1</i> (709)
HCO2198 R	TTAACITCAGGGTGACCAAAAAATCA	
12SlaF	CAGTTGTATACCGTCGTCAGGT	<i>rrnL-rrnS</i> (1.2K)
16sZouR	TCACGTAGAAATTAAATGGTCG	
coblaF	GAYCCWGARAAYTTATYCCTGCTAAYCC	<i>cob-nd4</i> (1.2K)
nd4lnd4R	GGTAATGAAGCTGCTACAGTGT	

Tritia tingitana Sequenced by Sanger

Long PCR

Primer	Sequence 5'-3'	Fragment (bp)
16SZouF	GCGGTACTCTGACCGTGCAA	<i>rrnL-cob</i> (2.5K)
coblaR	GCYCCTCARAARGATATYTGACCTCARGG	
12F	ATGGCRCGTAATCCTTTCATTT	<i>cox3-cox1</i> (3K)
cox11aR	CGAGGAAAAGCYATRTCAGGAGC	
5F	ATGAGCCTATGAGGACAAYTAGGATT	<i>cox2-rrnS</i> (3K)
12slaR	ATAGGCTGCACCTTGATCTGACGTYTT	
15F	TCAGCYTGTGGATTGRARAT	<i>trnH-trnF</i> (1.6K)
trnF-R	CACCCTAGCATCTCAGTGCTATGCTCT	
coblaF	GAYCCWGARAAYTTATYCCTGCTAAYCC	<i>cob-trnH</i> (2.5K)
13R	ATYTYCAAATCCACARGCTGA	

Walking Primers

Primer	Sequence 5'-3'	Fragment (bp)
1F	TGATTCTTARGAGAGGTTCA	<i>TrnQ-rrnS</i> (1K)
1R	TGCTATGTTACGACTTATCTC	
2F	AAGCTRTGGGTCATACCCC	<i>TrnM-TrnE</i> (0.5K)
2R	TAGATTTCATTCTAAARGRATA	
3F	ATGCTTGTAGACATTCTTC	<i>atp6-trnC</i> (0.9K)
3R	TCGATTTGCARRTCGATGTT	
4F	TTTAYGGTCARTGTTCYGAAAT	<i>cox2-atp6</i> (0.8K)
4R	ACAATATGYCCRGCYCTTATRTT	
5F	ATGAGCCTATGAGGACAAYTAGGATT	<i>cox2-trnD</i> (0.7K)
5R	GYRACRTAAGRCTGACAAYCT	
9F	AGGGCTGCTAACCTTGTTTG	<i>trnS-cox1</i> (1.1K)

9R	ACRTTRTAAAGTTGRTCRTCAACC	
10F	CTAGCTGTTAATTAGRAGAAT	<i>trnN-nd2</i> (0.75K)
10R	ATRAARTAYTTWACRGCYGAYTG	
11F	TTYTTYTGAGCTTAYTTTCAYAG	<i>cox3-trnI</i> (0.87K)
11R	ACATCAATGATTYCCGTTCAT	
12F	ATGGCRCGTAATCCTTTCATTT	<i>cox3-trnA</i> (0.8K)
12R	CTRAATGCAAATCARRTCTTT	
13F	TTTGAAGCTCTTTAATTCCWAC	<i>nd4-trnH</i> (0.8K)
13R	ATYTYCAAATCCACARGCTGA	
coblaF	GAYCCWGARAAYTTTATYCCTGCTAAYCC	<i>cob-nd4</i> (0.9K)
14R	TTKACYCTATTTGMCTYGCTAA	
15F	TCAGCYTGTGGATTGRARAT	<i>nd5</i> (0.9K)
15R	TTRTGRATAAATATHCCDGCRCA	
16F	ATTGGNGCHAAYTAYGAAAAYGA	<i>nd5-trnF</i> (0.9K)
trnF-R	CACCCCTAGCATCTCAGTGCTATGCTCT	
18F	DCATTCTGCCTGTTAKCAA	<i>rrnL-trnL2</i> (0.8K)
18R	GGGCTTAAACCTAACACTT	
19F	AATGCAATTGACTTAGGMTCA	<i>trnL1-trnP</i> (1K)
19R	ACCCAAGCTYTAGCTTCCAAT	
20F	TTGGCAGTCGCTTTTTACTCT	<i>nd1-nd6</i> (1K)
20R	CTAAARAYAATTARYGCTCTCAT	
21F	ATTAGCATTGGAAGCTARAGC	<i>trnP-cob</i> (0.6K)
21R	AARATRGGRGHTGHACTTTCGAAT	
22F	ATGCGAAGTCCYATTGAAAAGT	<i>cob</i> (1K)
22R	ACMGGACAAGCYCCAATTCAWGT	

Standard PCR

Primer	Sequence 5'-3'	Fragment (bp)
12SlaF	CAGTTGTATAACCGTCGTCGTCAGGT	<i>rrnL-rrnS</i> (1.2K)
16sZouR	TCACGTAGAAATTAAATGGTCG	
cob-12870F	GGGTATGTCTTACCCCTGAGGTCAGAT	<i>cob</i> (0.4K)
cob-12870R	GCATACGCAAAGAGGAAGTATCATTCTGG	

Anentome sp. Sequenced by NIMGenetics, in a whole library

Long PCR

Primer	Sequence 5'-3'	Fragment (bp)
cox1laF	AAYATRCGATGACGAGGRATRCARTTTGA	<i>cox1-rrnS</i> (4K)
12SlaR	ATAGGCTGCACCTTGATCTGACGTYTT	
12SlaF	CAGTTGTATAACCGTCGTCGTCAGGT	<i>rrnS-cob</i> (4.5K)
cobla2R	GGRTTAGCWGGRATAAARTTYTCWGGRTC	
cobla2F	CCYTGAGGTCARATATCYTTYTGAGGRGC	<i>cob-trnF</i> (4.3K)
trnF-R	CACCCCTAGCATCTCAGTGCTATGCTCT	
cox3la2F	ATGGCRCGNAATCCTTTCATTTAGTWGARTT	<i>cox3-cox1</i> (2.5K)
cox1laR	CGAGGAAAAGCYATRTCAGGAGC	

Primer Link *cox1*

Primer	Sequence 5'-3'	Fragment (bp)
LCO1490 F	GGTCAACAAATCATAAAGATATTGG	<i>cox1</i> (709)
HCO2198 R	TTAACCTCAGGGTGACCAAAAAATCA	

Table S2. Best fit partitions and substitution models.

	Set Partition (Conducted by PartitionFinder 2)	Best Model for BI (Selected by PartitionFinder 2)	Best Model for ML (Selected by IQtree 1.6.10)
Best Partition CDS genes (BIC= 254577.82)	<i>atp6-8</i> 1th <i>atp6-8</i> 2th <i>atp6-8</i> 3th <i>cox1-2-3</i> 1th <i>cox1-2-3</i> 2th <i>cox1-2-3</i> 3th <i>cob</i> 1th <i>cob</i> 2th <i>cob</i> 3th <i>nad1-2-3-4-4L-5-6</i> 1th <i>nad1-2-3-4-4L-5-6</i> 2th <i>nad1-2-3-4-4L-5-6</i> 3th	TRN+G K81UF+I TVM+I+G TRN+I+G TVM+I+G GTR+I+G TRN+I+G TVM+I+G K81UF+I+G GTR+I+G GTR+I+G	TN+F+G4 K3Pu+F+I K3Pu+F+I+G4 TN+F+I+G4 TVM+F+I+G4 TVM+F+I+G4 TIM2+F+I+G4 TVM+F+I+G4 K3Pu+F+I+G4 TIM3+F+I+G4 GTR+F+I+G4 TVM+F+I+G4
Best Partition to rRNA genes (BIC= 26625.61)	<i>rrnS-L</i>	GTR+I+G	GTR+F+I+G4

Table S3. Mitochondrial genome features*Tritia corniculum* 15,114 bp

Gene	Strand	Location	Size (bp)	Start Codon	Stop codon	Intergenic nucleotides
<i>Cox3</i>	H	1-747	incomplete	—	TAG	15
tRNA-Lys	H	763-827	65			1
tRNA-Ala	H	829-896	68			9
tRNA-Arg	H	906-974	69			5
tRNA-Asn	H	980-1047	68			15
tRNA-Ile	H	1063-1130	68			3
<i>Nad3</i>	H	1134-1487	354	ATG	TAA	0
tRNA-Ser	H	1488-1555	68			0
<i>Nad2</i>	H	1556-2610	1055	ATG	TA	0
<i>Cox1</i>	H	2611-4146	1536	ATG	TAA	29
<i>Cox2</i>	H	4176-4862	687	ATG	TAA	-2
tRNA-ASp	H	4861-4928	68			1
<i>Atp8</i>	H	4930-5088	159	ATG	TAA	7
<i>Atp6</i>	H	5096-5791	696	ATG	TAA	38
tRNA-Met	L	5830-5896	67			3
tRNA-Tyr	L	5900-5967	68			1
tRNA-Cys	L	5969-6033	65			0
tRNA-Trp	L	6034-6099	66			1
tRNA-Gln	L	6101-6162	62			1
tRNA-Gly	L	6164-6231	68			11
tRNA-Glu	L	6243-6307	65			0
12s	H	6308-7265	958			0
tRNA-Val	H	7266-7333	68			0
16s	H	7334-8685	1352			0
tRNA-Leu	H	8686-8757	72			2
tRNA-Leu	H	8760-8828	69			0
<i>Nad1</i>	H	8829-9770	942	ATG	TAA	6
tRNA-Pro	H	9777-9844	68			1
<i>Nad6</i>	H	9846-10346	501	ATG	TAG	5
<i>Cytb</i>	H	10352-11491	1140	ATG	TAA	9
tRNA-Ser	H	11502-11565	64			0
tRNA-Thr	L	11566-11630	65			20
<i>Nad4L</i>	H	11651-11947	297	ATG	TAG	11
<i>Nad4</i>	H	11959-13314	1356	ATA	TAG	-1
tRNA-His	H	13314-13378	65			0
<i>Nad5</i>	H	13379-15100	1722	ATG	TAG	14
tRNA-Phe	H	missing	—			—

Tritia cuvierii 15,185 bp

Gene	Strand	Location	Size (bp)	Start Codon	Stop codon	Intergenic nucleotides
<i>Cox3</i>	H	1-776	incomplete	—	TAA	12
tRNA-Lys	H	789-853	65			2
tRNA-Ala	H	856-922	67			10
tRNA-Arg	H	933-1001	69			8
tRNA-Asn	H	1010-1077	68			17
tRNA-Ile	H	1095-1162	68			3
<i>Nad3</i>	H	1166-1519	354	ATG	TAG	0
tRNA-Ser	H	1520-1587	68			0
<i>Nad2</i>	H	1588-2642	1055	ATG	TA	0
<i>Cox1</i>	H	2643-4178	1536	ATG	TAA	26
<i>Cox2</i>	H	4205-4891	687	ATG	TAA	-2
tRNA-Asp	H	4890-4957	68			1
<i>Atp8</i>	H	4959-5117	159	ATG	TAA	6
<i>Atp6</i>	H	5124-5819	696	ATG	TAA	42
tRNA-Met	L	5862-5928	67			4
tRNA-Tyr	L	5933-5999	67			1
tRNA-Cys	L	6001-6066	66			0
tRNA-Trp	L	6067-6132	66			0
tRNA-Gln	L	6133-6196	64			1
tRNA-Gly	L	6198-6264	67			14
tRNA-Glu	L	6279-6343	65			0
12s	H	6344-7302	959			0
tRNA-Val	H	7303-7370	68			0
16s	H	7371-8723	1353			0
tRNA-Leu	H	8724-8792	69			2
tRNA-Leu	H	8795-8863	69			0
<i>Nad1</i>	H	8864-9805	942	ATG	TAA	5
tRNA-Pro	H	9811-9878	68			1
<i>Nad6</i>	H	9880-10380	501	ATG	TAA	5
<i>Cytb</i>	H	10386-11525	1140	ATG	TAA	9
tRNA-Ser	H	11535-11599	65			0
tRNA-Thr	L	11600-11667	68			25
<i>Nad4L</i>	H	11693-11989	297	ATG	TAG	11
<i>Nad4</i>	H	12001-13356	1356	ATA	TAG	-1
tRNA-His	H	13356-13421	66			1
<i>Nad5</i>	H	13423-15144	1722	ATG	TAG	41
tRNA-Phe	H	missing	—			—

Tritia denticulata 15,167 bp

Gene	Strand	Location	Size (bp)	Start Codon	Stop codon	Intergenic nucleotides
<i>Cox3</i>	H	1-771	incomplete	—	TAA	15
tRNA-Lys	H	787-852	66			3
tRNA-Ala	H	856-923	68			8
tRNA-Arg	H	932-1002	71			7
tRNA-Asn	H	1010-1076	67			17
tRNA-Ile	H	1094-1161	68			3
<i>Nad3</i>	H	1165-1518	354	ATG	TAA	0
tRNA-Ser	H	1519-1586	68			0
<i>Nad2</i>	H	1587-2641	1055	ATG	TA	0
<i>Cox1</i>	H	2642-4177	1536	ATG	TAA	22
<i>Cox2</i>	H	4200-4886	687	ATG	TAA	-2
tRNA-Asp	H	4885-4952	68			1
<i>Atp8</i>	H	4954-5112	159	ATG	TAA	7
<i>Atp6</i>	H	5120-5815	696	ATG	TAA	42
tRNA-Met	L	5858-5924	67			6
tRNA-Tyr	L	5931-5998	68			1
tRNA-Cys	L	6000-6063	64			0
tRNA-Trp	L	6064-6129	66			-3
tRNA-Gln	L	6127-6193	67			-1
tRNA-Gly	L	6193-6261	69			12
tRNA-Glu	L	6274-6338	65			0
12s	H	6339-7296	958			0
tRNA-Val	H	7297-7364	68			0
16s	H	7365-8716	1352			0
tRNA-Leu	H	8717-8785	69			2
tRNA-Leu	H	8788-8856	69			0
<i>Nad1</i>	H	8857-9798	942	ATG	TAG	6
tRNA-Pro	H	9805-9872	68			1
<i>Nad6</i>	H	9874-10374	501	ATG	TAA	6
<i>Cytb</i>	H	10381-11520	1140	ATG	TAA	10
tRNA-Ser	H	11531-11595	65			-1
tRNA-Thr	L	11595-11664	70			18
<i>Nad4L</i>	H	11683-11979	297	ATG	TAG	11
<i>Nad4</i>	H	11991-13346	1356	ATA	TAG	-1
tRNA-His	H	13346-13412	67			1
<i>Nad5</i>	H	13414-15135	1722	ATG	TAG	32
tRNA-Phe	H	missing	—			—

Tritia elongata 15,145 bp

Gene	Strand	Location	Size (bp)	Start Codon	Stop codon	Intergenic nucleotides
<i>Cox3</i>	H	1-752	incomplete	—	TAA	12
tRNA-Lys	H	765-831	67			-1
tRNA-Ala	H	831-900	70			7
tRNA-Arg	H	908-978	71			2
tRNA-Asn	H	981-1047	67			14
tRNA-Ile	H	1062-1129	68			3
<i>Nad3</i>	H	1133-1486	354	ATG	TAG	0
tRNA-Ser	H	1487-1554	68			0
<i>Nad2</i>	H	1555-2609	1055	ATG	TA	0
<i>Cox1</i>	H	2610-4145	1536	ATG	TAA	29
<i>Cox2</i>	H	4175-4861	687	ATG	TAA	-2
tRNA-Asp	H	4860-4927	68			1
<i>Atp8</i>	H	4929-5087	159	ATG	TAA	7
<i>Atp6</i>	H	5095-5790	696	ATG	TAA	38
tRNA-Met	L	5829-5895	67			1
tRNA-Tyr	L	5897-5968	72			-1
tRNA-Cys	L	5968-6032	65			0
tRNA-Trp	L	6033-6098	66			-3
tRNA-Gln	L	6096-6162	67			0
tRNA-Gly	L	6163-6231	69			12
tRNA-Glu	L	6244-6308	65			0
12s	H	6309-7267	959			0
tRNA-Val	H	7268-7335	68			0
16s	H	7336-8686	1351			0
tRNA-Leu	H	8687-8756	70			1
tRNA-Leu	H	8758-8828	71			-1
<i>Nad1</i>	H	8828-9769	942	ATG	TAG	6
tRNA-Pro	H	9776-9843	68			1
<i>Nad6</i>	H	9845-10345	501	ATG	TAA	5
<i>Cytb</i>	H	10351-11490	1140	ATG	TAA	8
tRNA-Ser	H	11499-11569	71			-2
tRNA-Thr	L	11568-11635	68			19
<i>Nad4L</i>	H	11655-11951	297	ATG	TAG	11
<i>Nad4</i>	H	11963-13318	1356	ATA	TAG	-1
tRNA-His	H	13318-13382	65			0
<i>Nad5</i>	H	13383-15104	1722	ATG	TAG	41
tRNA-Phe	H	missing	—			—

Tritia ephamilla 15,186 bp

Gene	Strand	Location	Size (bp)	Start Codon	Stop codon	Intergenic nucleotides
<i>Cox3</i>	H	1-776	incomplete	—	TAA	15
tRNA-Lys	H	792-856	65			1
tRNA-Ala	H	858-925	68			9
tRNA-Arg	H	935-1003	69			9
tRNA-Asn	H	1013-1080	68			18
tRNA-Ile	H	1099-1166	68			3
<i>Nad3</i>	H	1170-1523	354	ATG	TAA	-1
tRNA-Ser	H	1523-1592	70			-1
<i>Nad2</i>	H	1592-2646	1055	ATG	TA	0
<i>Cox1</i>	H	2647-4182	1536	ATG	TAA	27
<i>Cox2</i>	H	4210-4896	687	ATG	TAA	-2
tRNA-Asp	H	4895-4962	68			1
<i>Atp8</i>	H	4964-5122	159	ATG	TAA	7
<i>Atp6</i>	H	5130-5825	696	ATG	TAA	43
tRNA-Met	L	5869-5935	67			2
tRNA-Tyr	L	5938-6003	66			1
tRNA-Cys	L	6005-6069	65			0
tRNA-Trp	L	6070-6135	66			-3
tRNA-Gln	L	6133-6199	67			-1
tRNA-Gly	L	6199-6267	69			13
tRNA-Glu	L	6281-6345	65			0
12s	H	6346-7301	956			0
tRNA-Val	H	7302-7369	68			0
16s	H	7370-8719	1350			0
tRNA-Leu	H	8720-8788	69			2
tRNA-Leu	H	8791-8861	71			-1
<i>Nad1</i>	H	8861-9802	942	ATG	TAA	6
tRNA-Pro	H	9809-9876	68			1
<i>Nad6</i>	H	9878-10378	501	ATG	TAA	4
<i>Cytb</i>	H	10383-11522	1140	ATG	TAA	16
tRNA-Ser	H	11539-11603	65			-1
tRNA-Thr	L	11603-11673	71			20
<i>Nad4L</i>	H	11694-11990	297	ATG	TAG	11
<i>Nad4</i>	H	12002-13357	1356	ATA	TAG	-1
tRNA-His	H	13357-13422	66			1
<i>Nad5</i>	H	13424-15145	1722	ATG	TAG	41
tRNA-Phe	H	missing	—			—

Tritia grana 15,198 bp

Gene	Strand	Location	Size (bp)	Start Codon	Stop codon	Intergenic nucleotides
<i>Cox3</i>	H	1-770	incomplete	—	TAA	15
tRNA-Lys	H	786-850	65			1
tRNA-Ala	H	851-918	68			9
tRNA-Arg	H	928-996	69			16
tRNA-Asn	H	1013-1080	68			12
tRNA-Ile	H	1093-1160	68			3
<i>Nad3</i>	H	1164-1517	354	ATG	TAG	0
tRNA-Ser	H	1518-1585	68			0
<i>Nad2</i>	H	1586-2641	1056	ATG	TAA	0
<i>Cox1</i>	H	2642-4177	1536	ATG	TAA	28
<i>Cox2</i>	H	4206-4892	687	ATG	TAA	-2
tRNA-Asp	H	4891-4958	68			1
<i>Atp8</i>	H	4960-5118	159	ATG	TAA	7
<i>Atp6</i>	H	5126-5821	696	ATG	TAA	41
tRNA-Met	L	5863-5929	67			2
tRNA-Tyr	L	5932-5999	68			1
tRNA-Cys	L	6001-6066	66			0
tRNA-Trp	L	6067-6132	66			1
tRNA-Gln	L	6134-6195	62			1
tRNA-Gly	L	6197-6264	68			12
tRNA-Glu	L	6277-6341	65			0
12s	H	6342-7302	961			0
tRNA-Val	H	7303-7370	68			0
16s	H	7371-8720	1350			0
tRNA-Leu	H	8721-8789	69			2
tRNA-Leu	H	8792-8860	69			0
<i>Nad1</i>	H	8861-9802	942	ATG	TAA	6
tRNA-Pro	H	9809-9876	68			1
<i>Nad6</i>	H	9878-10378	501	ATG	TAA	18
<i>Cytb</i>	H	10397-11536	1140	ATG	TAA	12
tRNA-Ser	H	11549-11614	66			0
tRNA-Thr	L	11615-11682	68			23
<i>Nad4L</i>	H	11706-12002	297	ATG	TAG	11
<i>Nad4</i>	H	12014-13369	1356	ATA	TAG	-1
tRNA-His	H	13369-13434	66			1
<i>Nad5</i>	H	13436-15157	1722	ATG	TAG	41
tRNA-Phe	H	missing	—			—

Tritia incrassata-Norway 15,170 bp

Gene	Strand	Location	Size (bp)	Start Codon	Stop codon	Intergenic nucleotides
<i>Cox3</i>	H	1-772	incomplete	—	TAA	14
tRNA-Lys	H	787-851	65			1
tRNA-Ala	H	853-920	68			9
tRNA-Arg	H	930-998	69			7
tRNA-Asn	H	1006-1072	67			15
tRNA-Ile	H	1088-1154	67			3
<i>Nad3</i>	H	1158-1511	354	ATG	TAA	0
tRNA-Ser	H	1512-1579	68			0
<i>Nad2</i>	H	1580-2634	1055	ATG	TA	0
<i>Cox1</i>	H	2635-4170	1536	ATG	TAG	28
<i>Cox2</i>	H	4199-4885	687	ATG	TAA	-2
tRNA-Asp	H	4884-4951	68			1
<i>Atp8</i>	H	4953-5111	159	ATG	TAA	7
<i>Atp6</i>	H	5119-5814	696	ATG	TAA	41
tRNA-Met	L	5856-5922	67			5
tRNA-Tyr	L	5928-5994	67			1
tRNA-Cys	L	5996-6061	66			0
tRNA-Trp	L	6062-6127	66			1
tRNA-Gln	L	6129-6190	62			1
tRNA-Gly	L	6192-6258	67			13
tRNA-Glu	L	6272-6336	65			0
12s	H	6337-7292	956			0
tRNA-Val	H	7293-7360	68			0
16s	H	7361-8711	1351			0
tRNA-Leu	H	8712-8780	69			2
tRNA-Leu	H	8783-8851	69			0
<i>Nad1</i>	H	8852-9793	942	ATG	TAG	6
tRNA-Pro	H	9800-9867	68			1
<i>Nad6</i>	H	9869-10369	501	ATG	TAA	4
<i>Cytb</i>	H	10374-11513	1140	ATG	TAA	11
tRNA-Ser	H	11525-11590	66			0
tRNA-Thr	L	11591-11658	68			19
<i>Nad4L</i>	H	11678-11974	297	ATG	TAG	11
<i>Nad4</i>	H	11986-13341	1356	ATA	TAA	1
tRNA-His	H	13343-13407	65			0
<i>Nad5</i>	H	13408-15129	1722	ATG	TAG	41
tRNA-Phe	H	missing	—			—

Tritia incrassata-Spain 15,159 bp

Gene	Strand	Location	Size (bp)	Start Codon	Stop codon	Intergenic nucleotides
<i>Cox3</i>	H	1-775	incomplete	—	TAA	14
tRNA-Lys	H	790-854	65			1
tRNA-Ala	H	856-923	68			9
tRNA-Arg	H	933-1001	69			7
tRNA-Asn	H	1009-1075	67			15
tRNA-Ile	H	1091-1157	67			3
<i>Nad3</i>	H	1161-1514	354	ATG	TAA	0
tRNA-Ser	H	1515-1582	68			0
<i>Nad2</i>	H	1583-2637	1055	ATG	TA	0
<i>Cox1</i>	H	2638-4173	1536	ATG	TAG	27
<i>Cox2</i>	H	4201-4887	687	ATG	TAA	-2
tRNA-Asp	H	4886-4953	68			1
<i>Atp8</i>	H	4955-5113	159	ATG	TAA	7
<i>Atp6</i>	H	5121-5816	696	ATG	TAA	41
tRNA-Met	L	5858-5924	67			5
tRNA-Tyr	L	5930-5996	67			1
tRNA-Cys	L	5998-6062	65			0
tRNA-Trp	L	6063-6128	66			1
tRNA-Gln	L	6130-6191	62			1
tRNA-Gly	L	6193-6259	67			13
tRNA-Glu	L	6273-6337	65			0
12s	H	6338-7293	956			0
tRNA-Val	H	7294-7361	68			0
16s	H	7362-8712	1351			0
tRNA-Leu	H	8713-8781	69			2
tRNA-Leu	H	8784-8852	69			0
<i>Nad1</i>	H	8853-9794	942	ATG	TAG	6
tRNA-Pro	H	9801-9868	68			1
<i>Nad6</i>	H	9870-10370	501	ATG	TAA	5
<i>Cytb</i>	H	10376-11515	1140	ATG	TAA	11
tRNA-Ser	H	11527-11591	65			0
tRNA-Thr	L	11592-11659	68			19
<i>Nad4L</i>	H	11679-11975	297	ATG	TAG	11
<i>Nad4</i>	H	11987-13342	1356	ATA	TAA	1
tRNA-His	H	13344-13408	65			0
<i>Nad5</i>	H	13409-15130	1722	ATG	TAG	29
tRNA-Phe	H	missing	—			—

Tritia mutabilis 15,148 bp

Gene	Strand	Location	Size (bp)	Start Codon	Stop codon	Intergenic nucleotides
<i>Cox3</i>	H	1-750	incomplete	—	TAA	15
tRNA- <i>Lys</i>	H	766-830	65			1
tRNA- <i>Ala</i>	H	832-899	68			7
tRNA- <i>Arg</i>	H	907-975	69			10
tRNA- <i>Asn</i>	H	986-1053	68			16
tRNA- <i>Ile</i>	H	1070-1137	68			3
<i>Nad3</i>	H	1141-1494	354	ATG	TAA	0
tRNA- <i>Ser</i>	H	1495-1562	68			0
<i>Nad2</i>	H	1563-2617	1055	ATG	TA	0
<i>Cox1</i>	H	2618-4153	1536	ATG	TAA	28
<i>Cox2</i>	H	4182-4868	687	ATG	TAA	-2
tRNA- <i>Asp</i>	H	4867-4934	68			1
<i>Atp8</i>	H	4936-5094	159	ATG	TAA	7
<i>Atp6</i>	H	5102-5797	696	ATG	TAG	42
tRNA- <i>Met</i>	L	5840-5906	67			2
tRNA- <i>Tyr</i>	L	5909-5975	67			1
tRNA- <i>Cys</i>	L	5977-6042	66			0
tRNA- <i>Trp</i>	L	6043-6108	66			1
tRNA- <i>Gln</i>	L	6110-6171	62			1
tRNA- <i>Gly</i>	L	6173-6239	67			14
tRNA- <i>Glu</i>	L	6254-6318	65			0
12s	H	6319-7278	960			0
tRNA- <i>Val</i>	H	7279-7346	68			0
16s	H	7347-8699	1353			0
tRNA- <i>Leu</i>	H	8700-8768	69			2
tRNA- <i>Leu</i>	H	8771-8839	69			0
<i>Nad1</i>	H	8840-9781	942	ATG	TAA	6
tRNA- <i>Pro</i>	H	9788-9855	68			1
<i>Nad6</i>	H	9857-10357	501	ATG	TAG	5
<i>Cytb</i>	H	10363-11502	1140	ATG	TAA	10
tRNA- <i>Ser</i>	H	11513-11577	65			0
tRNA- <i>Thr</i>	L	11578-11645	68			21
<i>Nad4L</i>	H	11667-11963	297	ATG	TAG	11
<i>Nad4</i>	H	11975-13330	1356	ATA	TAG	-1
tRNA- <i>His</i>	H	13330-13395	66			1
<i>Nad5</i>	H	13397-15118	1722	ATG	TAG	30
tRNA- <i>Phe</i>	H	missing	—			—

Tritia neritea 15,179 bp

Gene	Strand	Location	Size (bp)	Start Codon	Stop codon	Intergenic nucleotides
<i>Cox3</i>	H	1-771	incomplete	—	TAA	15
tRNA-Lys	H	787-851	65			0
tRNA-Ala	H	852-919	68			9
tRNA-Arg	H	929-997	69			16
tRNA-Asn	H	1014-1081	68			18
tRNA-Ile	H	1100-1167	68			3
<i>Nad3</i>	H	1171-1524	354	ATG	TAA	0
tRNA-Ser	H	1525-1592	68			0
<i>Nad2</i>	H	1593-2647	1055	ATG	TA	0
<i>Cox1</i>	H	2648-4183	1536	ATG	TAA	28
<i>Cox2</i>	H	4212-4898	687	ATG	TAA	-2
tRNA-Asp	H	4897-4964	68			1
<i>Atp8</i>	H	4966-5124	159	ATG	TAA	7
<i>Atp6</i>	H	5132-5827	696	ATG	TAA	41
tRNA-Met	L	5869-5935	67			3
tRNA-Tyr	L	5939-6006	68			1
tRNA-Cys	L	6008-6071	64			0
tRNA-Trp	L	6072-6137	66			1
tRNA-Gln	L	6139-6200	62			1
tRNA-Gly	L	6202-6268	67			11
tRNA-Glu	L	6280-6344	65			0
12s	H	6345-7300	956			0
tRNA-Val	H	7301-7368	68			0
16s	H	7369-8720	1352			0
tRNA-Leu	H	8721-8789	69			2
tRNA-Leu	H	8792-8860	69			0
<i>Nad1</i>	H	8861-9802	942	ATG	TAA	5
tRNA-Pro	H	9808-9875	68			1
<i>Nad6</i>	H	9877-10377	501	ATG	TAA	10
<i>Cytb</i>	H	10388-11527	1140	ATG	TAA	8
tRNA-Ser	H	11536-11600	65			0
tRNA-Thr	L	11601-11667	67			22
<i>Nad4L</i>	H	11690-11986	297	ATG	TAG	11
<i>Nad4</i>	H	11998-13353	1356	ATA	TAG	-1
tRNA-His	H	13353-13421	69			1
<i>Nad5</i>	H	13423-15144	1722	ATG	TAG	35
tRNA-Phe	H	missing	—			—

Tritia nitida 15,157 bp

Gene	Strand	Location	Size (bp)	Start Codon	Stop codon	Intergenic nucleotides
<i>Cox3</i>	H	1-750	incomplete	—	TAA	12
tRNA-Lys	H	763-827	65			1
tRNA-Ala	H	829-898	70			6
tRNA-Arg	H	905-975	71			8
tRNA-Asn	H	984-1051	68			20
tRNA-Ile	H	1072-1139	68			3
<i>Nad3</i>	H	1143-1496	354	ATG	TAG	0
tRNA-Ser	H	1497-1564	68			0
<i>Nad2</i>	H	1565-2619	1055	ATG	TA	0
<i>Cox1</i>	H	2620-4155	1536	ATG	TAA	26
<i>Cox2</i>	H	4182-4868	687	ATG	TAA	-1
tRNA-Asp	H	4868-4935	68			1
<i>Atp8</i>	H	4937-5095	159	ATG	TAA	7
<i>Atp6</i>	H	5103-5798	696	ATG	TAG	43
tRNA-Met	L	5842-5908	67			3
tRNA-Tyr	L	5912-5982	71			-1
tRNA-Cys	L	5982-6045	64			0
tRNA-Trp	L	6046-6111	66			-3
tRNA-Gln	L	6109-6175	67			-1
tRNA-Gly	L	6175-6243	69			14
tRNA-Glu	L	6258-6322	65			0
12s	H	6323-7282	960			0
tRNA-Val	H	7283-7349	67			0
16s	H	7350-8701	1352			0
tRNA-Leu	H	8702-8770	69			1
tRNA-Leu	H	8772-8840	69			0
<i>Nad1</i>	H	8841-9782	942	ATG	TAA	5
tRNA-Pro	H	9788-9855	68			1
<i>Nad6</i>	H	9857-10357	501	ATG	TAA	6
<i>Cytb</i>	H	10364-11503	1140	ATG	TAA	8
tRNA-Ser	H	11512-11576	65			3
tRNA-Thr	L	11580-11649	70			18
<i>Nad4L</i>	H	11668-11964	297	ATG	TAG	11
<i>Nad4</i>	H	11976-13331	1356	ATA	TAG	-1
tRNA-His	H	13331-13396	66			1
<i>Nad5</i>	H	13398-15119	1722	ATG	TAG	38
tRNA-Phe	H	missing	—			—

Tritia pallaryana 15,144 bp

Gene	Strand	Location	Size (bp)	Start Codon	Stop codon	Intergenic nucleotides
<i>Cox3</i>	H	1-753	incomplete	—	TAG	15
tRNA-Lys	H	769-833	65			1
tRNA-Ala	H	835-902	68			9
tRNA-Arg	H	912-980	69			5
tRNA-Asn	H	986-1053	68			15
tRNA-Ile	H	1069-1136	68			3
<i>Nad3</i>	H	1140-1493	354	ATG	TAA	0
tRNA-Ser	H	1494-1561	68			0
<i>Nad2</i>	H	1562-2616	1055	ATG	TA	0
<i>Cox1</i>	H	2617-4152	1536	ATG	TAA	29
<i>Cox2</i>	H	4182-4868	687	ATG	TAA	-2
tRNA-Asp	H	4867-4934	68			1
<i>Atp8</i>	H	4936-5094	159	ATG	TAA	7
<i>Atp6</i>	H	5102-5797	696	ATG	TAA	38
tRNA-Met	L	5836-5902	67			3
tRNA-Tyr	L	5906-5973	68			1
tRNA-Cys	L	5975-6039	65			0
tRNA-Trp	L	6040-6105	66			-3
tRNA-Gln	L	6103-6169	67			-1
tRNA-Gly	L	6169-6238	70			10
tRNA-Glu	L	6249-6313	65			0
12s	H	6314-7271	958			0
tRNA-Val	H	7272-7339	68			0
16s	H	7340-8690	1351			0
tRNA-Leu	H	8691-8762	72			1
tRNA-Leu	H	8764-8834	71			-1
<i>Nad1</i>	H	8834-9775	942	ATG	TAA	6
tRNA-Pro	H	9782-9849	68			1
<i>Nad6</i>	H	9851-10351	501	ATG	TAG	5
<i>Cytb</i>	H	10357-11496	1140	ATG	TAA	10
tRNA-Ser	H	11507-11570	64			-1
tRNA-Thr	L	11570-11636	67			19
<i>Nad4L</i>	H	11656-11952	297	ATG	TAG	11
<i>Nad4</i>	H	11964-13319	1356	ATA	TAG	-1
tRNA-His	H	13319-13383	65			0
<i>Nad5</i>	H	13384-15105	1722	ATG	TAG	39
tRNA-Phe	H	missing	—			—

Tritia pellucida 15,175 bp

Gene	Strand	Location	Size (bp)	Start Codon	Stop codon	Intergenic nucleotides
<i>Cox3</i>	H	1-771	incomplete	—	TAA	15
tRNA-Lys	H	787-851	65			0
tRNA-Ala	H	852-919	68			9
tRNA-Arg	H	929-997	69			16
tRNA-Asn	H	1014-1081	68			18
tRNA-Ile	H	1100-1167	68			3
<i>Nad3</i>	H	1171-1524	354	ATG	TAA	0
tRNA-Ser	H	1525-1592	68			0
<i>Nad2</i>	H	1593-2647	1055	ATG	TA	0
<i>Cox1</i>	H	2648-4183	1536	ATG	TAA	28
<i>Cox2</i>	H	4212-4898	687	ATG	TAA	-2
tRNA-Asp	H	4897-4964	68			1
<i>Atp8</i>	H	4966-5124	159	ATG	TAA	7
<i>Atp6</i>	H	5132-5827	696	ATG	TAA	41
tRNA-Met	L	5869-5935	67			3
tRNA-Tyr	L	5939-6006	68			1
tRNA-Cys	L	6008-6072	65			0
tRNA-Trp	L	6073-6138	66			1
tRNA-Gln	L	6140-6201	62			1
tRNA-Gly	L	6203-6269	67			11
tRNA-Glu	L	6281-6345	65			0
12s	H	6346-7301	956			0
tRNA-Val	H	7202-7369	68			0
16s	H	7370-8718	1349			0
tRNA-Leu	H	8719-8787	69			2
tRNA-Leu	H	8790-8858	69			0
<i>Nad1</i>	H	8859-9800	942	ATG	TAA	5
tRNA-Pro	H	9806-9873	68			1
<i>Nad6</i>	H	9875-10375	501	ATG	TAA	10
<i>Cytb</i>	H	10386-11525	1140	ATG	TAA	8
tRNA-Ser	H	11534-11598	65			0
tRNA-Thr	L	11599-11665	67			22
<i>Nad4L</i>	H	11688-11984	297	ATG	TAG	11
<i>Nad4</i>	H	11996-13351	1356	ATA	TAG	-1
tRNA-His	H	13351-13417	67			1
<i>Nad5</i>	H	13419-15140	1722	ATG	TAG	35
tRNA-Phe	H	missing	—			—

Tritia pfeifferi 15,142 bp

Gene	Strand	Location	Size (bp)	Start Codon	Stop codon	Intergenic nucleotides
<i>Cox3</i>	H	1-747	incomplete	—	TAA	15
tRNA-Lys	H	763-827	65			0
tRNA-Ala	H	828-895	68			5
tRNA-Arg	H	901-969	69			16
tRNA-Asn	H	986-1053	68			14
tRNA-Ile	H	1068-1135	68			3
<i>Nad3</i>	H	1139-1492	354	ATG	TAA	0
tRNA-Ser	H	1493-1560	68			0
<i>Nad2</i>	H	1561-2615	1055	ATG	TA	0
<i>Cox1</i>	H	2616-4151	1536	ATG	TAA	28
<i>Cox2</i>	H	4180-4866	687	ATG	TAA	-2
tRNA-Asp	H	4865-4932	68			1
<i>Atp8</i>	H	4934-5092	159	ATG	TAA	8
<i>Atp6</i>	H	5101-5796	696	ATG	TAA	42
tRNA-Met	L	5839-5905	67			1
tRNA-Tyr	L	5907-5974	68			1
tRNA-Cys	L	5976-6041	66			0
tRNA-Trp	L	6042-6107	66			1
tRNA-Gln	L	6109-6170	62			1
tRNA-Gly	L	6172-6238	67			12
tRNA-Glu	L	6251-6315	65			0
12s	H	6316-7271	956			0
tRNA-Val	H	7272-7339	68			0
16s	H	7340-8691	1352			0
tRNA-Leu	H	8692-8760	69			3
tRNA-Leu	H	8764-8832	69			0
<i>Nad1</i>	H	8833-9774	942	ATG	TAA	6
tRNA-Pro	H	9781-9848	68			1
<i>Nad6</i>	H	9850-10350	501	ATG	TAA	5
<i>Cytb</i>	H	10356-11495	1140	ATG	TAA	10
tRNA-Ser	H	11506-11570	65			0
tRNA-Thr	L	11571-11638	68			21
<i>Nad4L</i>	H	11660-11956	297	ATG	TAG	11
<i>Nad4</i>	H	11968-13323	1356	ATA	TAG	-1
tRNA-His	H	13323-13388	66			1
<i>Nad5</i>	H	13390-15111	1722	ATG	TAG	31
tRNA-Phe	H	missing	—			—

Tritia varicosa 15,142 bp

Gene	Strand	Location	Size (bp)	Start Codon	Stop codon	Intergenic nucleotides
<i>Cox3</i>	H	1-762	incomplete	—	TAA	18
tRNA- <i>Lys</i>	H	781-847	67			-1
tRNA- <i>Ala</i>	H	847-916	70			0
tRNA- <i>Arg</i>	H	917-985	69			20
tRNA- <i>Asn</i>	H	1006-1072	67			14
tRNA- <i>Ile</i>	H	1087-1154	68			3
<i>Nad3</i>	H	1158-1511	354	ATG	TAA	0
tRNA- <i>Ser</i>	H	1512-1579	68			0
<i>Nad2</i>	H	1580-2634	1055	ATG	TA	0
<i>Cox1</i>	H	2635-4170	1536	ATG	TAG	22
<i>Cox2</i>	H	4193-4879	687	ATG	TAA	-2
tRNA- <i>Asp</i>	H	4878-4945	68			1
<i>Atp8</i>	H	4947-5105	159	ATG	TAA	7
<i>Atp6</i>	H	5113-5808	696	ATG	TAA	41
tRNA- <i>Met</i>	L	5850-5916	67			2
tRNA- <i>Tyr</i>	L	5919-5985	67			1
tRNA- <i>Cys</i>	L	5987-6051	65			0
tRNA- <i>Trp</i>	L	6052-6117	66			-3
tRNA- <i>Gln</i>	L	6115-6181	67			0
tRNA- <i>Gly</i>	L	6182-6248	67			13
tRNA- <i>Glu</i>	L	6262-6326	65			0
12s	H	6327-7283	957			0
tRNA- <i>Val</i>	H	7284-7351	68			0
16s	H	7352-8701	1350			0
tRNA- <i>Leu</i>	H	8702-8770	69			2
tRNA- <i>Leu</i>	H	8773-8841	69			0
<i>Nad1</i>	H	8842-9783	942	ATG	TAA	5
tRNA- <i>Pro</i>	H	9789-9856	68			1
<i>Nad6</i>	H	9858-10358	501	ATG	TAA	2
<i>Cytb</i>	H	10361-11500	1140	ATG	TAA	8
tRNA- <i>Ser</i>	H	11509-11573	65			-1
tRNA- <i>Thr</i>	L	11573-11641	69			20
<i>Nad4L</i>	H	11662-11958	297	ATG	TAG	11
<i>Nad4</i>	H	11970-13325	1356	ATA	TAG	-1
tRNA- <i>His</i>	H	13325-13389	65			1
<i>Nad5</i>	H	13390-15111	1722	ATG	TAG	31
tRNA- <i>Phe</i>	H	missing	—			—

Tritia tenuicosta 15,169 bp

Gene	Strand	Location	Size (bp)	Start Codon	Stop codon	Intergenic nucleotides
<i>Cox3</i>	H	1-770	incomplete	—	TAA	12
tRNA-Lys	H	783-848	66			1
tRNA-Ala	H	850-919	70			8
tRNA-Arg	H	928-996	69			11
tRNA-Asn	H	1008-1074	67			15
tRNA-Ile	H	1090-1157	68			3
<i>Nad3</i>	H	1161-1514	354	ATG	TAA	-1
tRNA-Ser	H	1514-1583	70			-1
<i>Nad2</i>	H	1583-2637	1055	ATG	TA	0
<i>Cox1</i>	H	2638-4173	1536	ATG	TAA	25
<i>Cox2</i>	H	4199-4885	687	ATG	TAA	-2
tRNA-Asp	H	4884-4951	68			1
<i>Atp8</i>	H	4953-5111	159	ATG	TAA	6
<i>Atp6</i>	H	5118-5813	696	ATG	TAA	42
tRNA-Met	L	5856-5922	67			3
tRNA-Tyr	L	5926-5996	71			-1
tRNA-Cys	L	5996-6060	65			0
tRNA-Trp	L	6061-6126	66			-3
tRNA-Gln	L	6124-6190	67			0
tRNA-Gly	L	6191-6257	67			12
tRNA-Glu	L	6270-6335	65			0
12s	H	6336-7296	961			0
tRNA-Val	H	7297-7364	68			0
16s	H	7365-8716	1352			0
tRNA-Leu	H	8717-8785	69			1
tRNA-Leu	H	8787-8857	71			-1
<i>Nad1</i>	H	8857-9798	942	ATG	TAA	4
tRNA-Pro	H	9803-9870	68			1
<i>Nad6</i>	H	9872-10372	501	ATG	TAA	6
<i>Cytb</i>	H	10379-11518	1140	ATG	TAA	11
tRNA-Ser	H	11530-11593	64			-1
tRNA-Thr	L	11593-11662	70			24
<i>Nad4L</i>	H	11687-11983	297	ATG	TAG	11
<i>Nad4</i>	H	11995-13350	1356	ATA	TAG	-1
tRNA-His	H	13350-13415	66			1
<i>Nad5</i>	H	13417-15138	1722	ATG	TAG	31
tRNA-Phe	H	missing	—			—

Tritia unifasciata 15,168 bp

Gene	Strand	Location	Size (bp)	Start Codon	Stop codon	Intergenic nucleotides
<i>Cox3</i>	H	1-771	incomplete	—	TAG	12
tRNA-Lys	H	784-848	65			2
tRNA-Ala	H	851-918	68			10
tRNA-Arg	H	929-997	69			9
tRNA-Asn	H	1007-1074	68			17
tRNA-Ile	H	1092-1159	68			3
<i>Nad3</i>	H	1163-1516	354	ATG	TAG	0
tRNA-Ser	H	1517-1584	68			0
<i>Nad2</i>	H	1585-2639	1055	ATG	TA	0
<i>Cox1</i>	H	2640-4175	1536	ATG	TAA	25
<i>Cox2</i>	H	4201-4887	687	ATG	TAA	-2
tRNA-Asp	H	4886-4953	68			1
<i>Atp8</i>	H	4955-5113	159	ATG	TAA	7
<i>Atp6</i>	H	5121-5816	696	ATG	TAA	40
tRNA-Met	L	5857-5923	67			2
tRNA-Tyr	L	5926-5992	67			1
tRNA-Cys	L	5994-6057	64			0
tRNA-Trp	L	6058-6123	66			1
tRNA-Gln	L	6125-6186	62			1
tRNA-Gly	L	6188-6254	67			14
tRNA-Glu	L	6269-6333	65			0
12s	H	6334-7292	959			0
tRNA-Val	H	7293-7360	68			0
16s	H	7361-8712	1352			0
tRNA-Leu	H	8713-8781	69			2
tRNA-Leu	H	8784-8852	69			0
<i>Nad1</i>	H	8853-9794	942	ATG	TAA	5
tRNA-Pro	H	9800-9867	68			1
<i>Nad6</i>	H	9869-10369	501	ATG	TAA	6
<i>Cytb</i>	H	10376-11515	1140	ATG	TAG	11
tRNA-Ser	H	11527-11591	65			0
tRNA-Thr	L	11592-11659	68			21
<i>Nad4L</i>	H	11681-11977	297	ATG	TAG	11
<i>Nad4</i>	H	11989-13344	1356	ATA	TAG	-1
tRNA-His	H	13344-13408	65			1
<i>Nad5</i>	H	13410-15131	1722	ATG	TAG	37
tRNA-Phe	H	missing	—			—

Tritia vaucheri 15,153 bp

Gene	Strand	Location	Size (bp)	Start Codon	Stop codon	Intergenic nucleotides
<i>Cox3</i>	H	1-750	incomplete	—	TAA	13
tRNA-Lys	H	764-829	66			4
tRNA-Ala	H	834-901	68			8
tRNA-Arg	H	910-978	69			5
tRNA-Asn	H	984-1052	69			8
tRNA-Ile	H	1061-1128	68			3
<i>Nad3</i>	H	1132-1485	354	ATG	TAA	0
tRNA-Ser	H	1486-1553	68			0
<i>Nad2</i>	H	1554-2608	1055	ATG	TA	0
<i>Cox1</i>	H	2609-4144	1536	ATG	TAA	29
<i>Cox2</i>	H	4174-4860	687	ATG	TAA	-2
tRNA-Asp	H	4859-4926	68			1
<i>Atp8</i>	H	4928-5086	159	ATG	TAA	6
<i>Atp6</i>	H	5093-5788	696	ATG	TAG	40
tRNA-Met	L	5829-5895	67			8
tRNA-Tyr	L	5904-5970	67			1
tRNA-Cys	L	5972-6035	64			0
tRNA-Trp	L	6036-6102	67			1
tRNA-Gln	L	6104-6165	62			1
tRNA-Gly	L	6167-6233	67			13
tRNA-Glu	L	6247-6311	65			0
12s	H	6312-7264	953			0
tRNA-Val	H	7265-7332	68			0
16s	H	7333-8687	1355			0
tRNA-Leu	H	8688-8756	69			4
tRNA-Leu	H	8761-8829	69			0
<i>Nad1</i>	H	8830-9771	942	ATG	TAA	6
tRNA-Pro	H	9778-9846	69			1
<i>Nad6</i>	H	9848-10348	501	ATG	TAA	12
<i>Cytb</i>	H	10361-11500	1140	ATG	TAA	13
tRNA-Ser	H	11514-11578	65			0
tRNA-Thr	L	11579-11644	66			20
<i>Nad4L</i>	H	11665-11961	297	ATG	TAG	11
<i>Nad4</i>	H	11973-13328	1356	CTT	TAG	-1
tRNA-His	H	13328-13393	66			1
<i>Nad5</i>	H	13395-15116	1722	ATG	TAG	37
tRNA-Phe	H	missing	—			—

Tritia elata 15,167 bp

Gene	Strand	Location	Size (bp)	Start Codon	Stop codon	Intergenic nucleotides
<i>Cox3</i>	H	1-767	incomplete	—	TAA	15
tRNA-Lys	H	783-848	66			1
tRNA-Ala	H	850-919	70			8
tRNA-Arg	H	928-996	69			6
tRNA-Asn	H	1003-1070	68			18
tRNA-Ile	H	1089-1156	68			3
<i>Nad3</i>	H	1160-1513	354	ATG	TAA	-1
tRNA-Ser	H	1513-1582	70			-1
<i>Nad2</i>	H	1582-2636	1055	ATG	TA	0
<i>Cox1</i>	H	2637-4172	1536	ATG	TAA	30
<i>Cox2</i>	H	4203-4889	687	ATG	TAA	-2
tRNA-Asp	H	4888-4955	68			1
<i>Atp8</i>	H	4957-5115	159	ATG	TAA	6
<i>Atp6</i>	H	5122-5817	696	ATG	TAG	41
tRNA-Met	L	5859-5925	67			1
tRNA-Tyr	L	5927-5996	70			5
tRNA-Cys	L	6002-6066	65			0
tRNA-Trp	L	6067-6132	66			-3
tRNA-Gln	L	6130-6196	67			0
tRNA-Gly	L	6197-6263	67			15
tRNA-Glu	L	6279-6343	65			0
12s	H	6344-7295	952			0
tRNA-Val	H	7296-7363	68			0
16s	H	7364-8715	1352			0
tRNA-Leu	H	8716-8784	69			3
tRNA-Leu	H	8788-8858	71			-1
<i>Nad1</i>	H	8858-9799	942	ATG	TAA	6
tRNA-Pro	H	9806-9873	68			1
<i>Nad6</i>	H	9875-10375	501	ATG	TAA	5
<i>Cytb</i>	H	10381-11520	1140	ATG	TAA	10
tRNA-Ser	H	11531-11595	65			-1
tRNA-Thr	L	11595-11664	70			20
<i>Nad4L</i>	H	11685-11981	297	ATG	TAG	11
<i>Nad4</i>	H	11993-13348	1356	ATA	TAG	-1
tRNA-His	H	13348-13413	66			1
<i>Nad5</i>	H	13415-15136	1722	ATG	TAG	31
tRNA-Phe	H	missing	—			—

Tritia ovoidea partial mt genome

Gene	Strand	Location	Size (bp)	Start Codon	Stop codon	Intergenic nucleotides
<i>Cox3</i>	H	1-778	incomplete	—	TAA	15
tRNA-Lys	H	794-859	66			1
tRNA-Ala	H	861-928	68			10
tRNA-Arg	H	939-1007	69			7
tRNA-Asn	H	1015-1082	68			18
tRNA-Ile	H	1101-1168	68			3
<i>Nad3</i>	H	1172-1525	354	ATG	TAA	-1
tRNA-Ser	H	1525-1594	70			-1
<i>Nad2</i>	H	1594-2648	1055	ATG	TA	0
<i>Cox1</i>	H	2649-4184	1536	ATG	TAA	30
<i>Cox2</i>	H	4215-4901	687	ATG	TAA	-2
tRNA-Asp	H	4900-4968	69			0
<i>Atp8</i>	H	4969-5127	159	ATG	TAA	6
<i>Atp6</i>	H	5134-5829	696	ATG	TAA	41
tRNA-Met	L	5871-5937	67			1
tRNA-Tyr	L	5939-6008	70			6
tRNA-Cys	L	6015-6079	65			-2
tRNA-Trp	L	6078-6143	66			-1
tRNA-Gln	L	6143-6209	67			-1
tRNA-Gly	L	6209-6277	69			14
tRNA-Glu	L	6292-6356	65			0
12s	H	6357-7313	957			0
tRNA-Val	H	7314-7381	68			0
16s	H	7382-8733	1352			0
tRNA-Leu	H	8734-8802	69			3
tRNA-Leu	H	8806-8876	71			-1
<i>Nad1</i>	H	8876-9817	942	ATG	TAA	6
tRNA-Pro	H	9824-9890	67			1
<i>Nad6</i>	H	9892-10392	501	ATG	TAA	5
<i>Cytb</i>	H	10398-11537	1140	ATG	TAA	9
tRNA-Ser	H	11547-11611	65			-1
tRNA-Thr	L	11611-11679	69			20
<i>Nad4L</i>	H	11700-11996	297	ATG	TAG	11
<i>Nad4</i>	H	12008-13363	1356	ATA	TAG	66
missing tRNA-His						
<i>Nad5</i>	H	13430-15057	1628	—	—	0
tRNA-Phe	H	missing	—			—

Tritia tingitana partial mt genome

Gene	Strand	Location	Size (bp)	Start Codon	Stop codon	Intergenic nucleotides
<i>Cox3</i>	H	1-762	incomplete	—	TAA	12
tRNA- <i>Lys</i>	H	775-840	66			0
tRNA- <i>Ala</i>	H	841-910	70			6
tRNA- <i>Arg</i>	H	917-987	71			8
tRNA- <i>Asn</i>	H	996-1065	70			18
tRNA- <i>Ile</i>	H	1084-1151	68			3
<i>Nad3</i>	H	1155-1508	354	ATG	TAA	0
tRNA- <i>Ser</i>	H	1509-1577	69			-1
<i>Nad2</i>	H	1577-2631	1055	ATG	TA	0
<i>Cox1</i>	H	2632-4167	1536	ATG		28
<i>Cox2</i>	H	4196-4882	687		TAA	-2
tRNA- <i>Asp</i>	H	4881-4949	69			0
<i>Atp8</i>	H	4950-5108	159	ATG	TAA	8
<i>Atp6</i>	H	5117-5812	696	ATG	TAG	46
tRNA- <i>Met</i>	L	5859-5925	67			2
tRNA- <i>Tyr</i>	L	5928-5998	71			-1
tRNA- <i>Cys</i>	L	5998-6061	64			-2
tRNA- <i>Trp</i>	L	6060-6125	66			-1
tRNA- <i>Gln</i>	L	6125-6191	67			-1
tRNA- <i>Gly</i>	L	6191-6259	69			11
tRNA- <i>Glu</i>	L	6271-6335	65			0
12s	H	6336-7298	963			0
tRNA- <i>Val</i>	H	7299-7366	68			0
16s		7367-8725	1359			0
tRNA- <i>Leu</i>	H	8726-8796	71			3
tRNA- <i>Leu</i>	H	8797-8865	69			0
<i>Nad1</i>	H	8866-9807	942	ATG	TAA	6
tRNA- <i>Pro</i>	H	9814-9880	67			1
<i>Nad6</i>	H	9882-10382	501	ATG	TAA	6
<i>Cytb</i>	H	10389-11528	1140	ATG	TAA	10
tRNA- <i>Ser</i>	H	11539-11603	65			0
tRNA- <i>Thr</i>	L	11604-11671	68			19
<i>Nad4L</i>	H	11691-11987	297	ATG	TAG	11
<i>Nad4</i>	H	11999-13354	1356	ATA	TAG	-1
tRNA- <i>His</i>	H	13354-13419	66			1
<i>Nad5</i>	H	13421-15142	1722	ATG	TAG	30
tRNA- <i>Phe</i>	H	missing	—			—

Anentome sp. 15,069 bp

Gene	Strand	Location	Size (bp)	Start Codon	Stop codon	Intergenic nucleotides
<i>Cox3</i>	H	1-766	incomplete	—	TAA	4
tRNA-Lys	H	771-838	68			-1
tRNA-Ala	H	838-904	67			0
tRNA-Arg	H	905-973	69			5
tRNA-Asn	H	979-1047	69			6
tRNA-Ile	H	1054-1124	71			1
<i>Nad3</i>	H	1126-1479	354	ATG	TAA	10
tRNA-Ser	H	1490-1559	70			-1
<i>Nad2</i>	H	1559-2613	1055	ATG	TA	0
<i>Cox1</i>	H	2614-4149	1536	ATG	TAA	15
<i>Cox2</i>	H	4165-4851	687	ATG	TAA	-2
tRNA-Asp	H	4850-4917	68			1
<i>Atp8</i>	H	4919-5077	159	ATG	TAA	2
<i>Atp6</i>	H	5080-5772	693	ATG	TAA	31
tRNA-Met	L	5804-5868	65			1
tRNA-Tyr	L	5869-5934	66			5
tRNA-Cys	L	5940-6003	64			44
tRNA-Gln	L	6048-6114	67			0
tRNA-Trp	L	6115-6180	66			2
tRNA-Gly	L	6183-6251	69			-2
tRNA-Glu	L	6250-6315	66			0
12s	H	6316-7266	951			0
tRNA-Val	H	7267-7336	70			0
16s	H	7337-8671	1335			0
tRNA-Leu	H	8672-8741	70			3
tRNA-Leu	H	8745-8815	71			-1
<i>Nad1</i>	H	8815-9756	942	ATG	TAA	5
tRNA-Pro	H	9762-9828	67			1
<i>Nad6</i>	H	9830-10333	504	ATG	TAA	27
<i>Cytb</i>	H	10361-11500	1140	ATG	TAA	-1
tRNA-Ser	H	11500-11565	66			21
<i>Nad4L</i>	H	11587-11883	297	ATG	TAG	5
<i>Nad4</i>	H	11889-13244	1356	TTA	TAA	-1
tRNA-His	H	13244-13309	66			0
<i>Nad5</i>	H	13310-15022	1713	ATG	TAA	47
tRNA-Phe	H	missing	—			—

Table S4 Pairwise uncorrected sequence divergence within *Tritia*.

	1	2	3	4	5	6	7	8	9	10	11	12	13	14	15	16	17	18	19	20	21	22
1 <i>T. neritea</i>																						
2 <i>T. pellucida</i>	0.023																					
3 <i>T. grana</i>	0.129	0.128																				
4 <i>T. pfeifferi</i>	0.139	0.138	0.152																			
5 <i>T. mutabilis</i>	0.128	0.128	0.143	0.143																		
6 <i>T. pallaryana</i>	0.143	0.140	0.148	0.153	0.150																	
7 <i>T. corniculum</i>	0.143	0.140	0.149	0.154	0.151	0.006																
8 <i>T. elongata</i>	0.146	0.146	0.153	0.155	0.150	0.108	0.109															
9 <i>T. incrassata</i> -Spain	0.171	0.172	0.179	0.183	0.174	0.185	0.185	0.184														
10 <i>T. incrassata</i> -Norway	0.168	0.169	0.177	0.181	0.173	0.183	0.182	0.183	0.038													
11 <i>T. varicosa</i>	0.190	0.190	0.195	0.196	0.189	0.199	0.198	0.195	0.186	0.183												
12 <i>T. cuvierii</i>	0.151	0.150	0.164	0.167	0.158	0.163	0.163	0.166	0.184	0.179	0.199											
13 <i>T. tenuicosta</i>	0.148	0.150	0.160	0.165	0.157	0.166	0.167	0.168	0.177	0.173	0.198	0.125										
14 <i>T. unifasciata</i>	0.162	0.161	0.173	0.173	0.168	0.176	0.176	0.176	0.185	0.185	0.192	0.139	0.139									
15 <i>T. reticulata</i>	0.152	0.151	0.161	0.165	0.149	0.163	0.165	0.162	0.170	0.168	0.187	0.135	0.133	0.138								
16 <i>T. nitida</i>	0.156	0.154	0.162	0.169	0.152	0.164	0.166	0.169	0.171	0.168	0.189	0.133	0.136	0.141	0.106							
17 <i>T. denticulata</i>	0.132	0.130	0.147	0.146	0.136	0.143	0.143	0.149	0.164	0.163	0.179	0.135	0.135	0.149	0.135	0.136						
18 <i>T. ovoidea</i>	0.136	0.133	0.144	0.150	0.134	0.148	0.148	0.155	0.161	0.160	0.187	0.142	0.141	0.154	0.139	0.139	0.120					
19 <i>T. tingitana</i>	0.146	0.146	0.159	0.156	0.152	0.157	0.157	0.163	0.176	0.173	0.192	0.135	0.137	0.151	0.129	0.133	0.130	0.138				
20 <i>T. ephamilla</i>	0.130	0.129	0.143	0.148	0.132	0.141	0.142	0.149	0.159	0.158	0.184	0.144	0.142	0.151	0.133	0.137	0.110	0.116	0.134			
21 <i>T. elata</i>	0.129	0.127	0.139	0.140	0.129	0.141	0.141	0.150	0.160	0.157	0.181	0.137	0.139	0.149	0.133	0.136	0.113	0.073	0.131	0.110		
22 <i>I. obsoleta</i>	0.146	0.144	0.156	0.159	0.151	0.163	0.162	0.165	0.173	0.173	0.188	0.158	0.159	0.170	0.154	0.157	0.138	0.139	0.151	0.134	0.135	
23 <i>T. vaucheri</i>	0.160	0.159	0.166	0.171	0.162	0.174	0.174	0.177	0.186	0.184	0.203	0.175	0.175	0.183	0.173	0.172	0.158	0.160	0.166	0.159	0.155	0.166

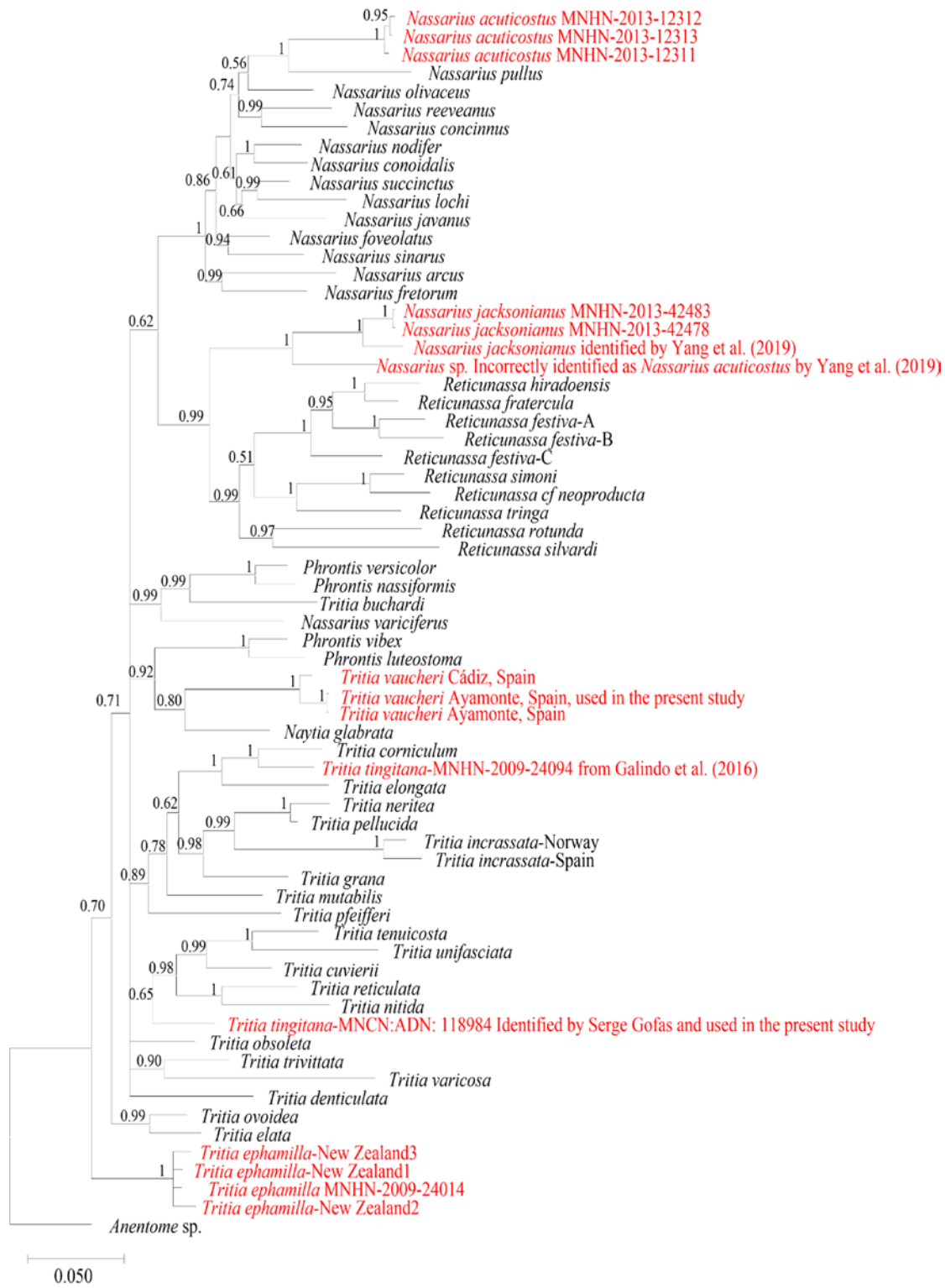


Figure S1. Phylogenetic relationships within Nassarrinae with *Anentome* sp. as outgroup based on the nucleotide sequences of *cox1* fragments. Numbers at nodes are statistical support values for BI (posterior probabilities). For species in red, several specimens were sequenced to ensure their correct identification.